SILICONE SURFACTANTS

THE ANTIBACTERIAL ACTIVITY OF SILICONE-POLYETHER SURFACTANTS

By MADIHA FAHEEM KHAN, M.A.Sc.

A Thesis

Submitted to the School of Graduate Studies

In Partial Fulfillment of the Requirements for the Degree of

Doctor of Philosophy

McMaster University Doctor of Philosophy (2017) Hamilton, Ontario (Biomedical Engineering)

TITLE: Antibacterial activity of silicone polyether surfactants

AUTHOR: Madiha F. Khan, M.A.Sc. (McMaster University)

SUPERVISOR: Professor Michael A. Brook

NUMBER OF PAGES: xxiv, 223

Abstract

The increase in microbial resistance to antibiotics underscores the need for novel antibacterial surfaces, particularly for silicone-based implants, because the hydrophobicity of silicones has been linked to undesirable microbial adhesion and biofilm formation. Unfortunately, current strategies for mitigation, such as pretreatment of surfaces with antiseptics/antibiotics, are not consistently effective. In fact, they can facilitate the prevalence of resistant pathogens by exposing bacteria to sublethal concentrations of biocides. Therefore, scientific interest has shifted to preventing *initial* adhesion (prior to surface colonization) by using surfactants as surface modifiers.

Accordingly, Chapter 2 studied the bioactivity of ACR-008 UP (an acrylic-terminated superwetting silicone surfactant) after it was copolymerized in increasing weight percentages with butyl methacrylate (BMA) and/or methyl methacrylate (MMA). Interestingly, copolymers of 20 wt % ACR showed at least 3x less adhesion by *Escherichia coli* BL21 (*E. coli*) than any other formulation. This was not a consequence of wettability, which followed a parabolic function with ACR concentration: high contact angles (CA) with sessile water drops were observed at both low (< 20 wt %) and high (> 80 wt %) concentrations of ACR in materials. The CA at 20 wt % ACR was 66°. The lack of *E. coli* adhesion was ascribed to surfactant-membrane interactions; hence, the antibacterial potential of compounds related to ACR was further probed.

Chapter 3, therefore, examines the structure-activity relationships of nonionic silicone polyether surfactants in solution. Azide/alkyne click chemistry was used to prepare a

series of eight compounds with consistent hydrophilic tails (8- 44 poly(ethylene glycol) units), but variable hydrophobic heads (branched silicones with 3-10 siloxane linkages, and in two cases phenyl substitutions). The compounds were tested for toxicity at 0.001 w/v %, 2.5 w/v % and their critical micelle concentrations (CMCs), against different concentrations of *E. coli* in a 3-step assay. Surfactants with smaller head groups had as much as 4x the bioactivity of larger analogues, with the smallest hydrophobe exhibiting potency equivalent to SDS. Smaller PEG chains were similarly associated with higher potency. This data suggests that lower micelle stability, and the theoretically enhanced permeability of smaller silicone head groups in membranes, is linked to antibacterial activity. The results further demonstrate that the simple manipulation of nonionic silicone polyether structures, leads to significant changes in antibacterial action.

To ensure similar results were achievable when such surfactants are immobilized on surfaces, 8 compounds with shorter, ethoxysilylpropyl-terminated PEG chains, and branched or linear hydrophobes, were incorporated into a homemade, room temperature vulcanization (RTV) silicone (Chapter 4). The materials, containing 0- 20 wt% surfactants) were then tested for contact killing and cytophobicity against the same *E. coli* strain. Elastomers modified with 0.5- 1 wt% of $(EtO)_3$Si-PEG- laurate, and separately $(EtO)_3$Si-PEG-*t*BS, were on average 2x more hydrophilic relative to controls (103°) and differed in their wettability by ~40°, yet *both* were anti-adhesive; a ~30-fold reduction in adhesion was seen on modified surfaces relative to the control PDMS. Additionally, the $(EtO)_3$Si-PEG-*t*BS surface demonstrated biocidal behavior, which further highlighted the importance of surfactant chemistry- not just wettability- in observing a specific

antibacterial response (if any).

Based on the data collated from each Chapter, silicone surfactants seem to have great potential as bioactive agents and warrant further systematic investigations into their mechanisms of action. In so doing, their chemistry may be optimized against different microbes for a variety of applications. In particular, their potential to create non-toxic, cytophobic silicones is particularly encouraging, given the need for anti-adhesive, biofilm preventing material surfaces.

Acknowledgements

As every past, present and future Doctoral Candidate will attest, the achievement of this milestone would not be possible without the support of a great many people. It is my good fortune that they are too numerous to list here in their entirety, but some in particular must be thanked.

The first is my supervisor, Dr. Michael Brook, who has taught me more than just good science. I am in awe of Mike's aptitude, but it is his unapologetic honesty, sincere convictions and lack of pretentiousness that I respect most. He is himself, in or outside of the spotlight, and that speaks to a formidable strength of character that I try hard to emulate. While I still have ways to go, I embrace each new challenge with a quite confidence that I hitherto lacked. Thank you, Mike. Thank you also for selecting an incredibly supportive committee to steer me throughout my academic journey. I am indebted to Dr. Carlos Filipe and Dr. Heather Sheardown for their patience, guidance and kind words whenever they were needed.

However, my warmest gratitude must go to my parents, without whom I would be lost in life. I hope to make you proud, so that you know your sacrifices for our family are not in vain. Your love and prayers are my greatest blessing.

Lastly, to all those unmentioned but dear to my heart, you know who you are. May my actions in life justify the privilege of your friendship and the good it inspires. You have my sincere thanks. Always.

TABLE OF CONTENTS

LIST OF FIGURES AND TABLES

List of Abbreviations and Symbols

AFM	Atomic force microscope
AH	4-diemthyaminobenzoate
BMA	Butyl methacrylate
BSC	Biosafety cabinet
CA	Contact Angle
CAA	2-carboxyethyl acrylate
CAI-1	Cholerae autoinducer-1
CLSM	Confocal laser scanning microscopy
CMC	Critical Micelle Concentration
CQ	Camphorquinone
CuAAC	Copper-catalyzed azide-alkyne 1,3-dipolar cycloaddition
DCM	Dichloromethane
DEGDA	Diethylene glycol diacrylate
DHPs	Dihydropyrrolones
GFP	Green Fluorescent Protein
HEMA	hydroxyethyl methacrylate
HLB	Hydrophilic-Lipophilic Balance
HPLC	High Performance Liquid Chromatography
IPTG	*Iso*propyl-beta-D-thiogalactopyranoside
LB	Luria-Bertani
LDR	Live:Dead Ratio
MMA	Methyl methacrylate
M_n	Number-average Molecular Weight
MOA	Mechanism of Action
MW	Molecular Weight
NMR	Nuclear Magnetic Resonance
OD_{600}	Optical Density measured at 600 nm
pBMA	Poly(butyl methacrylate)
PBS	Phosphate-buffered Saline
PDMS	Polydimethylsiloxane
PEG	Poly(ethylene glycol)
pMMA	Poly(methyl methacrylate)

PNIPAM	poly(N-*iso*propyl acrylamide)
PVAm	Polyvinylamine
PVP	polyvinylpyrrolidone
RFU	Relative Fluorescence Units
RTV	Room-temperature Vulcanization
SDS	Sodium Dodecyl Sulfate
*t*BS	*tert*-butylsilyl
TC	Tissue Culture
Tg	Glass transition temperature
TMA	(2-(acryloyloxy)ethyl)trimethyl ammonium chloride
QS	Quorum-sensing

CHAPTER 1: Introduction

1.1 The need for cytophobic antibacterial surfaces

Bacteria, like most other microorganisms, can form colonies that irreversibly adhere to surfaces in the form of biofilms.[1] These films are comprised of a fibrous, exopolysaccharide matrix,[2] which provides the encased microbes with 1,000-fold increase in resistance to eradication by biocides, surfactants, predators and antibiotics in comparison to their planktonic (free-floating) counterparts.[3] This is problematic, since biofilms are ubiquitous and detrimental in a variety of industries where their growth is undesirable. For example, microbially influenced corrosion (MIC) of pipelines and process equipment from biofilms, costs the oil and gas industry $10's millions per event.[4] Spoilage of petroleum products can occur due to an increase in suspended solids and a change in the bulk fluid composition,[5] while similar corrosion events and economic setbacks are evident in drinking water distribution systems,[6] fish farms,[7] and the food industry.[8] As important is the challenge of dealing with bacteria in hospitals, due to the increasing incidence of death caused by pathogenic and resistant bacteria (superbugs).[9] As a consequence, antibacterial agents, which kill bacteria or inhibit their growth,[10] are an active area of research.

Though colloquially interchangeable, the term 'antibacterial,' as opposed to 'antibiotic,' strictly refers to chemical agents that disinfect surfaces and prevent subsequent bacterial colonization.[11] They can be classified according to their speed of action and residue-

producing tendency,[12] but given their current, synonymous use with antibiotics,[13] they are also categorized based on biological activity and/ or origin (natural, synthetic, semi-synthetic)[14] (Figure 1). Their diversity allows their presence in a range of substances including soaps, household cleaners, detergents and skincare products, but they are notably absent in veterinary or human medicines, unlike antibiotics.[12] More frequently, antibacterial use is seen in the biomedical context.

It is well known, for example, that implant-related infections can cause both morbidity and a heavy financial toll on health care systems.[15, 16] There are ~80,000 annual catheter-related bloodstream infections linked with 24,000 patient deaths, and a $10,000- $63,000 increase in expenditure per case in the United States.[17] Health insurance companies consider such nosocomial infections as preventable, and since in the US, Medicare and Medicaid may longer reimburse associated costs, there is a big push for preventing biofilms on medical devices.[18, 19]

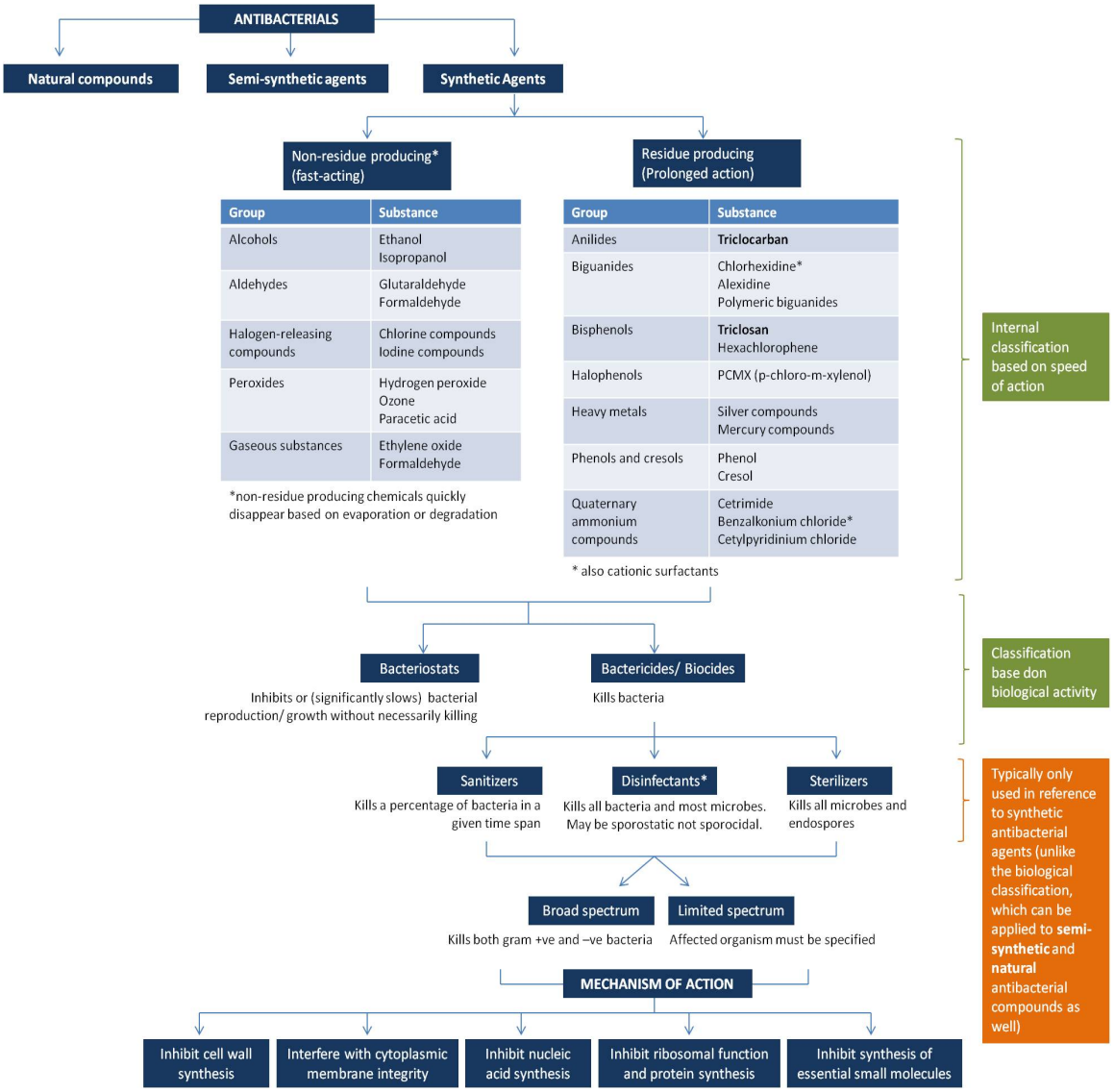

Figure 1: Overview of classification systems for antibacterial agents. Note that disinfectants can also be subcategorized as high-, intermediate- and low-level disinfectants, the distinction between which (along with other information in the diagram) can be found in Goldman and Green (2008).[20] Also note that the sub-classification above is by biological activity, not origin. Semi-synthetic compounds form the bulk of today's antibacterials.[21]

Generally medical devices, related equipment and other surfaces in hospitals are sterilized to counter microbial contamination. Low molecular weight disinfectants such as alcohols, hypochlorite, hydrogen peroxide (H_2O_2) or other reactive oxygen species (ROS) are often used.[22] However, the reintroduction of microbes to cleaned surfaces is frequent and common, due to the spread of pathogens (by patients or healthcare personnel)[23, 24] from other contaminated objects such as shared clinical equipment, floors, doorknobs, pagers and stethoscopes.[25-29] It was found, for example, that ~50% of toilet floors and bed frames sampled at a hospital were contaminated with *C. difficile*.[30] This persistence of bacteria, despite regular cleaning, is partly due to the resistance developed through the indiscriminate use of antibacterials, which are not always 100 % effective.[29]

Escherichia coli, the prototypical gram-negative bacteria, exemplifies many of the defenses possible against environmental stresses like antibacterials. When subjected to strong oxidizing agents such as H_2O_2, chlorine-based sanitizers or ultraviolet radiation (UV), *E. coli* upregulates the expression of protein catalases and superoxide dismutases, which neutralize the threat.[31-33] Other toxic molecules, such as ethanol, aminoglycosides and fluoroquinolones, which may cross the semi-permeable membrane, are promptly exported using the multi-drug and toxic compound extrusion (MATE) family of efflux pumps (an intrinsic bacterial defense).[34]

Unfortunately, many of these resistance mechanisms are encoded on mobile genetic elements such as plasmids, which can undergo horizontal or vertical transmission to other microbes, and are only one of the various and promiscuous gene transfer systems available to bacteria.[35] In fact, the genomes of human pathogens may be considered a

single gene pool that serves as a reservoir of survival genes for most, if not all, bacteria.[35] Unsurprisingly, such transfer of information is greatly facilitated in a structured consortium of microbes (biofilms). Since the ineffective use of antibacterial agents can facilitate resistance, which allows for problematic biofilm development and this in turn facilitates more resistance, scientific interest has shifted from killing bacteria to creating surfaces that, either through their physical characteristics or chemical composition, resist bacterial *attachment* (the first step towards successful bacterial colonization of materials).[36]

1.2 Mechanisms of bacterial adhesion [37-39]

The molecular mechanisms by which bacteria adhere to surfaces involve a series of nonspecific (long-range, >50 nm) and specific (short-range, <5 nm) interactions. Most, if not all, prokaryotic cells follow a similar multi-step process, despite the structural and functional diversity possible with biofilms. Initially, small molecules like water and salt ions adsorb to the interface. Then, depending on the contact media, a single layer of proteins and/or small organic molecules follows. Collectively these layers are termed the conditioning film, which is usually required for successful microbial attachment.[40, 41] In fact, the adhesion strength of nascent microcolonies depends on the structural integrity of the conditioning layer.[42, 43] Note, that while this term predominantly refers to protein deposition from the environment (aqueous liquids,[44, 45] laboratory growth media,[46] blood[47]), it should also include secreted bacterial proteins developed to facilitate

attachment.[48, 49] In some cases, an entirely microbially derived conditioning film has been observed.[50]

Regardless, bacteria reach the conditioned surfaces as single cells or aggregates via Brownian motion, gravitational forces and/or van der Waals, hydrophobic or electrostatic interactions with the material. Bacteria can also move along concentration gradients of diffusible ("chemotaxis") or surface-bound ("haptotaxis") chemoattractants such as amino acids or material debris in the event of surface damage. Since the initial attractive forces are relatively weak, microbial adsorption at this stage is considered reversible. Once near the surface, however, molecular- and species-specific interactions predominate. For example, *Staphylococcus epidermidis,* a skin saprophyte and common cause of biomaterial infections, preferentially binds to hydrophobic polymeric surfaces, whereas *S. aureus*, which is part of the indigenous microflora of humans, prefers metallic and/or hydrophilic implants;[51] successful colonization by *S. epidermidis* over *S. aureus* is attributed to its ability for rapid and maintained adhesion via slime production.[52-54] Similarly, bacterial fimbria, pilli, curli and other appendages, which are involved in the specific and more permanent adhesion to substrates, can have different subclasses of adhesin receptors (depending on the bacterial species/strain), some of which may better bind the proteins of the conditioning film.[55]

Note that while the surface hydrophobicity and membrane composition of bacteria is species-dependent, the surface charge of almost all bacteria in aqueous solutions is negative (bacterial pIs ≈1.5- 4.5).[56] The extent of this charge can vary with species, bacterial age, bacterial surface structure and the pH and ionic strength of the aqueous

solution that the microbe is in. However, there is a negative charge nonetheless. Hence, *S. aureus* adhesion is reduced on negatively charged PMMA/AA (acrylic acid), while it is increased on the positively charged PMMA/DMAEMA (dimethylamino ethyl methacrylate).[57] This example also illustrates the effects of material properties on bacterial attachment, that apart from charge, include porosity and surface roughness, both of which provide better colonization sites. Accordingly, roughening the surface of PMMA with silicone carbide paper (grade P1200) allows for a significant increase in bacterial adhesion.[58]

Once attached, bacteria begin the secretion of polysaccharides. The nature and production rate of the exopolymeric substances (slime) can vary (as abovementioned with *S. epidermidis* and *S. aureus*) but in all cases the secreted polysaccharides will integrate with the conditioning film, thereby strengthening its cohesiveness.[59, 60] At this point, the bacteria are irreversibly adhered and can attract other microbes. Within 24 hours, aggregates of adherent micro colonies form a microzone, a slime-covered area isolated from the external environment that is rich in trapped metal ions or metabolites from bacteria-induced material degradation, tissue trauma and/or previous surface disruption by wear or corrosion. Within 48 hours, bacteria from the biofilm can escape for the colonization of other niches. Hence, once a biofilm has formed it is difficult to treat and infection typically necessitates replacement of the material.

Clearly, the adhesion process is quite complex; in fact, much of the detailed molecular pathways involving specific receptors[38] have been omitted from the summary above. Even a superficial understanding of the adhesion steps, however, is useful in guiding

design parameters for materials. These, therefore, have been discussed in turn below.

1.3 The effect of material properties on bacterial adhesion

The attachment of bacteria to substrates is influenced by several interfacial characteristics. These include the surface chemistry,[61, 62] hydrophobicity (or wettability),[63, 64] roughness and topography,[65, 66] modulus (stiffness or elasticity)[67] and the surface charge.[68] Many of these properties are interrelated, hence attributing adhesion to just one characteristic can be challenging. Increases in surface roughness, for example, can increase hydrophobicity,[69] as is seen by the increased contact angles observed on hydrophobic PTFE (poly-tetrafluoroethylene) after nanoscale imperfections are introduced on its surface.[70]

In general, surface roughness (at the macro, micro or nano scale) refers to the height, width and distribution of surface irregularities on an otherwise ideal surface.[71-73] More specifically, a surface is termed rough when the distance between adjacent hills is ~5-100x greater than the depth.[71] Therefore, roughness, which is indicated by a two-dimensional parameter (R_a or R_q value), is actually the mean deviation of the height profile.[74] This distance between peaks and valleys is what can affect wettability, since the drop edge of the contact angle can become 'arrested' by the borders of grooves,[72, 75] which can also accommodate pockets of air that contribute to the overall hydrophobicity of the interface. Similarly, there is a positive correlation between bacterial adhesion and material roughness,[76-78] however, this trend is seen to a limit. For example, as aforementioned, using silicone carbide paper (grade P1200) to increase the surface

roughness of PMMA greatly increases bacterial adhesion, but larger increases in roughness (produced using grades P400 an P120) had an insignificant effect compared to the control.[58]

Related to roughness is the concept of surface topography, which is the controlled distribution and periodicity of interfacial irregularities that results in patterned surfaces (such as braided, porous or grid-like interfaces).[79] It is a three dimensional parameter observable by electron microscopy. Unsurprisingly, the differences in such physical configurations cause differing amounts of adhesion; porous materials can shelter microbes from environmental antagonists, for example, and are associated with an increased rate of bacterial attachment than denser materials.[80] In another study, spatially controlled microtopographical features were introduced onto PDMS using soft lithography, and the adhesion response of *E. coli, S. epidermidis,* and *Bacillus subtilis* was studied.[81] All topographies discouraged adhesion relative to controls by 35-40 %, and selective adhesion was observed on specific surfaces that correlated to the size and shape of the adhering bacterium. It may seem, therefore, that the surface provides 'contact cues' to proximal microbes. In fact, cells generally contain complex molecular signaling pathways[82, 83] that respond to chemical and biomechanical signals from the underlying substrates, such as the extracellular matrix (ECM) in the context of multicellular organisms.[84-87] These bacterial systems allow the detection of not just topography, but

also the pliability of the material.

The latter may also be described by its stiffness and hardness. Collectively, these terms refer to elastic (temporary)[88] and plastic (permanent) deformation[89] at the interface. Plastic changes can be measured on the Mohs scale and can be further classified into scratch hardness,[90] dynamic or absolute hardness,[89] and indentation hardness (which is commonly used in lab settings). Elasticity is measured differently (using Newtons per meter and Young's modulus), but the term is used synonymously with 'hardness' and surface 'rigidity'. Regardless, the correlation between stiffness and adhesion seems contentious. Recently, for example, an inverse relationship between PDMS rigidity and the adhesion of *E. coli* and *Pseudomonas aeruginosa* was reported.[91] Contrary to this, another study found that by increasing the rigidity of media using agar, an increased production of IV pilli required for adhesion could be observed in cells of *P. aeruginosa*.[92]

Less debatable is the effect of surface charge on preliminary bacterial attachment. At a critical proximity (typically <1 mm) the net sum of attractive or repulsive forces determines the outcome.[93] Electrostatic interactions, for example, favor repulsion, since many surfaces (bacterial and material) are negatively charged.[94, 95] Bacteria that are positively charged at physiological pH seem to be a rare exception, and unsurprisingly, such strains adhere better to negatively charged surfaces like Teflon.[95] In general,

however, there is a dearth of reports studying this phenomenon relative to those dedicated to surface wettability effects.

Wettability refers to the polar dispersive forces at the interface, and is related to the terms 'surface free energy' and 'surface tension'.[96] Wetting typically occurs when the substrate has a higher interfacial free energy than the wetting agent (e.g. water). In such cases, the material is said to be hydrophilic, a measurable characteristic indicated by the contact angle produced from a drop of water on the surface. Materials with contact angles $< 5°$, $< 90°$, $90° \leq \theta \leq 150°$, $> 150°$ are considered super-hydrophilic, hydrophilic, hydrophobic and super-hydrophobic, respectively.[97, 98] Each of these can influence the adhesion and proliferation of bacteria at the interface.[99-102]

While the attachment of bacteria to wettable materials varies with bacterial strains, generally hydrophobic surfaces are implicated in enhanced adhesion. In one study, for example, four different bacterial strains were adsorbed to silica surfaces that had been hydrophobized with alkylsilanes.[103] The modified surfaces had higher bacterial sticking coefficients and stronger adhesion forces than the unmodified controls. Similarly, when comparing the adhesion response of clinical isolates of *S. epidermidis* to hydrophilic (glass) and hydrophobic (acrylic) surfaces, it was found that all strains adhered to a greater extent on the latter.[104] The preference for hydrophobic surfaces may stem from the

creation of stable interfacial water layers on their hydrophilic counterparts, which may prevent direct bacterial-surface interactions.[105] However, as aforementioned, designing an experiment to probe the effect of only one material characteristic on bacterial adhesion can be tricky; in the case of the second study, for example, the comparison of adhesion was done for two chemically different interfaces (acrylic and glass), and it is well-established that the surface chemical composition influences bacterial attachment.[79]

In fact, a recent seminal report examined the effect of interfacial chemistry on the adhesion of *P. aeruginosa, E. coli,* and *S. aureus* to hundreds of polymeric biomaterials with different types of surface hydrocarbons.[106] It was found that *in vitro* bacterial attachment could be decreased by 67-fold when medical-grade silicones were coated with cyclic and aromatic hydrocarbon groups. Other coatings with different functionalities effected the extent of observed adhesion. Hence, alteration of the surface chemistry can significantly affect bacterial attachment, and many anti-biofilm materials are generated based on this concept. Therefore, within the framework of an ideal surface (nonionic, smooth, and relatively hydrophilic) the chemical strategies used to create anti-adhesive materials are critically reviewed.

1.4 Chemical strategies for biofilm prevention

Given the relevance of antibacterial coatings to the biomedical industry, many of the material examples described below were developed with the intent of serving as implantable biomaterials. As such they are reviewed first in that context, and then more generally as surface coatings for industries where biofilms are problematic. Note that the work discussed below provides excellent proof-of-concept prototypes; therefore, it is well understood, that all materials, including the body of work presented in this thesis, would need further testing prior to practical use. Hence, the goal of this section is not to criticize but to highlight the challenges inherent in designing antibacterial surfaces.

1.4.1 Silver (Ag) containing materials

The use of Ag as an antibacterial agent against protozoa, viruses, gram-negative and gram-positive bacteria is well documented,[107-110] owing in part to its broad-spectrum and lasting biocidal effects.[111] Consequently, dressings, catheters and other surface coatings impregnated with Ag are commercially available, and the rise in antibacterial-resistant microbes has renewed interest in their use.[112] The silver in such materials can exist in its elemental state, as nanoparticles (SN), zeolites or simply ions,[113] however, the nanoparticle format seems particularly common.

In one instance, when SNs (Ø <5 nm, 0-500 ppm) and nanofillers were incorporated into orthodontic adhesives, the adhesion of carcinogenic streptococci was significantly reduced (even though the integration of SNs increased the surface roughness of the materials).[114] In fact, coating of the adhesive with saliva did not mitigate the antibacterial

affect. However, the amount of SNs used in materials must be carefully considered to ensure a reasonable longevity. Modified polysulfone membranes for the ultrafiltration of water, for example, lost their antibacterial effect within a short filtration timeframe (0.4 L/cm^2) due to significant silver loss from the surface.[115] During their period of bioactivity, the membranes were resistant to adhesion by *E. coli* K12, *Pseudomonas mendocina* KR1 and MS2 bacteriophage. Furthermore, the adhesion on membrane coupons immersed in *E. coli* cultures was reduced by 2-log (99 %), likely due to decreased cell viability of *E. coli*. It is interesting to note that the leachates from the membranes contained primarily silver ions, and the number of nanoparticles in the filtrate approximated to less than 10^{-7} %. This is important because it highlights the uncertainty surrounding the MOA of SNs.

Many believe that the antimicrobial activity stems from its ionic form.[110, 116-121] Even when using nanoparticles, the release of SIs is detected as shown above, and as evident in the case where composites of polyamide and SNs were used.[122] This is concerning for several reasons, the first of which has already been underscored in Section 1.1; SIs are potent bactericidal agents, which may facilitate the formation of resistance in cases where they are not 100 % effective. Their efficacy results from their multiple modes of action within cells: SIs form strong bonds with molecules containing sulphur, oxygen or nitrogen (which impairs the integrity of bacterial cell walls)[121]; they can associate with bacterial DNA to prevent cellular reproduction[121]; and SIs can complex proteins to prohibit normal metabolic functions like respiration.[110, 121] The high affinity of ionic silver

for proteins can actually decrease the antibacterial activity of biomaterials, since conditioning films have been implicated in the inactivation of released SIs.[112, 117, 123]

However, even more concerning is the concentration-dependent toxicity seen with the use of silver-containing materials. One study examined the *in vitro* cytotoxicity of different nanoparticles against a mouse spermatogonial stem cell line, because gametogenesis in general is highly sensitive to environmental insults, and therefore, related cell lines are useful in preliminary screens of adverse effects.[124] Out of the 3 different types of nanoparticles tested (silver, Ø = 15 nm; molybdenum trioxide, Ø = 30 nm; aluminum, Ø = 30nm) at concentrations that ranged from 5 -100 μg/mL, SNs were by far the most toxic (for example, the EC_{50} required for impaired mitochondrial function in cells was ~8.75 μg/mL for silver, and 90 μg/mL for molybdenum). This potency is unsurprising given the range of effects that silver has within cells. Consequently, the use of silver-containing materials is of equal concern to the environment, where heavy metal accumulation and toxicity to wildlife may be problematic.[125] For all these reasons, other antibacterial surface types have been explored.

1.4.2 Antimicrobial polymers

A common approach to prevent bacterial colonization of surfaces is the use of antimicrobial polymers. These have been extensively reviewed throughout the literature and only a brief overview is provided herein.[22, 126-128] In general, antimicrobial polymers can provide passive or active protection.[129] The former category includes polymers that impair the formation of a conditioning layer by reducing unspecific protein adsorption.

Consequently this limits bacterial adhesion. The most commonly used passive polymer is poly(ethylene glycol) (PEG, with repeating units of $–CH_2CH_2-O-$),[130] which forms hydrated brush layers at the interface of materials, thereby sterically hindering the access of microbes to the surface.[131] PEG-based monomers can be incorporated at the interface through covalent attachment or adsorption (chemisorption or physisorption), and the diversity of surfaces possible has been reviewed elsewhere.[132, 133]

Like PEGylated interfaces, polysaccharide coatings also create a hydration shell that limits undesirable surface adsorption of proteins and therefore microbial contaminants. Hyaluronan (the anionic form of hyaluronic acid) is an obvious fit for such applications, because it is a naturally occurring glycosaminoglycan, which constitutes the extracellular matrix (ECM) of multiple cell types.[134-136] As a result, it and its derivatives have been used as biocompatible coatings on different implantable devices, such as endovascular stents made of stainless steel.[137] For example, 326L stainless steel plates (25 x 25 mm^2) that had been electrosprayed with hyaluronan ions showed no activated platelets as per SEM versus the unmodified controls, which had a dense coverage of the same.[138] Results like these, which show disruption of protein layers that facilitate microbial adhesion, have prompted the exploration of other suitable polysaccharides like maltose.

A derivative of maltose, *n*-dodecyl-β-D-maltoside (a very mild nonionic surfactant, DDM), was used to render polydimethylsiloxane (PDMS) relatively hydrophilic.[139] A concentration of 0.1 w/v % of DDM was sufficient to completely prohibit nonspecific adsorption of streptavidin and bovine serum albumin (BSA). Similarly, a novel self-assembling surfactant polymer designed from maltose dendrons on a polyvinylamine

(PVAm) backbone, was qualitatively shown to reduce platelet adhesion by 90 % compared to unmodified octadecyltrichlorosilane (OTS) controls.[139] As with other passive antimicrobial polymers, the antifouling properties were attributed to the glycocalyx-like brush layers that had formed over the surface.

While polysaccharide coatings may provide excellent adhesion resistance, their widespread use has been limited for several reasons. The first is the batch-to-batch differences observed in the quality of commercially available saccharides.[140] Since most are extracted and purified from natural sources, they are subject to natural variation, which also affects the polydispersity of the purchased product. This in turn can hinder the reproducibility of experimental results.[140] Additionally, their low flexibility, hydration shell, and poor solubility in organic solvents can limit their versatility of use in comparison to synthetic analogues.[140] Many of these limitations may also be true for other naturally derived polymers. Note that not all polysaccharides are nonionic, therefore, not all provide passive protection through steric hindrance; some carry charge and therefore constitute the active category of antimicrobial polymers.

The most obvious example of this is chitosan, a semi-synthetic, polycationic, natural copolymer created from the deactylation of chitin, which is the second most abundant natural polysaccharide after cellulose.[141] It has broad-spectrum activity against bacteria and fungi[142] that depends in part on its electrostatic interactions with the anionic cell walls/membranes of microbes.[143, 144] However, the antibacterial MOA varies depending on the charge density, molecular weight, microbe type, environmental pH, concentration and temperature.[145] For example, in one study that synthesized polyurethane films and

modified them with low viscosity (< 200 mPa s) chitosan (75-85 % deacetylated, 5 mg/mL or 20 mg/mL), greater antibacterial activity was seen against gram-negative *P. aeruginosa* than gram-positive *S. aureus.*[146] In fact, viable colony counts of the former (from a suspension that had been exposed to the surfaces) were reduced by 65 % in comparison to controls, while the latter exhibited a 49 % reduction. It is unclear from the report whether this reduction resulted from contact-killing by the modified surface, or whether it was a function of bacterial loss to the interface due to adhesion; a surface that allows adhesion will remove bacteria from suspension and therefore, decreases the colony forming units available in solution. However, based on the reported MOAs for chitosan in the literature, bactericidal activity is quite possible, and in this case problematic since it seems discriminate.

Like chitosan, many active biocidal polymers that kill adhering bacteria are cationic in nature. Of these, polymers functionalized with quaternary ammonium compounds (QACs), which are effectively cationic surfactants, are most common and highly potent.[147] In fact, they have been heavily utilized in products that range from facial cleansers to nose decongestants and hand sanitizers to hair conditioners.[148] Their positive charge disrupts the anionic microbial membranes resulting in lysis and release of intracellular components.[147] Representative polymers include polyethylenimine, polyguanidine and *N*-halamine,[128] and various techniques have been developed to tether them and their relatives on to surfaces. These include plasma polymerization, surface grafting, layer-by-layer deposition[149-153] and even UV-dependent radical copolymerization. In one example,[154] contact-active, non-leaching, acrylate-based

materials were synthesized using hydroxyethyl methacrylate (HEMA), 1,3-glyceroldimethacrylate, and 0.4 % of heterofunctional monomers with QAC and methylacrylamide terminal groups separated by a poly(2-methyl-1,3-oxazoline) chain of different spacer lengths. Each of the resulting polymeric films, regardless of spacer length, retained high antimicrobial activity against *S. aureus* even after 45 days. This is interesting, since one might assume that copolymerization of biocidal macromers into the bulk material may limit their existence at the interface. However, using confocal Raman spectroscopy, the authors found that the biocides were migrating to the surface during polymerization.

While QACs clearly provide stellar, and well-documented biocidal activity, their use has been contentious. It has been suggested for example, that QACs more than other antibacterial agents have been key in facilitating the emergence of antimicrobial resistance.[155] This may be because the use of QAC formulations typically does not require rinsing after the fact;[156] hence, bacteria may have long-term exposure to sub-inhibitory concentrations (ICs) of QACs with low reactivity. Consequently, only those clones with higher ICs may be favored.[157] Additionally, QACs have poor environmental degradability, perhaps due to their adsorption onto suspended solids that could shield them from primary biodegradation.[158, 159] This is undesirable, since QACs can be toxic at relatively low concentrations to algae, daphnids and fish, and therefore, may be harmful to aquatic ecosystems.[160-163] Similarly, one study found that two common and commercially available QACs (benzalkonium chloride and dimethyldioctadecyl-ammonium bromide) produced moderate but significant genotoxic effects in primary rat

hepatocytes and plant cells at relevant environmental concentrations.[164] It should be noted that many of the environmental challenges posed by the use of QACs are being addressed by the development of 'soft antibacterials'.[165] These labile long-chain QACs are characterized by facile enzymatic and non-enzymatic degradation. Hence, QACs are not to be avoided in their entirety. However, the associated issues have at the very least prompted exploration of other strategies.

Not all antimicrobial polymers, for example, need to be bound *in* or *on* the material, as has been the case with all the surfaces discussed so far. Some can be biocide-releasing such that the polymer backbone functions as a carrier for active compounds like antibiotics.[129] As with all drug-releasing systems, the release kinetics and impermanence of the antibacterial action can be problematic. Other antimicrobial polymers can be mobile in materials to produce self-replenishing, wetting films at the interface. This is most beautifully exemplified by the SLIPS technology developed at Harvard University.[166] Two types of Slippery, Liquid-Infused Porous surfaces were fabricated: the first had periodically ordered epoxy-resin nanoposts (Ø = 300 nm, height = 5 mm) modified with a polyfluoroalkyl silane, and the second was comprised of randomly distributed Teflon nanofibres (thickness = 60-80 μm, average pore size ≥ 200 nm). Both materials were subjected to liquid imbibition with perfluorinated liquids (3M Fluorinert FC-70) that were immiscible with both aqueous and hydrocarbon phases. The resulting surfaces showed impressive repellency of a variety of liquids (water, blood, hydrocarbons and crude oil), negligible contact angle hysteresis (< 2.5 °) and instantaneous, repeated self-healing when damaged. While the report did not evaluate the antibacterial activity of

the surfaces, or even protein adsorption at the interface, the authors did propose an antifouling application for the SLIPs technology. This seems apt, however, the shelf life of such materials is suspect given the high evaporative rates of perfluorinated liquids, and potential loss of the liquids in high-shear conditions. Further development of the technology may overcome this limitation and so it is noteworthy. In the interim, longer antibacterial activity may be achieved through multifunctional systems that are not dependent on a depletable reservoir of fluid.

1.4.3 Stimuli-responsive, multifunctional systems

Responsive antibacterial surfaces often incorporate, biocidal, anti-adhesive and/or self-replenishing characteristics that predominate in turn, depending on the environmental stimuli.[22] Consequently, they are quite complex and often impractical from an industrial manufacturing perspective, however, some repelling and releasing coatings do exist commercially. An obvious example is the use of antifouling paints on ships, the hulls of which are often coated with a biocide-releasing surface that self-polishes in response to movement-induced shear.[167-169] Typically such paints are copper-ion releasing, hydrophobic organocopper esters of poly(methacrylic acid) copolymers, which may also contain pesticides to kill adhesive marine organisms.[167]

Lab-based prototypes of multifunctional, antibacterial surfaces are generally geared towards biomedical applications but need further development. For example, photoresponsive porphyrin and metalloporphyrin derivatives have demonstrated biocidal

activity, but predominantly to bacteria with thinner walls (gram-positive types).[170] Hence, they may not mitigate surface infections led by common gram-negative bacteria such as *E. coli* and *P. aeruginosa.* More troublesome is the antibacterial mechanism of action; the porphyrin is thought to undergo proton absorption through a catalytic reaction with peroxidase and oxidase, thereby resulting in the generation of reactive oxygen species (ROS) that disrupt the bacterial lipid membrane. Specifically, short lifetime singlet oxygen $^1O_2$ is produced, and this targets unsaturated molecules.[171, 172] Though ROS are inevitably produced in aerobic environments, and most organisms have developed strategies to combat ROS accumulation,[173] a surface that actively produces such chemical species may cause damage to proximal proteins, nucleic acids and lipid membranes of eukaryotic cells.[173]

Surfaces that respond to local pH changes may provide a gentler approach to combat microbial colonization of the interface. Mi et al.[174] reported a tunable mixed-charge copolymer surface containing positively charged (2-(acryloyloxy)ethyl)trimethyl ammonium chloride (TMA) and negatively charged 2-carboxyethyl acrylate (CAA) that exhibited pH-dependent nonfouling. The surface of P(TMA-*co*- CAA) lacks charge under neutral and basic conditions, but is positively charged in acidic environments, such that changing the solution pH from 4.5 to 10.0 caused a six-fold decrease in the number of adhered *S. epidermidis* cells. Even more interesting than this example is another surface with pH-dependent switching between bactericidal and bacteria-repellent properties.[175] Under dry conditions, the immobilized cationic *N*,*N*-dimethyl-2-morpholinone(CB-ring) can kill over 99.9 % of adhered *E. coli* K12 cells. Once immersed in neutral or basic

aqueous medium, the CB-ring hydrolyzes to the zwitterionic betaine (CB-OH) state, which causes the release of the dead bacteria and makes the surface bacteria-repellent. Acidic conditions would once again regenerate the killing-state. Although the shelf life of the surface was not clear, the simple switching between two functions makes the surface a promising model for *in vivo* coatings, albeit with other stimuli. The concern with pH responsive materials in general, is (1) making them sensitive to small pH fluctuations and (2) ensuring a rapid response in that range. An environment that changes pH from 4.0-10.0 may be an extreme example. In the biomedical context, for example, blood pH is tightly regulated between ~7.3- 7.4 due to an excellent buffering system and homeostatic process.

Thermoresponsive polymers have similar concerns despite showing much promise. Hyperbranched PNIPAM (HB-PNIPAM) with bound antibiotics (vancomycin/ polymyxin), for example, can selectively bind gram-positive and gram negative bacteria at physiological temperatures before coiling to form bacteria-polymer complexes.[176, 177] Cooling the system reverses the effect. Although the antibiotics are no longer antimicrobial on the surface, they retain their selective binding ability. If this surface were on a wound dressing, then the removal of the dressing from the wound (e.g. skin burn) would also remove the complexes and therefore the bacteria. Alternatively, it may be utilized in pipes where hot and cold water can be run though the system. In any instance, where the temperature cannot be varied, however, the device may actually contribute to subsequent bacterial adhesion (since it is binding bacteria). Therefore, despite the increasing complexity of synthetic surfaces for antibacterial applications, their efficacy is

limited for several reasons. Naturally produced antimicrobial compounds (used in the defense systems of living entities) are now being explored, since they have evolved over time to keep pace with changing microbial floras and any resistance acquired by microbial threats. The three prominent categories of these compounds are discussed in turn below.

1.4.4 Antimicrobial peptides (AMPs)

AMPs are compounds that constitute the immune system systems of most vertebrates and invertebrates.[178] Consequently, they are structurally and functionally diverse with over 2000 identified compounds.[179-181] All, however, are highly cationic in nature with significant amounts of hydrophobic residues, and are classified according to their secondary structures.[182, 183] They also discriminate between host and microbial cells, have broad-spectrum and rapid MOAs against even multi-drug resistance strains, and are poor facilitators of resistance in microbes.[184-187] Hence, AMPs are promising compounds with which to functionalize surfaces in an attempt to create antibacterial materials.

In fact, the inspiration to do so comes from amphibians and fish, which secrete a dermal slime comprised of AMPs to prevent microbial colonization of their skins.[188, 189] Accordingly, AMPs have been immobilized at interfaces using a layer-by-layer deposition technique. Briefly, this strategy alternates the adsorption of polycations and polyanions on the underlying surface such that AMPs are trapped in the resulting matrix.[190] Varying the thickness and number of layers controls the interfacial concentration of AMPs.

This approach has successfully produced functional surfaces on different occasions, one of which utilized the peptide defensin from mosquitos.[191] A surface created with 10 layers reduced *E. coli* growth on the surface by 98 % in comparison to controls. Unfortunately, many layer-by-layer techniques allow for leaching of AMPs into the surrounding media. This can lead to the development of bacterial AMP-resistance.

Low concentrations of free-floating peptides allow bacteria to counter them as is seen with other small molecules like antibiotics; namely efflux pumps and proteases are developed to cleave and inactivate the AMP. *S. aureus* for example utilizes its QacA pump to expel any AMPs that gain entry to the cell.[192] However, it takes 30 passages of *P. aeruginosa* in sub-inhibitory concentrations of AMPs to increase its resistance by 2-4x,[193] whereas the resistance to gentamicin (a known antibiotic) under the same conditions would have increased by 190x.[194] The more pressing concern is that most AMPs like LL-37 and Omiganan have cytotoxic profiles with associated hemolytic activity.[195]

To mitigate these leaching-associated issues, the covalent tethering of AMPs to surfaces has been explored.[196, 197] Typically, surfaces functionalized with PEG or other polymeric brushes ending in appropriate reactive groups are used to immobilize the AMP,[198, 199] and an infection-resistant coating that used this binding mechanism was recently reported.[200] The coatings proved to be non-toxic to osteoblast-like cells with limited platelet adhesion and activation. Furthermore, at least one of the AMP's utilized allowed for a surface with only 8.4 ± 6.6 adhered *P. aeruginosa* per 0.035 mm^2 after 7 days of incubation (versus the unmodified control that had 1268 ± 695 colonies).

These results are surprising in light of the fact that the activity of bound peptides is lower than their mobile and soluble analogues.[199, 201-203] However, optimizing the immobilization conditions can ensure more effective surfaces,[197] since links have been observed between interfacial AMP activity and the attachment method.[204] For example, during melimine immobilization with two different bifunctional azides as crosslinking agents, one clearly produced a higher concentration of AMP at the interface and a corresponding greater antimicrobial activity than the other.[205] Therefore, inadequate interfacial activity of AMPs is not the reason for their limited widespread use. Rather the cost and complexity of synthesis are their main disadvantages, despite the option of non-natural and rationally engineered mimics.[206, 207]

1.4.5 Molecules of quorum sensing

In general, quorum sensing involves the response to, and release and detection of, diffusible chemical signals by microbes as a function of their population density; the greater the density the higher the observable concentration of signals.[208-213] The constituent molecules are typically acylated homoserine lactones in Gram-negative bacteria, and processed oligopeptides in Gram-positive species.[208] However, in both cases, the signals function as autoinducers that alter gene function in the receiving cell.[208] The resulting intercellular communication allows microbes to achieve a range of physiological activities including symbiosis, antibiotic production, sporulation, conjugation and biofilm formation.[209-211]

Quorum sensing is particularly evident within biofilms,[214] the exact molecular

mechanisms for which are poorly understood. However, it is widely accepted that the release of these signals by bacteria induces the biofilm phenotype in neighboring clusters.[215] Similarly, when the biofilm has reached a critical mass, a different set of quorum molecules signal bacteria to leave the biofilm for colonization of surfaces elsewhere. Consequently, there is much interest in isolating molecules that can cause adherent cells to revert back to their planktonic (free-floating) state, or the use of quorum signal inhibitors that disrupt key signaling pathways involved in biofilm maintenance.[216, 217] In each case, the now loose bacteria would become susceptible to bactericides in the environment, phagocytes of the immune system and/or any circulating antibiotics.

An example of such a molecule is cholerae autoinducer-1 (CAI-1), which naturally occurs in *Vibrio cholerae* and was isolated by Higgins et al.[218] By varying the concentrations of CAI-1, they were able to control the sessile/planktonic behavior of the bacteria; in the absence of signal, the bacteria remained attached in biofilms, but at high levels of the same, the bacteria stopped producing an exopolysaccharide matrix. Although the bacteria may communicate via signals other than CAI-1, the study exemplified the significance of signaling molecules in general, and there have been several reports of molecules identified for specific species since then, some of which are clinically relevant. Farnesol, for example, is the quorum signaling molecule that inhibits biofilm formation in *Candida albicans.*[219] Interest in the use of quorum molecules for the functionalization of surfaces was heightened by the eventual synthesis of CAI-1, with no apparent difference in functionality between the synthetic analogue and the natural molecule.[218] This suggested that other molecules could also be synthesized.

It is important to note that the efficacy of CAI-1 after immobilization has not been determined, so it is unclear whether surface modification with the molecule will prevent biofilm formation on a material. However, similar molecules have been shown to remain efficacious after binding. Dihydropyrrolones (DHPs) are quorum-sensing (QS) inhibitors that block communication within biofilms and can prevent bacterial colonization. In a study by Kitty et al.[220] these molecules were covalently bound to glass surfaces via copper-catalyzed azide-alkyne 1,3-dipolar cycloaddition (CuAAC) click reaction, and the antibacterial activity of the coatings against *P. aeruginosa* and *S. aureus* was analyzed by confocal laser scanning microscopy (CLSM). The results demonstrated that the covalently bound DHP compounds reduced bacterial adhesion of both species by 97% ($p < 0.05$). Hence, strategies based on the incorporation of QS inhibitors or other signaling molecules may be useful in combating bacterial colonization at an interface. Unfortunately, like AMPs, the isolation, characterization and synthesis of quorum sensing molecules remains difficult, as does the determination of their MOA. This has hindered their widespread study as antibacterial agents on surfaces.

1.4.6 Biosurfactants

Interestingly, biosurfactants have also been implicated in quorum sensing and biofilm formation.[221] Like other natural compounds, they are structurally diverse (and can exist as glycolipids, lipopeptides, phospholipids and polysaccharide-protein complexes) with certain shared characteristics: they are microbially derived, amphipathic molecules with high surface and emulsifying activities.[222-226] Such diversity is mirrored in their functions,

which range from bacterial pathogenesis to increasing the bioavailability of hydrophobic nutrients.[227] Some biosurfactants are considered secondary metabolites, others, however, may be essential for microbial survival. Regardless, they have garnered interest because they are diverse, biodegradable, selective, functional at extreme temperatures or pH values, and less toxic than their synthetic counterparts.[228-230] Many of them also have demonstrated antimicrobial activity even at low concentrations.[231, 232] For example, the biosurfactant secreted by *Lactobacillus fermentum* RC-14 inhibits *S. aureus* infections of implants in rats.[233]

In the study, the biosurfactant was collected,[234] filter-sterilized, and incubated overnight at 4 °C with a 1 cm^2 sterile piece of silicone. The pre-soaked rubbers were then surgically introduced to dorsal, subcutaneous pockets (with 10^8 cfu of *S. aureus*) in anesthetized rats, which were euthanized 3 days later. Abscess formation was significantly reduced (89 %) in experimental animals versus controls. Similar efficacy has been reported for rhamnolipids (another class of biosurfactants),[235, 236] that also show excellent antifungal properties in the context of soybean oil refineries.[234]

More interestingly, however, biosurfactants can reduce microbial adhesion to solid surfaces.[221] Adsorbing surfactin solution on vinyl urethral catheters, for example, before exposing them to *Salmonella typhimurium, Salmonella enterica and E. coli* decreases the amount of biofilm formed by each.[237] In another instance, biosurfactants from the probiotic strains *L. lactis 53* and *S. thermophillis* A. decreased the initial deposition rates and number of adhered cells of 4 bacterial and 2 yeast strains from explanted, contaminated voice prostheses by 90 %.[238, 239]

There are many similar examples of the antimicrobial and anti-adhesive effects of biosurfactants,[227] however, much work still needs to be done before their mainstream adoption as surface modifiers. Note, for example, that in the cases above, the toxicity of the surfactants to mammalian cells and natural microbial flora has not been examined, which is particularly important since none of the biosurfactants were covalently tethered at the interface to create non-leaching surfaces. Neither the ease with which this can be done, nor the ability to chemically modify biosurfactants without altering their physiochemical properties, has been extensively described in the literature. Hence, this requires investigation to maximally exploit the potential of these compounds. In the interim, another unexplored class of surfactants may be explored for their biological activity.

1.5 The case for silicone surfactants as anti-adhesive surface modifiers

As aforementioned, a large number of potent antimicrobial agents are commercially available or currently in development for the functionalization of materials. Key among them are quaternary ammonium ions, silver-containing compounds or charged entities, but these can cause contact-related toxicity to mammalian cells,[240, 241, 242] aggravate unspecific protein adsorption by virtue of their charge, or raise environmental concerns due to their poor biodegradability. Antibiotics are another relevant class of compounds, however, while they retain their selectivity in binding target bacteria, many seem to lose their antimicrobial activity. Consequently, the bound bacteria can now signal other

microbes in the vicinity towards the surface. The cost of antibiotics is another prohibition to their widespread use as surface modifiers outside of the biomedical context, as may be there inability to address complex bacterial adhesion mechanisms. Stimuli-responsive materials may better address the latter issue, however, their intricacy is only theoretically beneficial, and may be difficult to manufacture and reproduce from a practical standpoint. Additionally the pre-requisite conditions for their efficacy (light/ pH/ electrolytes) may not be readily available, depending on the application. Hence, other antimicrobial strategies (that are less biocidal, and therefore less likely to facilitate antimicrobial resistance) have been explored. These include use of more natural compounds like quorum sensing molecules, AMPs and biosurfactants. Unfortunately, such molecules are often costly and difficult to synthesize or modify in large quantities with controlled polydispersities. Note that all of these routes to anti-adhesive materials have much potential, particularly, the use of surface-active biosurfactants. However, their current limitations warrant exploration of other options, and silicone surfactants have much potential.

Polymeric in nature, silicone surfactants contain a methylated, hydrophobic siloxane group bound to polar entities that are typically nonionic derivatives of polyoxyethylene and polyoxypropylene.[243, 244] A subset of these amphiphilic compounds includes trisiloxane surfactants that have remarkable superwetting properties,[245-247] a characteristic that is not shared by their hydrocarbon counterparts. In fact, there are many similarities and differences between the two groups of surfactants. These include:[248]

- Significant surface activity in aqueous media (silicone surfactants can reduce the surface tension of water to values of 21-30 mN m^{-1}, which is 10-20 % lower than organic surfactants, and are additionally active in organic media);[249-253]
- Use as wetting agents for aqueous mixtures (trisiloxane surfactants are superwetting); and
- The ability to synthesize nonionic and ionic (cationic,[254-257] anionic,[258, 259] zwitterionic[260]) derivatives (silicone surfactants are usually the former).

The last point refers to the hydrophilic segment of the molecule. However structural diversity can also be achieved by altering the hydrophobe structure. Generally the silicone component can exist as linear (AB, ABA, BAB) structures,[248] branched (graft, comb or rake) varieties,[248] or as a siloxane unit within a network or other groups. Consequently, there exist a rich variety of commercial applications for silicone surfactants, from emulsifiers in personal care products to foam control agents in pain and coating products.[248] In all these cases, there is little environmental concern since silicone surfactants have excellent degradability; the breakdown of silicones results in sand, carbon dioxide and water,[261] while polyethers degrade to glycolic acids via oxidation and hydrolysis.[262] Despite this, comparatively little has been done to evaluate the biomedical use of such surfactants, specifically as potential antimicrobial agents.

This is surprising given that they are derivatives of silicones, which have a well-documented role in the biomedical industry (from lubricants to hydrocephalus shunts),[263] and which are the usual material of choice for functionalization to produce anti-adhesive materials.[264-268] It is likely therefore, that on top of their high surface activity silicone

surfactants may have some, if not all, of the advantageous properties of silicone-based elastomers such as high chemical, oxidative and thermal stability,[269-271] high permeability to gases, durability, transparency, hypoallergenic nature[272, 273] and moldability.[274] Furthermore, functionalization of silicones with silicone surfactants may provide two more advantages: (1) better adsorption of surfactant to the interface if physisorption is explored as a modification route (the hydrophobic silicones have higher affinity for each other than surrounding polar/aqueous media); and (2) the link between silicone hydrophobicity and undesirable adhesion of biologicals[60, 275] may be mitigated by the presence of superwetting trisiloxane surfactants. This rationale became the premise for **Chapter 2** of the thesis, where the correlation between *E. coli* adhesion to a substrate with trisiloxane-modulated wettability was explored.

Perhaps the limited research on the bioactivity of silicone surfactants was linked with the inherent difficulty in creating explicit hydrophobes for such compounds. Theoretically, this would complicate the predication and tunability of biological behavior, since function is often associated with structure for most molecules. However, the synthesis of explicit surfactant structures was made possible with the recent use of metal-free click chemistry and the Piers–Rubinsztajn reaction.[276] The latter can be used to create highly defined hydrophobes.

As a result, the potential use of silicone surfactants as antibacterial agents needs to be revaluated. The hydrophobes of nonionic surfactants generally play a key role in the solubilization of membrane lipid bilayers (e.g., Triton X-100),[277, 278] and the known hydrophobicity of silicones should make their surfactant derivatives good candidates for

antimicrobial compounds. In fact, any biocidal activity of silicone surfactants (if this was the intended application) may be comparable to that of other non-related and potent compounds by virtue of the fact that they target bilayers; (1) this non-discriminate MOA would confer broad-spectrum activity, and (2) disruption of membrane integrity beyond a critical point is almost always lethal for cells.[279] To overcome this kind of environmental insult, microbes would need to change the composition and/or organization of their lipids to prevent penetration by surfactants. Since this constitutes a costly and unlikely solution for most microbial species,[280] it may be difficult for bacteria to develop resistance against surface-active silicone surfactants. Accordingly, compounds with defined hydrophobes containing allyl, phenolic, or alkyl groups, constituted the study of **Chapter 3**.

Armed with the tentative design criteria for biocidal and benign surfactants provided by its predecessor, **Chapter 4** used the structure-activity information to generate another set of silicone surfactants in pursuit of anti-adhesive materials. The new group contained (among other things) hydrophobes of varying length since the literature reports hydrophobic length-dependent activity of antimicrobials.[281, 282]

1.6 References

1. T.-F. C. Mah and G. A. O'Toole, *Trends in Microbiology*, 2001, **9**, 34-39.
2. J. W. Costerton, Z. Lewandowski, D. DeBeer, D. Caldwell, D. Korber and G. James, *Journal of Bacteriology*, 1994, **176**, 2137-2142.
3. K. Lewis, *Antimicrobial Agents and Chemotherapy*, 2001, **45**, 999-1007.
4. C. D. Stephen Maxwell, Fiona Rooney, presented in part at the Corrosion, New Orleans, March 28, 2004.
5. M. Magot, B. Ollivier and B. C. Patel, *Antonie Van Leeuwenhoek*, 2000, **77**, 103-116.
6. F. Teng, Y. T. Guan and W. P. Zhu, *Corrosion Science*, 2008, **50**, 2816-2823.
7. S. L. Hodson, C. M. Burke and A. P. Bissett, *Aquaculture*, 2000, **184**, 277-290.
8. C. G. Kumar and S. K. Anand, *International Journal of Food Microbiology*, 1998, **42**, 9-27.
9. H. Hanberger, S. Walther, M. Leone, P. S. Barie, J. Rello, J. Lipman, J. C. Marshall, A. Anzueto, Y. Sakr, P. Pickkers, P. Felleiter, M. Engoren and J.-L. Vincent, *International journal of antimicrobial agents*, 2011, **38**, 331-335.
10. A. J. O'Neill and I. Chopra, *Expert Opinion on Investigational Drugs*, 2004, **13**, 1045-1063.
11. S. Waksman, *Journal of the History of Medicine and Allied Sciences*, 1973, **28**, 284-286.
12. A. f. t. P. U. o. A. (APUA), General Background: Antibiotic Agents, http://www.tufts.edu/med/apua/about_issue/agents.shtml, (accessed February 5, 2014).
13. W. H. Organization, *Tackling antibiotic resistance from a food safety perspective in Europe*, World Health Organization, 2011.
14. P. M. Davidson, *Chemical preservatives and naturally antimicrobial compounds, in: Food Microbiology. Fundamentals and Frontiers*, ASM Press, Washington, 2nd edn., 2001.
15. J. E.-M. Albert and H. Jeffries, in *Textbook of Clinical Pediatrics*, eds. A. Elzouki, H. Harfi, H. Nazer, F. B. Stapleton, W. Oh and R. Whitley,

Springer Berlin Heidelberg, 2012, DOI: 10.1007/978-3-642-02202-9_67, ch. 67, pp. 833-845.

16. M. Hellmann, S. D. Mehta, D. M. Bishai, S. C. Mears and J. M. Zenilman, *The Journal of arthroplasty*, 2010, **25**, 766-771.e761.
17. K. Halton and N. Graves, *Emerging infectious diseases*, 2007, **13**, 815.
18. E. N. Perencevich and D. Pittet, *JAMA*, 2009, **301**, 1285-1287.
19. N. L. Moureau, *Nursing2013*, 2009, **39**, 14-15.
20. E. Goldman and L. H. Green, *Practical Handbook of Microbiology, Second Edition*, Taylor & Francis, 2008.
21. F. von Nussbaum, M. Brands, B. Hinzen, S. Weigand and D. Häbich, *Angewandte Chemie International Edition*, 2006, **45**, 5072-5129.
22. F. Siedenbiedel and J. C. Tiller, *Polymers*, 2012, **4**, 46-71.
23. D. J. Weber, W. A. Rutala, M. B. Miller, K. Huslage and E. Sickbert-Bennett, *American journal of infection control*, 2010, **38**, S25-S33.
24. M. Falagas, P. Thomaidis, I. Kotsantis, K. Sgouros, G. Samonis and D. Karageorgopoulos, *Journal of Hospital Infection*, 2011, **78**, 171-177.
25. D. Talon, *Journal of Hospital Infection*, 1999, **43**, 13-17.
26. C. Zollfrank, K. Gutbrod, P. Wechsler and J. P. Guggenbichler, *Materials Science and Engineering: C*, 2012, **32**, 47-54.
27. J. M. Boyce, *Journal of Hospital Infection*, 2007, **65**, 50-54.
28. S. J. Dancer, *Journal of hospital Infection*, 2009, **73**, 378-385.
29. A. E. Berendt, L. Turnbull, D. Spady, R. Rennie and S. E. Forgie, *American journal of infection control*, 2011, **39**, 442-443.
30. M. Wilcox, W. Fawley, N. Wigglesworth, P. Parnell, P. Verity and J. Freeman, *Journal of Hospital Infection*, 2003, **54**, 109-114.
31. B. Demple and J. Halbrook, *Nature*, 1983, **304**, 466-468.
32. P. J. Pomposiello, M. H. Bennik and B. Demple, *Journal of bacteriology*, 2001, **183**, 3890-3902.
33. M. Zheng, F. Åslund and G. Storz, *Science*, 1998, **279**, 1718-1722.
34. L. Fernández and R. E. Hancock, *Clinical microbiology reviews*, 2012, **25**, 661-681.
35. P. Bennett, *British journal of pharmacology*, 2008, **153**, S347-S357.

36. M. L. W. Knetsch and L. H. Koole, *Polymers*, 2011, **3**, 340-366.

37. C. J. Wilson, R. E. Clegg, D. I. Leavesley and M. J. Pearcy, *Tissue Engineering*, 2005, **11**, 1-18.

38. T. Boland, R. Latour and F. Stutzenberger, in *Handbook of Bacterial Adhesion*, eds. Y. An and R. Friedman, Humana Press, 2000, DOI: 10.1007/978-1-59259-224-1_2, ch. 2, pp. 29-41.

39. K. C. Dee, D. A. Puleo and R. Bizios, in *An Introduction To Tissue-Biomaterial Interactions*, John Wiley & Sons, Inc., 2003, DOI: 10.1002/0471270598.ch3, pp. 37-52.

40. A. G. Gristina, P. T. Naylor and Q. N. Myrvik, in *Pathogenesis of Wound and Biomaterial-Associated Infections*, Springer, 1990, pp. 193-216.

41. R. P. Schneider and K. C. Marshall, *Colloids and surfaces B: Biointerfaces*, 1994, **2**, 387-396.

42. H. Busscher and H. Van der Mei, *Methods in enzymology*, 1995, **253**, 455-477.

43. H. Busscher, G. Doornbusch and H. Van der Mei, *Journal of dental research*, 1992, **71**, 491-500.

44. O. Habimana, A. Semião and E. Casey, *Journal of Membrane Science*, 2014, **454**, 82-96.

45. A. Matin, Z. Khan, S. Zaidi and M. Boyce, *Desalination*, 2011, **281**, 1-16.

46. G. S. Lorite, C. M. Rodrigues, A. A. De Souza, C. Kranz, B. Mizaikoff and M. A. Cotta, *Journal of colloid and interface science*, 2011, **359**, 289-295.

47. L. G. Harris and R. G. Richards, *Injury*, 2006, **37**, S3-S14.

48. E. R. Green and J. Mecsas, *Microbiology spectrum*, 2016, **4**.

49. T. R. Costa, C. Felisberto-Rodrigues, A. Meir, M. S. Prevost, A. Redzej, M. Trokter and G. Waksman, *Nature Reviews Microbiology*, 2015, **13**, 343-359.

50. D. Bradshaw, P. Marsh, G. Watson and C. Allison, *Biofouling*, 1997, **11**, 217-226.

51. J. Dankert, A. Hogt and J. Feijen, *CRC critical reviews in biocompatibility*, 1986, **2**, 219-301.

52. Y. H. An and R. J. Friedman, *Journal of biomedical materials research*, 1998, **43**, 338-348.

53. D. Mack, W. Fischer, A. Krokotsch, K. Leopold, R. Hartmann, H. Egge and R. Laufs, *Journal of bacteriology*, 1996, **178**, 175-183.

54. M. E. Rupp, J. S. Ulphani, P. D. Fey, K. Bartscht and D. Mack, *Infection and immunity*, 1999, **67**, 2627-2632.

55. G. E. Soto and S. J. Hultgren, *Journal of bacteriology*, 1999, **181**, 1059-1071.

56. V. P. Harden and J. O. Harris, *Journal of Bacteriology*, 1953, **65**, 198.

57. M. Kiremitçi-Gümüşderelioğlu and A. Peşmen, *Biomaterials*, 1996, **17**, 443-449.

58. R. L. Taylor, J. Verran, G. C. Lees and A. P. Ward, *Journal of Materials Science: Materials in Medicine*, 1998, **9**, 17-22.

59. Y. F. Dufrêne, C. J.-P. Boonaert and P. G. Rouxhet, *Colloids and Surfaces B: Biointerfaces*, 1996, **7**, 113-128.

60. T. R. Neu and K. C. Marshall, *Journal of biomaterials applications*, 1990, **5**, 107-133.

61. E. Barth, Q. M. Myrvik, W. Wagner and A. G. Gristina, *Biomaterials*, 1989, **10**, 325-328.

62. M. Oga, Y. Sugioka, C. Hobgood, A. Gristina and Q. Myrvik, *Biomaterials*, 1988, **9**, 285-289.

63. J. Pringle and M. Fletcher, *Applied and environmental microbiology*, 1986, **51**, 1321-1325.

64. E. C. Reynolds and A. Wong, *Infection and immunity*, 1983, **39**, 1285-1290.

65. Y. H. An, R. J. Friedman, R. A. Draughn, E. A. Smith, J. H. Nicholson and J. F. John, *Journal of Microbiological Methods*, 1995, **24**, 29-40.

66. R. Locci, G. Peters and G. Pulverer, *Zentralblatt fur Bakteriologie, Mikrobiologie und Hygiene. 1. Abt. Originale B, Hygiene*, 1981, **173**, 285.

67. D. F. Gerson and D. Scheer, *Biochimica et Biophysica Acta (BBA)-Biomembranes*, 1980, **602**, 506-510.

68. A. H. Hogt, J. DANKERT and J. Feijen, *Microbiology*, 1985, **131**, 2485-2491.

69. S. Shibuichi, T. Onda, N. Satoh and K. Tsujii, *The Journal of Physical Chemistry*, 1996, **100**, 19512-19517.

70. S. Veeramasuneni, J. Drelich, J. D. Miller and G. Yamauchi, *Progress in Organic Coatings*, 1997, **31**, 265-270.

71. B. D. Ratner, A. S. Hoffman, F. J. Schoen and J. E. Lemons, *Biomaterials science: an introduction to materials in medicine*, Academic press, 2004.

72. K. Hay, M. Dragila and J. Liburdy, *Journal of colloid and interface science*, 2008, **325**, 472-477.

73. M. J. Biggs, R. Richards, N. Gadegaard, C. Wilkinson and M. Dalby, *Journal of Orthopaedic Research*, 2007, **25**, 273-282.

74. H. Tang, T. Cao, X. Liang, A. Wang, S. O. Salley, J. McAllister and K. Ng, *Journal of Biomedical Materials Research Part A*, 2009, **88**, 454-463.

75. C. Extrand, *Langmuir*, 2004, **20**, 5013-5018.

76. A. Gallardo-Moreno, M. González-Martín, J. Bruque and C. Pérez-Giraldo, *Colloids and Surfaces A: Physicochemical and Engineering Aspects*, 2004, **249**, 99-103.

77. M. Quirynen, H. Van der Mei, C. Bollen, A. Schotte, M. Marechal, G. Doornbusch, I. Naert, H. v. Busscher and D. Van Steenberghe, *Journal of dental research*, 1993, **72**, 1304-1309.

78. E. W. McAllister, L. C. Carey, P. G. Brady, R. Heller and S. G. Kovacs, *Gastrointestinal endoscopy*, 1993, **39**, 422-425.

79. K. Merritt and Y. H. An, in *Handbook of Bacterial Adhesion*, Springer, 2000, pp. 53-72.

80. K. Merritt, J. W. Shafer and S. A. Brown, *Journal of Biomedical Materials Research Part A*, 1979, **13**, 101-108.

81. D. Perera-Costa, J. M. Bruque, M. L. González-Martín, A. C. Gómez-García and V. Vadillo-Rodríguez, *Langmuir*, 2014, **30**, 4633-4641.

82. E. Zamir and B. Geiger, *Journal of cell science*, 2001, **114**, 3583-3590.

83. C. A. Reinhart-King, M. Dembo and D. A. Hammer, *Biophysical journal*, 2005, **89**, 676-689.

84. C. E. Chan and D. J. Odde, *Science*, 2008, **322**, 1687-1691.

85. A. L. Plant, K. Bhadriraju, T. A. Spurlin and J. T. Elliott, *Biochimica et Biophysica Acta (BBA)-Molecular Cell Research*, 2009, **1793**, 893-902.

86. E. L. Baker and M. H. Zaman, *Journal of biomechanics*, 2010, **43**, 38-44.

87. D. Choquet, D. P. Felsenfeld and M. P. Sheetz, *Cell*, 1997, **88**, 39-48.

88. J. N. Lee, X. Jiang, D. Ryan and G. M. Whitesides, *Langmuir*, 2004, **20**, 11684-11691.

89. R. G. Parr and R. G. Pearson, *J. Am. Chem. Soc.;(United States)*, 1983, **105**.

90. C. Brookes, P. Green, P. Harrison and B. Moxley, *Journal of Physics D: Applied Physics*, 1972, **5**, 1284.

91. F. Song and D. Ren, *Langmuir*, 2014, **30**, 10354-10362.

92. K. N. Cowles and Z. Gitai, *Molecular microbiology*, 2010, **76**, 1411-1426.

93. W. M. Dunne, *Clinical microbiology reviews*, 2002, **15**, 155-166.

94. B. Carpentier and O. Cerf, *Journal of Applied Bacteriology*, 1993, **75**, 499-511.

95. B. A. Jucker, H. Harms and A. Zehnder, *Journal of Bacteriology*, 1996, **178**, 5472-5479.

96. M. Dahlström, H. Jonsson, P. R. Jonsson and H. Elwing, *Journal of Experimental Marine Biology and Ecology*, 2004, **305**, 223-232.

97. R. Förch and A. T. A. Jenkins, *Surface design: applications in bioscience and nanotechnology*, John Wiley & Sons, 2009.

98. L. Feng, S. Li, Y. Li, H. Li, L. Zhang, J. Zhai, Y. Song, B. Liu, L. Jiang and D. Zhu, *Advanced materials*, 2002, **14**, 1857-1860.

99. R. E. Baier, *Marine biodeterioration: an interdisciplinary study*, 1984, **1**, 57-62.

100. M. Fletcher and J. H. Pringle, *Journal of Colloid and Interface Science*, 1985, **104**, 5-14.

101. A. Meyer, R. Baier and R. King, *The canadian journal of chemical engineering*, 1988, **66**, 55-62.

102. Y. Arima and H. Iwata, *Biomaterials*, 2007, **28**, 3074-3082.

103. M. B. Salerno, B. E. Logan and D. Velegol, *Langmuir*, 2004, **20**, 10625-10629.

104. N. Cerca, G. B. Pier, M. Vilanova, R. Oliveira and J. Azeredo, *Research in microbiology*, 2005, **156**, 506-514.

105. V. A. Tegoulia and S. L. Cooper, *Colloids and Surfaces B: Biointerfaces*, 2002, **24**, 217-228.

106. A. L. Hook, C.-Y. Chang, J. Yang, J. Luckett, A. Cockayne, S. Atkinson, Y. Mei, R. Bayston, D. J. Irvine, R. Langer, D. G. Anderson, P. Williams, M. C. Davies and M. R. Alexander, *Nat Biotech*, 2012, **30**, 868-875.

107. D. Balazs, K. Triandafillu, P. Wood, Y. Chevolot, C. van Delden, H. Harms, C. Hollenstein and H. Mathieu, *Biomaterials*, 2004, **25**, 2139-2151.

108. D. Parikh, T. Fink, K. Rajasekharan, N. Sachinvala, A. Sawhney, T. Calamari and A. D. Parikh, *Textile Research Journal*, 2005, **75**, 134-138.

109. E. Ülkür, O. Oncul, H. Karagoz, E. Yeniz and B. Çeliköz, *Burns*, 2005, **31**, 874-877.

110. A. Panáček, L. Kvítek, R. Prucek, M. Kolář, R. Večeřová, N. Pizúrová, V. K. Sharma, T. j. Nevěčná and R. Zbořil, *The Journal of Physical Chemistry B*, 2006, **110**, 16248-16253.

111. R. Kumar and H. Münstedt, *Biomaterials*, 2005, **26**, 2081-2088.

112. N. Stobie, B. Duffy, D. E. McCormack, J. Colreavy, M. Hidalgo, P. McHale and S. J. Hinder, *Biomaterials*, 2008, **29**, 963-969.

113. D. R. Monteiro, L. F. Gorup, A. S. Takamiya, A. C. Ruvollo-Filho, E. R. de Camargo and D. B. Barbosa, *International journal of antimicrobial agents*, 2009, **34**, 103-110.

114. S.-J. Ahn, S.-J. Lee, J.-K. Kook and B.-S. Lim, *Dental Materials*, 2009, **25**, 206-213.

115. K. Zodrow, L. Brunet, S. Mahendra, D. Li, A. Zhang, Q. Li and P. J. Alvarez, *Water research*, 2009, **43**, 715-723.

116. A. Melaiye and W. J. Youngs, *Journal*, 2005.

117. F. Furno, K. S. Morley, B. Wong, B. L. Sharp, P. L. Arnold, S. M. Howdle, R. Bayston, P. D. Brown, P. D. Winship and H. J. Reid, *Journal of Antimicrobial Chemotherapy*, 2004, **54**, 1019-1024.

118. K. Kawahara, K. Tsuruda, M. Morishita and M. Uchida, *Dental materials*, 2000, **16**, 452-455.

119. T. Matsuura, Y. Abe, Y. Sato, K. Okamoto, M. Ueshige and Y. Akagawa, *Journal of dentistry*, 1997, **25**, 373-377.

120. E. Weir, A. Lawlor, A. Whelan and F. Regan, *Analyst*, 2008, **133**, 835-845.

121. C. Damm, H. Münstedt and A. Rösch, *Materials Chemistry and Physics*, 2008, **108**, 61-66.

122. C. Damm and H. Münstedt, *Applied Physics A*, 2008, **91**, 479-486.

123. J. Schierholz, L. Lucas, A. Rump and G. Pulverer, *Journal of Hospital Infection*, 1998, **40**, 257-262.

124. L. Braydich-Stolle, S. Hussain, J. J. Schlager and M.-C. Hofmann, *Toxicological sciences*, 2005, **88**, 412-419.

125. J. J. Harrison, H. Ceri and R. J. Turner, *Nature Reviews Microbiology*, 2007, **5**, 928-938.

126. L. Timofeeva and N. Kleshcheva, *Applied microbiology and biotechnology*, 2011, **89**, 475-492.

127. E.-R. Kenawy, S. Worley and R. Broughton, *Biomacromolecules*, 2007, **8**, 1359-1384.

128. A. Jain, L. S. Duvvuri, S. Farah, N. Beyth, A. J. Domb and W. Khan, *Advanced healthcare materials*, 2014, **3**, 1969-1985.

129. K.-S. Huang, C.-H. Yang, S.-L. Huang, C.-Y. Chen, Y.-Y. Lu and Y.-S. Lin, *International Journal of Molecular Sciences*, 2016, **17**, 1578.

130. K. Yu, Y. Mei, N. Hadjesfandiari and J. N. Kizhakkedathu, *Colloids and Surfaces B: Biointerfaces*, 2014, **124**, 69-79.

131. H. Zhang and M. Chiao, *Journal of medical and biological engineering*, 2015, **35**, 143-155.

132. M. Heuberger, T. Drobek and N. D. Spencer, *Biophysical journal*, 2005, **88**, 495-504.

133. S. R. Meyers and M. W. Grinstaff, *Chemical reviews*, 2011, **112**, 1615-1632.

134. T. C. Laurent and J. Fraser, *The FASEB Journal*, 1992, **6**, 2397-2404.

135. E. Balazs, E. Leshchiner, N. Larsen and P. Band, *Handbook of Biomaterials and Applications*, 1995, **52**, 2719-2741.

136. J. Necas, L. Bartosikova, P. Brauner and J. Kolar, *Veterinarni medicina*, 2008, **53**, 397-411.

137. S. Verheye, C. P. Markou, M. Y. Salame, B. Wan, S. B. King, K. A. Robinson, N. A. Chronos and S. R. Hanson, *Arteriosclerosis, thrombosis, and vascular biology*, 2000, **20**, 1168-1172.

138. M. Volný, W. T. Elam, B. D. Ratner and F. Tureček, *Journal of Biomedical Materials Research Part B: Applied Biomaterials*, 2007, **80**, 505-510.

139. B. Huang, H. Wu, S. Kim and R. N. Zare, *Lab on a Chip*, 2005, **5**, 1005-1007.

140. T. Crouzier, T. Boudou and C. Picart, *Current Opinion in Colloid & Interface Science*, 2010, **15**, 417-426.

141. V. E. Tikhonov, E. A. Stepnova, V. G. Babak, I. A. Yamskov, J. Palma-Guerrero, H.-B. Jansson, L. V. Lopez-Llorca, J. Salinas, D. V. Gerasimenko and I. D. Avdienko, *Carbohydrate polymers*, 2006, **64**, 66-72.

142. C. R. Allan and L. A. Hadwiger, *Experimental mycology*, 1979, **3**, 285-287.

143. S. Hirano and N. Nagao, *Agricultural and biological chemistry*, 1989, **53**, 3065-3066.

144. D. F. Kendra and L. A. Hadwiger, *Experimental Mycology*, 1984, **8**, 276-281.

145. M. Kong, X. G. Chen, K. Xing and H. J. Park, *International journal of food microbiology*, 2010, **144**, 51-63.

146. F. Kara, E. A. Aksoy, Z. Yuksekdag, N. Hasirci and S. Aksoy, *Carbohydrate polymers*, 2014, **112**, 39-47.

147. Y. Xue, H. Xiao and Y. Zhang, *International journal of molecular sciences*, 2015, **16**, 3626-3655.

148. P. Gilbert and L. Moore, *Journal of applied microbiology*, 2005, **99**, 703-715.

149. Y. Sang and H. Xiao, *Colloids and Surfaces A: Physicochemical and Engineering Aspects*, 2009, **335**, 121-127.

150. D. Zhang and H. Xiao, *ACS applied materials & interfaces*, 2013, **5**, 3464-3468.

151. D. Roy, J. S. Knapp, J. T. Guthrie and S. Perrier, *Biomacromolecules*, 2007, **9**, 91-99.

152. K. Bazaka, M. V. Jacob, R. J. Crawford and E. P. Ivanova, *Acta biomaterialia*, 2011, **7**, 2015-2028.

153. M. Charnley, M. Textor and C. Acikgoz, *Reactive and Functional Polymers*, 2011, **71**, 329-334.

154. C. J. Waschinski, J. Zimmermann, U. Salz, R. Hutzler, G. Sadowski and J. C. Tiller, *Advanced Materials*, 2008, **20**, 104-108.

155. S. Buffet-Bataillon, P. Tattevin, M. Bonnaure-Mallet and A. Jolivet-Gougeon, *International journal of antimicrobial agents*, 2012, **39**, 381-389.

156. W. H. Organization, *World Health Organization*, 2007.

157. A. McBain, A. Rickard and P. Gilbert, *Journal of industrial microbiology & biotechnology*, 2002, **29**, 326-330.

158. J. Cross and E. J. Singer, *Cationic surfactants: analytical and biological evaluation*, CRC Press, 1994.

159. M. Garcia, E. Campos, J. Sanchez-Leal and I. Ribosa, *Chemosphere*, 1999, **38**, 3473-3483.

160. X. Y. Qv and J. G. Jiang, *Environmental toxicology and chemistry*, 2013, **32**, 426-433.

161. G. Ying, *Journal*, 2004, 78-109.

162. Z. Liang, F. Ge, H. Zeng, Y. Xu, F. Peng and M. Wong, *Aquatic toxicology*, 2013, **138**, 81-87.

163. J. C. Cooper, *Ecotoxicology and environmental safety*, 1988, **16**, 65-71.

164. F. Ferk, M. Mišík, C. Hoelzl, M. Uhl, M. Fuerhacker, B. Grillitsch, W. Parzefall, A. Nersesyan, K. Mičieta and T. Grummt, *Mutagenesis*, 2007, **22**, 363-370.

165. T. Thorsteinsson, M. Másson, K. G. Kristinsson, M. A. Hjálmarsdóttir, H. Hilmarsson and T. Loftsson, *Journal of medicinal chemistry*, 2003, **46**, 4173-4181.

166. T.-S. Wong, S. H. Kang, S. K. Tang, E. J. Smythe, B. D. Hatton, A. Grinthal and J. Aizenberg, *Nature*, 2011, **477**, 443-447.

167. P.-L. Kuo, T.-F. Chuang and H.-L. Wang, *Journal of Coatings Technology*, 1999, **71**, 77-83.

168. D. Ibbitson, A. Johnson, N. Morley and A. Penman, ACS Publications, 1986.

169. P.-Y. Qian, Y. Xu and N. Fusetani, *Biofouling*, 2009, **26**, 223-234.

170. I. Stojiljkovic, B. D. Evavold and V. Kumar, *Expert Opinion on Investigational Drugs*, 2001, **10**, 309-320.

171. J. Sherrill, S. Michielsen and I. Stojiljkovic, *Journal of Polymer Science Part A: Polymer Chemistry*, 2003, **41**, 41-47.

172. S. Cannistraro, A. van de Vorst and G. Jori, *Photochemistry and Photobiology*, 1978, **28**, 257-259.

173. C. M. Bergamini, S. Gambetti, A. Dondi and C. Cervellati, *Current pharmaceutical design*, 2004, **10**, 1611-1626.

174. L. Mi, M. T. Bernards, G. Cheng, Q. Yu and S. Jiang, *Biomaterials*, 2010, **31**, 2919-2925.

175. Z. Cao, L. Mi, J. Mendiola, J. R. Ella‐Menye, L. Zhang, H. Xue and S. Jiang, *Angewandte Chemie International Edition*, 2012, **51**, 2602-2605.

176. J. Shepherd, P. Sarker, K. Swindells, I. Douglas, S. MacNeil, L. Swanson and S. Rimmer, *Journal of the American Chemical Society*, 2010, **132**, 1736-1737.

177. J. Shepherd, P. Sarker, S. Rimmer, L. Swanson, S. MacNeil and I. Douglas, *Biomaterials*, 2011, **32**, 258-267.

178. D. Alves and M. Olívia Pereira, *Biofouling*, 2014, **30**, 483-499.

179. D. Andreu and L. Rivas, *Peptide Science*, 1998, **47**, 415-433.

180. E. Guaní-Guerra, T. Santos-Mendoza, S. O. Lugo-Reyes and L. M. Terán, *Clinical Immunology*, 2010, **135**, 1-11.

181. K. Reddy, R. Yedery and C. Aranha, *International journal of antimicrobial agents*, 2004, **24**, 536-547.

182. R. E. Hancock and R. Lehrer, *Trends in biotechnology*, 1998, **16**, 82-88.

183. R. E. Hancock and H.-G. Sahl, *Nature biotechnology*, 2006, **24**, 1551-1557.

184. H. Altman, D. Steinberg, Y. Porat, A. Mor, D. Fridman, M. Friedman and G. Bachrach, *Journal of Antimicrobial Chemotherapy*, 2006, **58**, 198-201.

185. K. A. Brogden, *Nature Reviews Microbiology*, 2005, **3**, 238-250.

186. K. Matsuzaki, *Biochimica et Biophysica Acta (BBA)-Biomembranes*, 1999, **1462**, 1-10.

187. L. Yang, T. M. Weiss, R. I. Lehrer and H. W. Huang, *Biophysical Journal*, 2000, **79**, 2002-2009.

188. M. Simmaco, G. Mignogna and D. Barra, *Peptide Science*, 1998, **47**, 435-450.

189. K. Glinel, P. Thebault, V. Humblot, C.-M. Pradier and T. Jouenne, *Acta biomaterialia*, 2012, **8**, 1670-1684.

190. K. Ariga, J. P. Hill and Q. Ji, *Physical Chemistry Chemical Physics*, 2007, **9**, 2319-2340.

191. O. Etienne, C. Picart, C. Taddei, Y. Haikel, J. Dimarcq, P. Schaaf, J. Voegel, J. Ogier and C. Egles, *Antimicrobial agents and chemotherapy*, 2004, **48**, 3662-3669.

192. B. A. Mitchell, M. H. Brown and R. A. Skurray, *Antimicrobial agents and chemotherapy*, 1998, **42**, 475-477.

193. L. Zhang, J. Parente, S. M. Harris, D. E. Woods, R. E. Hancock and T. J. Falla, *Antimicrobial agents and chemotherapy*, 2005, **49**, 2921-2927.

194. D. A. Steinberg, M. A. Hurst, C. A. Fujii, A. Kung, J. Ho, F. Cheng, D. J. Loury and J. C. Fiddes, *Antimicrobial agents and chemotherapy*, 1997, **41**, 1738-1742.

195. C. D. Ciornei, T. Sigurdardóttir, A. Schmidtchen and M. Bodelsson, *Antimicrobial agents and chemotherapy*, 2005, **49**, 2845-2850.

196. J. M. Goddard and J. Hotchkiss, *Progress in polymer science*, 2007, **32**, 698-725.

197. S. A. Onaizi and S. S. Leong, *Biotechnology advances*, 2011, **29**, 67-74.

198. I. Banerjee, R. C. Pangule and R. S. Kane, *Advanced Materials*, 2011, **23**, 690-718.

199. S. L. Haynie, G. A. Crum and B. A. Doele, *Antimicrobial agents and chemotherapy*, 1995, **39**, 301-307.

200. G. Gao, D. Lange, K. Hilpert, J. Kindrachuk, Y. Zou, J. T. Cheng, M. Kazemzadeh-Narbat, K. Yu, R. Wang and S. K. Straus, *Biomaterials*, 2011, **32**, 3899-3909.

201. W.-M. Cho, B. P. Joshi, H. Cho and K.-H. Lee, *Bioorganic & medicinal chemistry letters*, 2007, **17**, 5772-5776.

202. M. Bagheri, M. Beyermann and M. Dathe, *Antimicrobial agents and chemotherapy*, 2009, **53**, 1132-1141.

203. K. Hilpert, M. Elliott, H. Jenssen, J. Kindrachuk, C. D. Fjell, J. Körner, D. F. Winkler, L. L. Weaver, P. Henklein and A. S. Ulrich, *Chemistry & biology*, 2009, **16**, 58-69.

204. F. Costa, I. F. Carvalho, R. C. Montelaro, P. Gomes and M. C. L. Martins, *Acta Biomaterialia*, 2011, **7**, 1431-1440.

205. R. Chen, N. Cole, M. D. Willcox, J. Park, R. Rasul, E. Carter and N. Kumar, *Biofouling*, 2009, **25**, 517-524.

206. B. P. Mowery, S. E. Lee, D. A. Kissounko, R. F. Epand, R. M. Epand, B. Weisblum, S. S. Stahl and S. H. Gellman, *Journal of the American Chemical Society*, 2007, **129**, 15474-15476.

207. G. N. Tew, D. Liu, B. Chen, R. J. Doerksen, J. Kaplan, P. J. Carroll, M. L. Klein and W. F. DeGrado, *Proceedings of the National Academy of Sciences*, 2002, **99**, 5110-5114.

208. M. B. Miller and B. L. Bassler, *Annual Reviews in Microbiology*, 2001, **55**, 165-199.

209. C. M. Waters and B. L. Bassler, *Annu. Rev. Cell Dev. Biol.*, 2005, **21**, 319-346.

210. S. B. von Bodman, J. M. Willey and S. P. Diggle, *Journal of bacteriology*, 2008, **190**, 4377-4391.

211. G. M. Dunny and B. A. Leonard, *Annual Reviews in Microbiology*, 1997, **51**, 527-564.

212. M. J. Federle and B. L. Bassler, *The Journal of clinical investigation*, 2003, **112**, 1291-1299.

213. S. Schauder and B. L. Bassler, *Genes & Development*, 2001, **15**, 1468-1480.

214. C. Solano, M. Echeverz and I. Lasa, *Current Opinion in Microbiology*, 2014, **18**, 96-104.

215. Y.-H. Li and X. Tian, *Sensors*, 2012, **12**, 2519-2538.

216. T. Bjarnsholt and M. Givskov, *Philosophical Transactions of the Royal Society B: Biological Sciences*, 2007, **362**, 1213-1222.

217. M. Hentzer, H. Wu, J. B. Andersen, K. Riedel, T. B. Rasmussen, N. Bagge, N. Kumar, M. A. Schembri, Z. Song and P. Kristoffersen, *The EMBO journal*, 2003, **22**, 3803-3815.

218. D. A. Higgins, M. E. Pomianek, C. M. Kraml, R. K. Taylor, M. F. Semmelhack and B. L. Bassler, *Nature*, 2007, **450**, 883-886.

219. G. Ramage, S. P. Saville, B. L. Wickes and J. L. López-Ribot, *Applied and Environmental Microbiology*, 2002, **68**, 5459-5463.

220. K. K. K. Ho, R. Chen, M. D. P. Willcox, S. A. Rice, N. Cole, G. Iskander and N. Kumar, *Biomaterials*, 2014, **35**, 2336-2345.

221. P. Singh and S. S. Cameotra, *TRENDS in Biotechnology*, 2004, **22**, 142-146.

222. S. C. Lin, *Journal of Chemical Technology and Biotechnology*, 1996, **66**, 109-120.

223. M. Morikawa, H. Daido, T. Takao, S. Murata, Y. Shimonishi and T. Imanaka, *Journal of Bacteriology*, 1993, **175**, 6459-6466.

224. J. D. Desai and I. M. Banat, *Microbiology and Molecular biology reviews*, 1997, **61**, 47-64.

225. B. Angelova and H.-P. Schmauder, *Journal of biotechnology*, 1999, **67**, 13-32.

226. F. Ahimou, P. Jacques and M. Deleu, *Enzyme and microbial technology*, 2000, **27**, 749-754.

227. L. Rodrigues, I. M. Banat, J. Teixeira and R. Oliveira, *Journal of Antimicrobial Chemotherapy*, 2006, **57**, 609-618.

228. I. M. Banat, R. S. Makkar and S. S. Cameotra, *Applied microbiology and biotechnology*, 2000, **53**, 495-508.

229. N. Kosaric, *Pure and Applied Chemistry*, 1992, **64**, 1731-1737.

230. S. S. Cameotra and R. Makkar, *Applied microbiology and Biotechnology*, 1998, **50**, 520-529.

231. S. S. Cameotra and R. S. Makkar, *Current opinion in microbiology*, 2004, **7**, 262-266.

232. L. Rodrigues, H. C. Van der Mei, J. Teixeira and R. Oliveira, *Applied and environmental microbiology*, 2004, **70**, 4408-4410.

233. B. S. Gan, J. Kim, G. Reid, P. Cadieux and J. C. Howard, *Journal of infectious Diseases*, 2002, **185**, 1369-1372.

234. G. Reid, C. Heinemann, M. Velraeds, H. C. van der Mei and H. J. Busscher, *Methods in enzymology*, 1999, **310**, 426-433.

235. M. Benincasa, A. Abalos, I. Oliveira and A. Manresa, *Antonie Van Leeuwenhoek*, 2004, **85**, 1-8.

236. G. Bai, M. L. Brusseau and R. M. Miller, *Applied and environmental microbiology*, 1997, **63**, 1866-1873.

237. J. R. Mireles, A. Toguchi and R. M. Harshey, *Journal of Bacteriology*, 2001, **183**, 5848-5854.

238. L. Rodrigues, H. Van der Mei, J. A. Teixeira and R. Oliveira, *Applied microbiology and biotechnology*, 2004, **66**, 306-311.

239. L. Rodrigues, H. Van Der Mei, I. M. Banat, J. Teixeira and R. Oliveira, *FEMS Immunology & Medical Microbiology*, 2006, **46**, 107-112.

240. M. Zilberman and J. J. Elsner, *Journal of Controlled Release*, 2008, **130**, 202-215.

241. K. Hegstad, S. Langsrud, B. T. Lunestad, A. A. Scheie, M. Sunde and S. P. Yazdankhah, *Microbial Drug Resistance*, 2010, **16**, 91-104.

242. E. M. Hetrick and M. H. Schoenfisch, *Chemical Society Reviews*, 2006, **35**, 780-789.

243. R. M. Hill, *Silicone surfactants*, CRC Press, 1999.

244. I. Schlachter and G. Feldmann-Krane, *Surfactant science series*, 1998, **74**, 201-239.

245. R. M. Hill, *Current opinion in colloid & interface science*, 1998, **3**, 247-254.

246. N. Churaev, N. Esipova, R. Hill, V. Sobolev, V. Starov and Z. Zorin, *Langmuir*, 2001, **17**, 1338-1348.

247. T. Stoebe, Z. Lin, R. M. Hill, M. D. Ward and H. T. Davis, *Langmuir*, 1996, **12**, 337-344.

248. M. J. Owen and P. R. Dvornic, *Advances in Silicon Science*, 2012, 374.

249. H. Hoffmann and W. Ulbricht, *Surfactant science series*, 1999, 97-136.

250. G. Wang, W. Qu, Z. Du, Q. Cao and Q. Li, *The Journal of Physical Chemistry B*, 2011, **115**, 3811-3818.

251. W. Guoyong, D. Zhiping, L. Qiuxiao and Z. Wei, *The Journal of Physical Chemistry B*, 2010, **114**, 6872-6877.

252. D.-W. Kim, C.-H. Lim, J.-K. Choi and S.-T. Noh, *Bulletin of the Korean Chemical Society*, 2004, **25**, 1182-1188.

253. D.-W. Kim, S.-T. Noh and B.-W. Jo, *Colloids and Surfaces A: Physicochemical and Engineering Aspects*, 2006, **287**, 106-116.

254. G. Schmaucks, G. Sonnek, R. Wuestneck, M. Herbst and M. Ramm, *Langmuir*, 1992, **8**, 1724-1730.

255. S. A. Snow, *Langmuir*, 1993, **9**, 424-430.

256. R. M. Hill and S. A. Snow, *Journal*, 1993.

257. R. Wagner and G. Sonnek, *Organosilicon Chemistry Set: From Molecules to Materials*, 1994, 267-268.

258. N. Meguriya, S. Azechi and M. Tanaka, *Journal*, 1991.

259. A. R. Colas and F. A. Renauld, *Journal*, 1988.

260. S. A. Snow, W. N. Fenton and M. J. Owen, *Langmuir*, 1991, **7**, 868-871.

261. M. A. Brook, *Silicon in organic, organometallic, and polymer chemistry*, J. Wiley, 2000.

262. F. Kawai and B. Schink, *Critical reviews in biotechnology*, 1987, **6**, 273-307.

263. B. D. Ratner, A. S. Hoffman, F. Schoen and J. E. Lemons, *San Diego, California*, 2004, 162-164.

264. R. Malcolm, S. McCullagh, A. Woolfson, S. Gorman, D. Jones and J. Cuddy, *Journal of Controlled Release*, 2004, **97**, 313-320.

265. O. Girshevitz, Y. Nitzan and C. N. Sukenik, *Chemistry of Materials*, 2008, **20**, 1390-1396.

266. Y. Inoue, Y. Kurihara and S. Susumu, *Journal*, 1995.

267. K. J. Quinn and J. M. Courtney, *British polymer journal*, 1988, **20**, 25-32.

268. S. Perni, C. Piccirillo, A. Kafizas, M. Uppal, J. Pratten, M. Wilson and I. P. Parkin, *Journal of Cluster Science*, 2010, **21**, 427-438.

269. L. V. Interrante, Q. Shen and J. Li, *Macromolecules*, 2001, **34**, 1545-1547.

270. J. H. Park, K. D. Park and Y. H. Bae, *Biomaterials*, 1999, **20**, 943-953.

271. A. Mata, A. J. Fleischman and S. Roy, *Biomedical microdevices*, 2005, **7**, 281-293.

272. S. I. Ertel, B. D. Ratner, A. Kaul, M. B. Schway and T. A. Horbett, *Journal of Biomedical Materials Research*, 1994, **28**, 667-675.

273. T. G. van Kooten, J. F. Whitesides and A. F. von Recum, *Journal of biomedical materials research*, 1998, **43**, 1-14.

274. M. V. Kunnavakkam, F. M. Houlihan, M. Schlax, J. A. Liddle, P. Kolodner, O. Nalamasu and J. A. Rogers, *Applied Physics Letters*, 2003, **82**, 1152-1154.

275. H. J. Busscher, G. I. Geertsema-Doornbusch and H. C. van der Mei, *Journal of Biomedical Materials Research*, 1997, **34**, 201-209.

276. F. Gonzaga, J. B. Grande and M. A. Brook, *Chemistry – A European Journal*, 2012, **18**, 1536-1541.

277. J. B. Cornett and G. D. Shockman, *Journal of bacteriology*, 1978, **135**, 153-160.

278. P. Schlieper and E. De Robertis, *Archives of Biochemistry and Biophysics*, 1977, **184**, 204-208.

279. I. R. Booth, *International journal of food microbiology*, 2002, **78**, 19-30.

280. M. Zasloff, *nature*, 2002, **415**, 389-395.

281. T. Abel, J. I. Cohen, R. Engel, M. Filshtinskaya, A. Melkonian and K. Melkonian, *Carbohydrate research*, 2002, **337**, 2495-2499.

282. B. Dizman, M. O. Elasri and L. J. Mathias, *Journal of applied polymer science*, 2004, **94**, 635-642.

CHAPTER 2: Superwetting comonomers reduce bacterial adhesion[†]

2.1 Abstract

The adhesion of *Escherichia coli* to copolymers of methacrylates and a trisiloxane-polyether acrylate surfactant was found to be at a minimum with copolymers containing a low (20 %) fraction of the surfactant monomer. Rather than wettability, hardness, or water uptake, adhesion was found to be limited by the presence of low concentrations of bound surfactant that can interact with hydrophobic domains on the bacterium inhibiting anchoring to the polymer surface.

2.2 Introduction

The increase in nosocomial infections associated with antibacterial-resistant pathogens,[1] such as *Clostridium difficile*,[2] is of concern with regards to patient safety and associated healthcare costs.[3] The common strategy to manage bacterial persistence in hospitals involves stringent surface disinfection protocols with

---

[†] This chapter is taken from a an article accepted by the journal *Chemical Communications* by M. F. Khan, N. Luong, J. Kurian and M. A. Brook (2017). It is reproduced by permission of Royal Society of Chemistry, 2017. Khan synthesized all materials (with occasional help from Kurian) using a formulation developed by Luong. Khan performed all characterization and analyses except the water contact angle work that was conducted by Luong. Khan wrote the manuscript with additions, edits and guidance from Brook.

biocides.[4] However, bacteria can form biofilms that protect the constituents from such broad-spectrum antibacterials,[5] thereby allowing them to persist after cleaning.[6] A companion strategy for bacterial management may be the utilization of surfaces to which bacteria have difficulty adhering, such that it is difficult for bacteria to proliferate and establish biofilms.[7]

Many seminal studies have examined the facility with which various bacteria are able to adhere to surfaces.[8, 9] Although the behaviours vary with organism type,[10] several general trends have been noted. The extent of adhesion seems low with: i) low or very high roughness[11-13] (e.g. Ra <0.05 μm, lower limit[14]; undefined upper limit[15]); ii) high stiffness;[16, 17] iii) negative charge[18-20, 21] and, iv) high hydrophilicity (contact angles < 90°).[22-24] The latter, which describes the wettability of a surface, is a well-exploited characteristic for anti-adhesive materials, and may be achieved through the use of surfactants.

In solution, surfactants tend to decrease bacterial adhesion, even at concentrations well below that needed to lyse the cells.[25] When anchored to a surface, surface active molecules can similarly disrupt adhesion,[26, 27] but the specific type and concentration of surfactant, underlying substrate,[28] and organism all play roles in establishing the degree to which adhesion is affected.

One class of silicone surfactants is ‘superwetting’, leading to much more rapid and extensive water wetting of hydrophobic surfaces than traditional organic surfactants;[29] they are used to facilitate delivery of agricultural pesticide formulations. The compounds in solution are biocidal, with toxicity slightly higher than sodium dodecyl sulfate (SDS), a

commonly used surfactant for disinfection.[30, 31] We were interested in testing if improved wetting (resulting from surfactants at the interface) would decrease bacterial adhesion and/or viability when compared to hardness and other parameters.

2.3 Results and Discussion

We describe the systematic preparation of acrylate (co)polymer surfaces derived from methyl methacrylate (MMA), butyl methacrylate (BMA) or a combination of the two, with increasing amounts of a silicone surfactant-based acrylic comonomer (ACR-008 UP - designated ACR, Figure 2-1); acrylate-terminated PEG was used as a control.

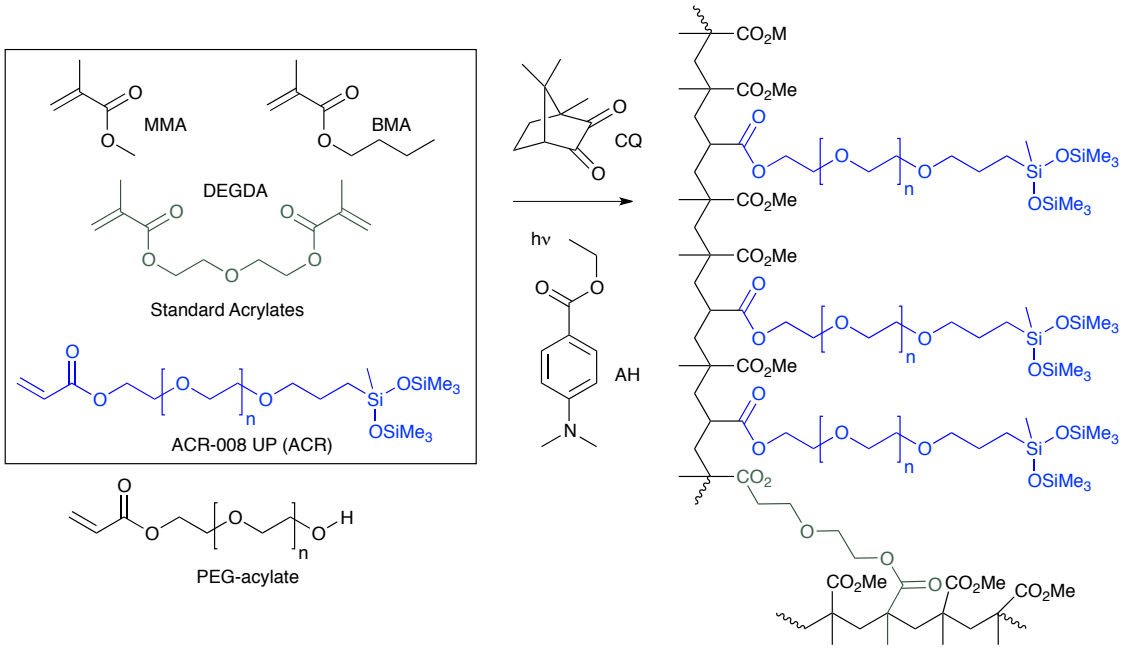

Figure 2-1. (a) Chemical structure of **ACR**; (b) Proposed dilution effect of ACR after addition of co-constituent(s)

An additional consequence of the oligoether chains in ACR is a decrease in stiffness of the copolymers with increasing ACR content. Combinations of BMA and MMA were therefore chosen to allow for the preparation of hydrophobic materials with tuneable hardness; atactic poly(butyl methacrylate)(PBMA) has a glass transition temperature (Tg) of ~20 °C while the value for atactic poly(methyl methacrylate)(PMMA) is much higher at ~105 °C.[32]

Radical polymerization of the (meth)acrylic comonomers was performed as previously reported for methacrylates[33] using camphorquinone (CQ) and 4-dimethylaminobenzoate (AH) as photoinitiators excited by a blue light LED (at 480 nm, provided by Kerber Science).[34] Briefly, inhibitor-free MMA and BMA (0.04 g, 20 wt% each), diethylene glycol diacrylate (DEGDA), CQ and AH (0.02 g, 1 wt% each) were mixed in a test tube, and the solution was purged with N_2 (g). ACR (1.2 g, 60 wt%) was added and the entire mixture was poured into a 10 mm, Teflon-lined Petri dish and irradiated for 30 min, after which the solid elastomer was removed and swelled in isopropanol overnight to extract unreacted monomers. The materials were dried in a vacuum oven (50 °C, 51 mm Hg), and a 0.64 mm punching tool was used to obtain circular disks (2 mm thick). The process was used to create three distinct polymer series: ACR:BMA:MMA (with equal parts BMA and MMA), ACR:MMA and ACR:BMA, respectively. For each series, the ACR content was varied from 0- 100 % at 20 wt% intervals (Appendix section 2.7.2.10).

Gram-negative, *E. coli* B21 was selected as a model organism to test the different surfaces.[35] Qualitative bacterial adhesion assays were performed using an *E. coli*

strain capable of producing green fluorescent protein (GFP) upon induction with isopropyl-β-D-1-thiogalactopyranoside (IPTG). Briefly, copolymer coupons (n=4) obtained from leachate-free polymers in the three series were incubated for 12 h at 37 °C with 400 µL each of phosphate buffered saline (PBS) inoculated with IPTG-induced *E. coli*. The coupons were rinsed with PBS then measured for GFP fluorescence using a Gemini XPS microplate reader (excitation: 395 nm, emission: 509 nm, Figure 2-2).

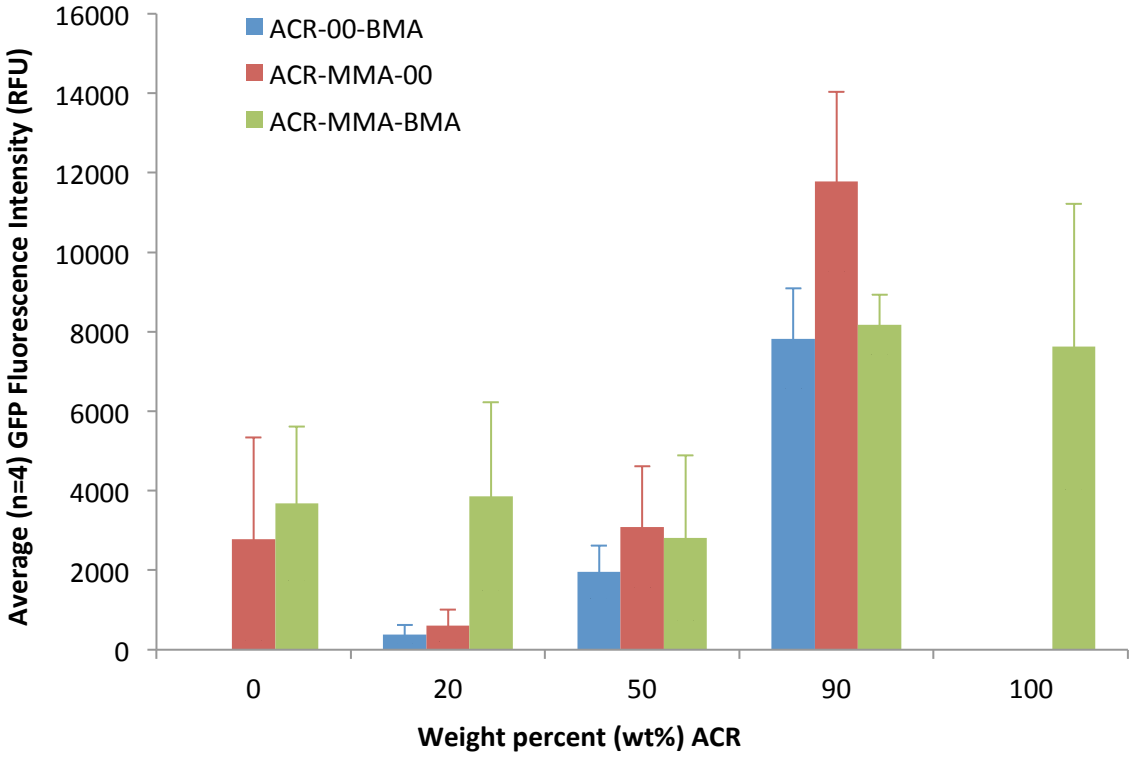

Figure 2-2. Average (n = 4) GFP fluorescence readings from IPTG-induced *Escherichia coli* adhered to surfaces

The average hardnesses (n=6) for coupons of each copolymer type were measured using a Shore OO Rex Durometer (Model 1600). As shown in Figure 2-3.A, polymer stiffness was unsurprisingly lower for the BMA-containing polymer series. However, the concentration of ACR was an even stronger contributor to lower modulus (Appendix section 2.7.2.1).[36] Note that the homopolymer of ACR was too soft to measure by the Shore OO instrument.

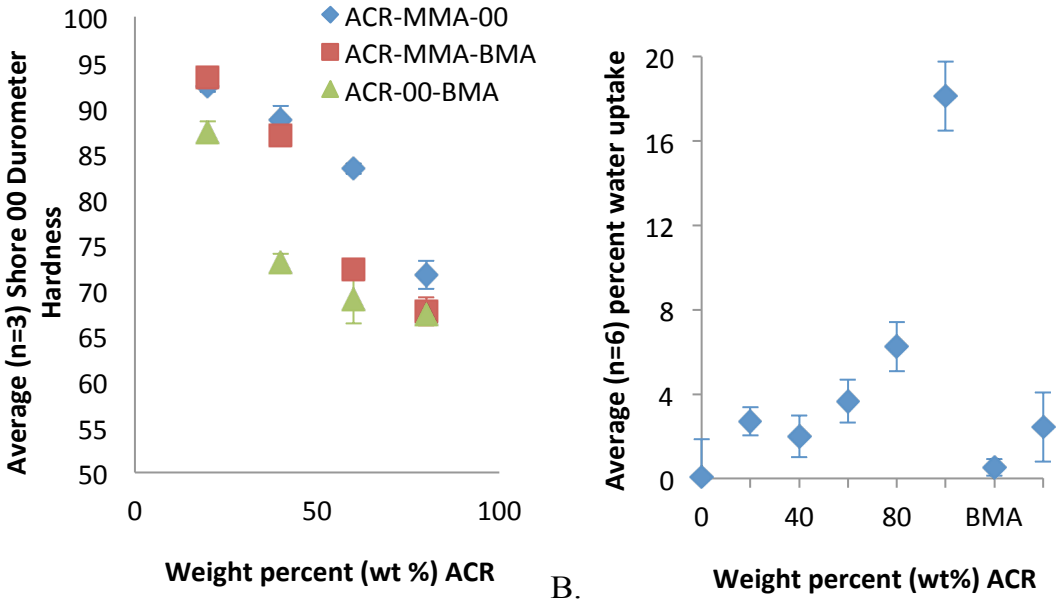

Figure 2-3. A: Average (n=3) Shore OO hardness values for **ACR**-methacrylate copolymer series. B: Average (n=6) percent water uptake for terpolymers of the ACR-MMA-BMA series.

Since the literature cites positive correlations between *E. coli* adhesion and surface roughness[11 12] it was important to ensure the consistency of this parameter across all **ACR**-methacrylate polymer series. Triplicate measurements of surface roughnesses over a 1 μm^2 area, using an atomic force microscope (AFM) with a

silicon tapping probe, yielded consistent roughness (2-3 nm) across all copolymers, removing this parameter as a basis for differentiation.

The average percent water uptake for 6 coupons of each copolymer type in the ACR-MMA-BMA series was determined. Calculated weight differences before and after immersion of the coupon in distilled water for 30 min showed that the highest percent increase (18.2 %) was seen for pACR while the lowest uptake was observed for the pMMA (0.5 %) and pBMA (2.4 %) coupons (Figure 2-3.B). Given the hydrophilic nature of PEG, the presence of ACR in the co- and terpolymers would be expected to facilitate water penetration into the polymer due to the osmotic differential that exists between spaces in polymer matrices and an aqueous external environment.[37]

Surface wettability, measured using milliQ water and a sessile-drop contact angle (CA) goniometer, showed that the contact angle of the surfaces decreased as the concentration of the surfactant increased in any of the polymeric series (Figure 2-4). However, starting at about 60 wt% ACR, the contact angle began to increase with increasing ACR content. This phenomenon is ascribed to the assembly of siloxane surfactants at the interface. At low concentrations of ACR, a water droplet will mostly see the underlying hydrophobic methacrylate body (Figure 2-4.A). With increasing concentration, an increase in wetting will be observed as the tethered surfactant comes into play[38] (Figure 2-4.B). At high concentrations (>60 wt%), however, the surfactant will form a brush that presents siloxane head groups at the interface, leading to an increase in contact angle (Figure 2-4.C).

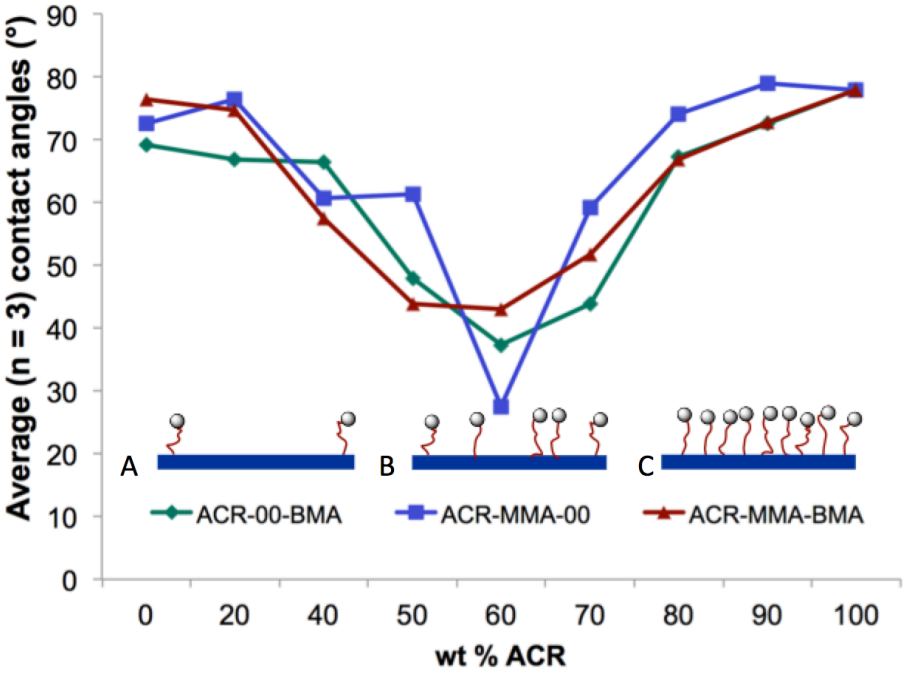

Figure 2-4. Sessile-drop contact angles obtained for the different ACR-MMA-BMA copolymers

With the exception of pure pMMA or pBMA, the average relative fluorescence (Figure 2-2) resulting from bacterial growth on the surface was higher as the fraction of ACR increased in each copolymer series. The greatest value was observed for 80 wt% ACR in the ACR-MMA series (11,778 RFUs), which was somewhat higher than the other copolymers: 8180 and 7823 RFUs for the 90 wt% polymers of ACR-BMA and ACR-MMA-BMA, respectively. The hard surfaces of pMMA and pBMA were not consistent with good bacterial adhesion. *E. coli* growth is higher on soft versus rigid surfaces,[39] possibly because the elasticity of the former allows for better interactions between material and bacterial membranes, thereby allowing better adhesion.[40-42] Surprisingly,

however, the lowest adhesion level was observed at 20 % ACR-BMA and 20 % ACR-MMA copolymers, likely because of the presence of surfactants as explained below.

In general, the normal factors associated with bacterial adhesion were observed with the ACR-MMA and ACR-BMA copolymers. Enhanced adhesion was observed with softer (and wetter) and more hydrophobic interfaces. The exceptions to this were the 20 wt% ACR polymers for the ACR-BMA and ACR-MMA copolymers, which showed the lowest RFUs (389 and 3859, respectively) of the samples tested, including pMMA and pBMA. This is of interest, because the hard, non-water wettable materials could make excellent coatings that do not promote biofilm formation.

The presence of surfactants can dramatically reduce the level of bacterial adhesion at synthetic surfaces. For example, as little as 0.002 % of non-ionic surfactants led to a 95 % reduction in adhesion of *V. proteolyrica*, *P. arlanrica*, and *V. alginolyricus* to (hydrophobic) polystyrene. This has been attributed to disruption of hydrophobic interactions with the hydrophobic surface; less significant effects were noted on high energy glass surfaces.[25] When surfactants are tethered to the surface, bacterial adhesion becomes increasingly limited as the surface density of surface-active groups increase. In the case of PEG based surfactants, this is particularly noticeable.[43]

We propose that the absence of adhesion of *E. coli* on 20 wt% ACR/acrylic surfaces is similarly a consequence of surface activity provided by low concentrations of the surfactants that disrupt hydrophobic interactions. (Note, that

the materials were extensively extracted so this effect is not a consequence of surfactant being released from these surfaces; the surfactant monomer is highly toxic to these bacteria).[44] The surface concentration of surfactant groups is insufficient to show a net change in sessile drop contact angle. However, the siloxane hydrophobe on the very mobile superwetting PEG chains can interact with the surface hydrophobes typically found on bacterial surfaces, which interrupts more enhanced binding with the pMMA or pBMA surface per se. That mobility disfavors anchoring. At much higher levels, the tethered surfactant provides multiple contact points to which attachment becomes more facile. In the limit, a hydrophobic silicone brush (sitting on a layer of hydrated PEG) presents a surface that particularly facilitates adhesion.

2.4 Conclusion

The incorporation of superwetting monomer ACR into acrylic copolymers leads to many of the expected changes in physical behaviour. With an increase in ACR concentration in the copolymer there is an increase of water uptake, decrease in hardness and, until 60 wt%, an increase in water wettability. At higher concentrations, the surface becomes more hydrophobic as silicone brush forms. All these factors lead to increasing bacterial adhesion that tracks with ACR concentration; the samples were smooth on the nm scale as shown by AFM. The exceptions were the samples of 20 % ACR-MMA and ACR-BMA which, while

exhibiting only poor wetting, were hard, did not imbibe much water yet led to very low bacterial adhesion. We ascribe this effect to weak interactions between the bacterial interface and the very mobile siloxane that prevent proper anchoring to the underlying interface. Such observations, if more general, provide a strategy to manipulate the magnitude of biofouling.

2.5 Acknowledgements

We acknowledge with gratitude the financial support of the Natural Sciences and Engineering Research Council of Canada.

2.6 References

1. H. Ammerlaan, S. Harbarth, A. Buiting, D. Crook, F. Fitzpatrick, H. Hanberger, L. Herwaldt, P. Van Keulen, J. Kluytmans and A. Kola, *Clinical infectious diseases*, 2013, **56**, 798-805.
2. C. P. Kelly and J. T. LaMont, *New England Journal of Medicine*, 2008, **359**, 1932-1940.
3. G. M. Eliopoulos, S. E. Cosgrove and Y. Carmeli, *Clinical Infectious Diseases*, 2003, **36**, 1433-1437.
4. T. C. Penna, P. G. Mazzola and A. M. S. Martins, *BMC Infect. Dis.*, 2001, **1**, 16.
5. J. Otter, K. Vickery, J. Walker, E. deLancey Pulcini, P. Stoodley, S. Goldenberg, J. Salkeld, J. Chewins, S. Yezli and J. Edgeworth, *Journal of Hospital Infection*, 2015, **89**, 16-27.
6. V. Sigler and S. Hensley, *Journal of Hospital Infection*, 2013, **83**, 253-256.
7. T. R. Garrett, M. Bhakoo and Z. Zhang, *Progress in Natural Science*, 2008, **18**, 1049-1056.
8. N. P. Boks, W. Norde, H. C. van der Mei and H. J. Busscher, *Microbiology*, 2008, **154**, 3122-3133.
9. Y. H. An and R. J. Friedman, *J. Biomed. Mater. Res.*, 1998, **43**, 338-348.
10. G. M. Bruinsma, H. C. van der Mei and H. J. Busscher, *Biomaterials*, 2001, **22**, 3217-3224.
11. H. Tang, T. Cao, X. Liang, A. Wang, S. O. Salley, J. McAllister and K. Y. S. Ng, *J. Biomed. Mater. Res. A*, 2009, **88A**, 454-463.
12. A. M. Gallardo-Moreno, M. L. González-Martín, J. M. Bruque and C. Pérez-Giraldo, *Colloids Surf. A Physicochem. Eng. Asp.*, 2004, **249**, 99-103.
13. E. W. McAllister, L. C. Carey, P. G. Brady, R. Heller and S. G. Kovacs, *Gastrointest. Endosc.*, 1993, **39**, 422-425.
14. J. Verran and R. D. Boyd, *Biofouling*, 2001, **17**, 59-71.
15. I. Yoda, H. Koseki, M. Tomita, T. Shida, H. Horiuchi, H. Sakoda and M. Osaki, *BMC Microbiology*, 2014, **14**, 234.
16. J. A. Lichter, M. T. Thompson, M. Delgadillo, T. Nishikawa, M. F. Rubner and K. J. Van Vliet, *Biomacromolecules*, 2008, **9**, 1571-1578.
17. K. N. Cowles and Z. Gitai, *Molec. Microbiol.*, 2010, **76**, 1411-1426.

18. A. Terada, A. Yuasa, T. Kushimoto, S. Tsuneda, A. Katakai and M. Tamada, *Microbiology*, 2006, **152**, 3575-3583.

19. M. Gross, S. E. Cramton, F. Götz and A. Peschel, *Infection and immunity*, 2001, **69**, 3423-3426.

20. M. Hermansson, *Colloids and Surfaces B: Biointerfaces*, 1999, **14**, 105-119.

21. B. Gottenbos, D. W. Grijpma, H. C. van der Mei, J. Feijen and H. J. Busscher, *Journal of Antimicrobial Chemotherapy*, 2001, **48**, 7-13.

22. U. Husmark and U. Rönner, *Biofouling*, 1992, **5**, 335-344.

23. P. Teixeira and R. Oliveira, *J. Adhesion Sci. Tech.*, 1999, **13**, 1287-1294.

24. E. Sinde and J. Carballo, *Food Microbio.*, 2000, **17**, 439-447.

25. J. H. Paul and W. H. Jeffrey, *Can. J. Microbiol.*, 1985, **31**, 224-228.

26. J. Treter, F. Bonatto, C. Krug, G. V. Soares, I. J. R. Baumvol and A. J. Macedo, *Appl. Surf. Sci.*, 2014, **303**, 147-154.

27. M. J. Bridgett, M. C. Davies and S. P. Denyer, *Biomaterials*, 1992, **13**, 411-416.

28. K. Vacheethasanee and R. E. Marchant, *J. Biomed. Mater. Res.*, 2000, **50**, 302-312.

29. T. Svitova, R. M. Hill, Y. Smirnova, A. Stuermer and G. Yakubov, *Langmuir*, 1998, **14**, 5023-5031.

30. P. V. Gawande, K. LoVetri, N. Yakandawala, T. Romeo, G. G. Zhanel, D. G. Cvitkovitch and S. Madhyastha, *Journal of Applied Microbiology*, 2008, **105**, 986-992.

31. V. C. Kramer, K. W. Nickerson, N. V. Hamlett and C. O'Hara, *Canadian Journal of Microbiology*, 1984, **30**, 711-713.

32. D. Porter, *Group Interaction Modelling of Polymer Properties*, Taylor & Francis, 1995.

33. J. P. Fisher, D. Dean, P. S. Engel and A. G. Mikos, *Ann. Rev. Mater. Res.*, 2001, **31**, 171-181.

34. K.-D. Ahn, C.-M. Chung and Y.-H. Kim, *J. Appl. Polym. Sci.*, 1999, **71**, 2033-2037.

35. O. Vidal, R. Longin, C. Prigent-Combaret, C. Dorel, M. Hooreman and P. Lejeune, *Journal of Bacteriology*, 1998, **180**, 2442-2449.

36. K. Sungsanit, N. Kao and S. N. Bhattacharya, *Polymer Engineering & Science*, 2012, **52**, 108-116.

37. N. Yui, R. J. Mrsny and K. Park, *Reflexive polymers and hydrogels: understanding and designing fast responsive polymeric systems*, CRC Press, 2004.

38. J. M. Harris, *Poly(Ethylene Glycol) Chemistry: Biotechnical and Biomedical Applications*, Springer, 1992.

39. F. Song and D. Ren, *Langmuir*, 2014, **30**, 10354-10362.

40. H. J. Busscher and H. C. van der Mei, *PLoS Pathogens*, 2012, **8**, e1002440.

41. I. Iscla, R. Wray and P. Blount, *Protein Science : A Publication of the Protein Society*, 2011, **20**, 1638-1642.

42. M. J. Whitfield, J. P. Luo and W. E. Thomas, *PLoS Computational Biology*, 2014, **10**, e1003971.

43. P. Kingshott, J. Wei, D. Bagge-Ravn, N. Gadegaard and L. Gram, *Langmuir*, 2003, **19**, 6912-6921.

44. M. F. Khan, L. Zepeda-Velazquez and M. A. Brook, *Colloids and Surfaces B: Biointerfaces*, 2015.

45. M. L. De Castro and L. Garcıa-Ayuso, *Analytica chimica acta*, 1998, **369**, 1-10.

46. M. Katsikogianni and Y. Missirlis, *Eur Cell Mater*, 2004, **8**, 37-57.

2.7 Appendix

2.7.1 Materials

Ethyl 4-(dimethylamino)benzoate (EDB), acryloyl chloride, butyl methacrylate (BMA), camphorquinone (CQ), diethyl ether, diethylene glycol diacrylate (DEGDA), hydroquinone monomethyl ether (MEHQ) inhibitor remover, methyl methacrylate (MMA), poly(ethylene glycol) acrylate (Mn ≈ 375) (hPEG), poly(ethylene glycol) monooleate (Mn ≈ 860), and triethylamine were purchased from Sigma Aldrich. EDB, acryloyl chloride, CQ, diethyl ether, DEGDA, MEHQ inhibitor remover, and triethylamine were used as received. MMA, BMA, PEG, poly(ethylene glycol) monooleate had the radical inhibitors removed by passage through a column packed with MEHQ inhibitor remover and stored at 2 °C until used. Silmer ACR A008-UP (ACR) was a gift from Siltech Corporation and was used as received. Photopolymerization was initiated by a blue light source, Kerber Applied Research BlueCure 25, which was graciously provided by Kerber Applied Research Inc.

2.7.2 Methods

2.7.2.1 Shore hardness measurements

Shore hardness measurements were taken using a Type OO Model 1600 Rex® Durometer purchased from Rex Gauge Company, Inc. Three small discs were punched out from the main polymer body and stacked, before the hardness reading was obtained. By stacking

them, this prevents the durometer measured only the polymer and not the metal substrate beneath.

2.7.2.2 Wettability measurements

Water contact angles measurements were obtained through manual measurements of digital images depicting the water droplets on the surface of the polymers. The images were obtained through the use of a Krüss Contact Angle Measuring Instrument G10 and the manual measurements were obtained through the use of an angling tool function in GIMP 2.6.8, a GNU image manipulation program. While monitoring the surface using the Krüss instrument, a 3 μL droplet of Milli-Q water was placed onto of the surface of the polymer being examined. A digital image of the water droplet on the surface is captured, and by using the angling tool provided by GIMP, a contact angle was determined by averaging the left and right angles of the droplet.

2.7.2.3 Soxhlet extraction

A conventional Soxhlet extractor was used to extract the unreacted material and low molecular weight oligomers from the matrix of the copolymers. The extraction solvent used was 2-propanol and the extraction process ran overnight at 90 °C following a procedure described by Luque de Castro and García-Ayuso.[45]

2.7.2.4 Surface analysis

The topographical features of the polymers were obtained using a Tescan Vega II LSU scanning electron microscope (Tescan USA, Pennsylvania, United States) operating at 10

kV. In order to optimize imaging of the pattern, the stage was slightly tilted approximately 28°.

2.7.2.5 Chemical structure analysis

^{1}H NMR data was obtained using a Bruker AVANCE 200 MHz nuclear magnetic resonance spectrometer (Bruker Corp., Milton, Canada); samples were measured in deuterated chloroform.

2.7.2.6 Mass determination

The mass spectrum of the oPEG monomer was obtained using a Waters/Micromass Global Q-TOF (Quadrupole-Time of Flight) mass spectrometer. The sample was run in ESI(+ve) mode at 6000 mass resolution.

2.7.2.7 Bacterial adhesion studies

LB agar plates were created using 10 g of tryptone, 5 g of yeast extract, 10 g of NaCl, 15 g of agar and 1 L of distilled water (dH_2O). The dry ingredients were measured into a 2 L Erlenmeyer flask followed by 500 mL of dH_2O and the mixture was stirred to achieve complete solvation of the starting materials. The agar was added along with the rest of the H_2O before the solution was autoclaved. Following autoclaving, approximately 12 mL of the media were transferred into a dish in a laminar flow hood and the process was continued until all the media had been utilized. The media in the dishes was left to solidify for 30 min, after which the capped plates were stacked in their original packaging, sealed and stored at 4 °C until further use. LB media for culturing E. coli in solution was

made in the same manner with the exception of agar. The autoclaved solution was sealed and stored at room temperature. The protocol for the adhesion assay was based on published results [10, 46]. Exactly 100 μL of *E. coli* culture broth were streaked on an agar plate that was incubated overnight. Multiple colonies (3-4) were obtained from the resultant lawn using an autoclaved pipette tip and a new vial of broth (200 mL) was inoculated. This vial was placed in an incubator from where 1 mL aliquots were taken every 30 min to measure the OD_{600} of the solution. Once the OD_{600} value reached 0.7, 0.5-1 mM, IPTG was added to the vial, which was incubated for 5-6 h. E. coli from the vial was filtered using a cellulose acetate filter 0.45 microns (37 mm diameter) and the filter paper was washed thrice with autoclaved 0.9% PBS into new vial. 100 mL of PBS were added to the vial, which was supplemented with 2% w/v nutrient broth. The solution was agitated to facilitate equal dispersion of E. coli. Copolymer coupons (n = 4 for each type) were placed in a 48- well polystyrene, flat- bottom plate and to each polymer-containing well, 400 μL of the broth-supplemented E. coli mixture were added. The plate was incubated overnight (12 h), after which each coupon was removed from its well using sterile forceps, rinsed thrice with autoclaved PBS and placed in a well of a fresh plate. A microplate reader (Gemini XPS) was used to obtain GFP fluorescence readings using an excitation and emission wavelength of 395 nm and 509 nm, respectively, from the rinsed polymer coupons in the new plate. The procedure was repeated for hydrated coupons (coupons that had been soaked in dH_2O for 30 min prior to incubation with 400 μL of broth-supplemented E. coli in PBS). The fluorescence readings for each set were plotted for comparison after the background fluorescence (reading from a sample of each type

incubated with uninduced E. coli) had been subtracted. Readings for the dry set were also plotted against the average percent water uptake and the sessile drop contact angles to determine the correlation, if any, between the three different variables.

2.7.2.8 Synthesis of oPEG

To a stirring and sealed 500 mL round-bottomed flask, under nitrogen, was added poly(ethylene glycol) monooleate (9.04 g, 0.011 mol, 1.0 eq, Mn ≈ 860) and dry diethyl ether (250 mL). Once the mixture was homogenized, triethylamine (7.33 mL, 0.053 mol, 5.0 eq) was slowly introduced to the reaction. Then, while stirring vigorously, acryloyl chloride (1.70 mL, 0.021 mol, 2.0 eq) was slowly introduced dropwise to the reaction mixture. A white precipitate formed instantaneously when acryloyl chloride was added to the mixture. After stirring overnight, solvents were removed using evaporation under reduced pressure until a thick, viscous slushy residue remained. The residue was diluted with diethyl ether and filtered through a pad of Celite using vacuum filtration to collect the product. The process was repeated 3 times. The ether extracts were dried over magnesium sulfate and, after filter, the solvents were removed obtain the purified oPEG monomer (9.162 g, 91.62 %).

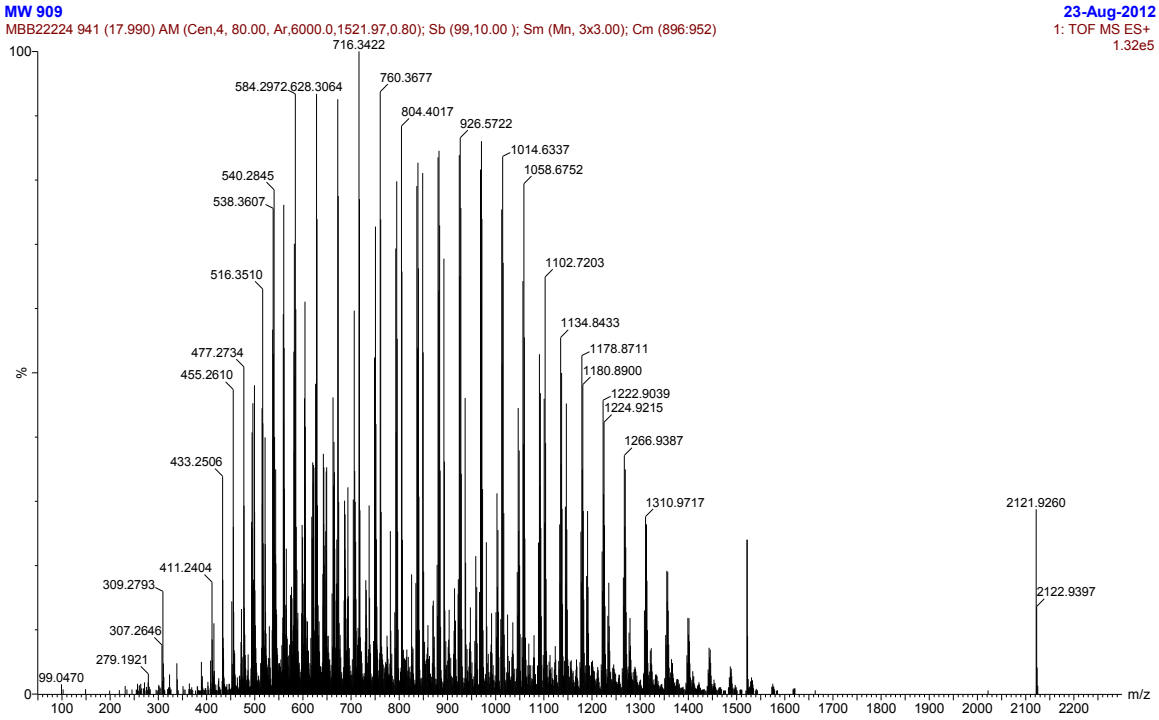

Figure 2-5. Mass spectrum of oPEG

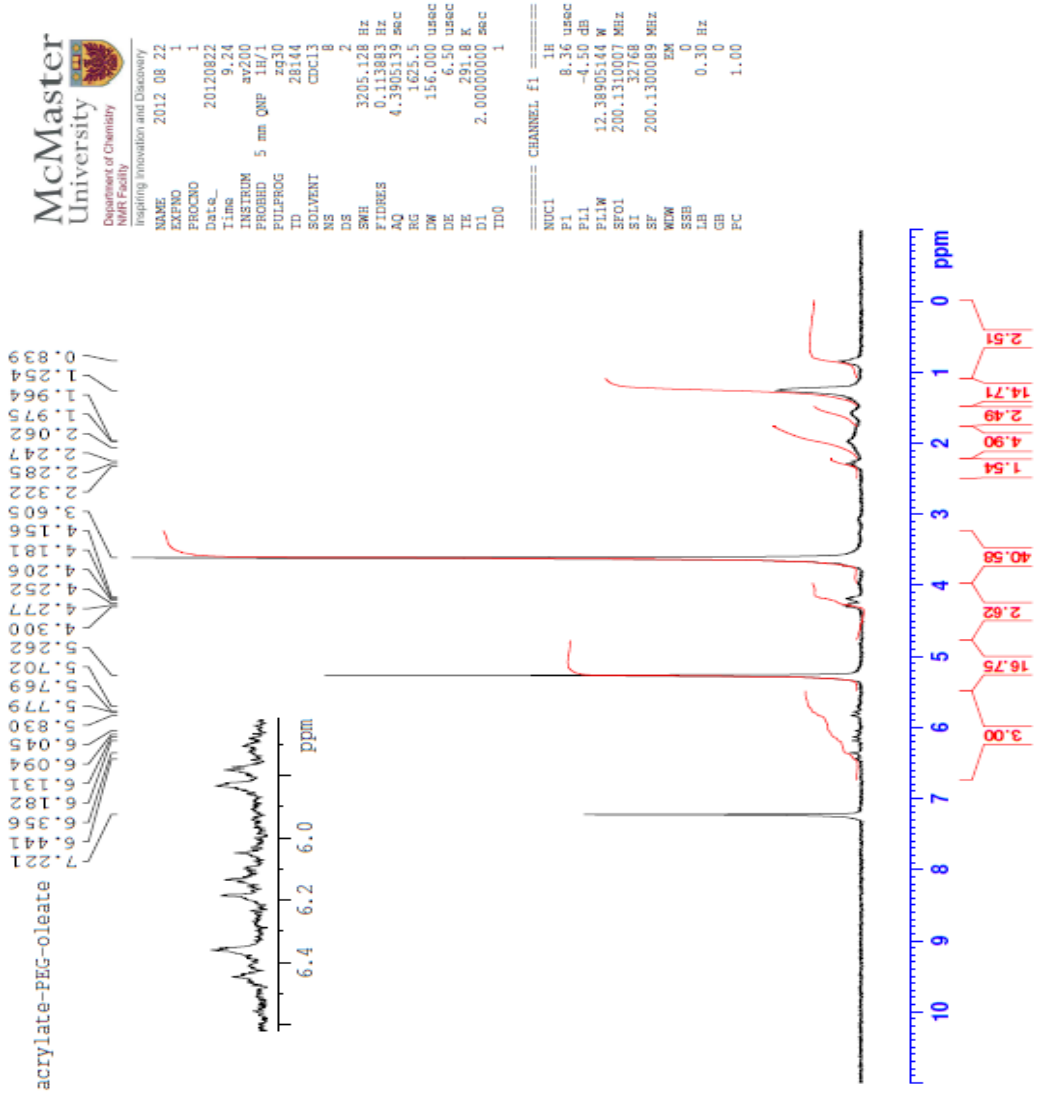

Figure 2-6. The NMR spectrum of oPEG monomer

2.7.2.9 Polymer synthesis

As the syntheses of the various polymers are similar, differing only by the natures of the monomers ACR, hPEG, or oPEG, and quantities added (Table 2-1), a general

procedure will be described. All polymers synthesized were formed using a total of 2 g of monomers, contained 1 wt% CQ and 1 wt% EDB as the photoinitiating system, 1 wt% DEGDA as the crosslinker, and all monomers in their respective weight percent ratios.

2.7.2.10 Synthesis of ACR-MMA-BMA polymers

CQ (0.02 g, 1 wt%) and EDB (0.02 g, 1 wt%) were weighed into a 10 mL glass test tube. Uninhibited MMA and BMA were added to the test tube followed by the addition of DEGDA (0.02 g, 1 wt%). The reaction mixture was stirred gently to facilitate the dissolution of the solid reagents to give a homogeneous solution. ACR was then added. After the mixture was thoroughly mixed, it was golden yellow in color. The reaction mixture was deoxygenated by bubbling nitrogen gas, through a glass pipette into the solution for 30 s, and then poured into a small Teflon-lined plastic Petri dish and irradiated for 1 h. Solutions with greater percentages of ACR were found to cure more slowly. The solid elastomer was then removed from the Teflon-lined Petri dish and soaked in 2-propanol (40 mL) overnight. The elastomer was removed and dried in a vacuum oven (50 °C, 500 mm Hg) overnight to afford the final product.

Table 2-1. Formulation for ACR-MMA-BMA polymers

CQ (g)	EDB (g)	ACR (g)	MMA (g)	MMA (uL)	BMA (g)	BMA (uL)	DEGDA (g)	DEGDA (µL)
0.02	0.02	0.8	1.2	1282.1	0	0.0	0.02	13.7
0.02	0.02	0.9	1.1	1175.2	0	0.0	0.02	13.7
0.02	0.02	1	1	1068.4	0	0.0	0.02	13.7
0.02	0.02	1.1	0.9	961.5	0	0.0	0.02	13.7
0.02	0.02	1.2	0.8	854.7	0	0.0	0.02	13.7
0.02	0.02	1.3	0.7	747.9	0	0.0	0.02	13.7
0.02	0.02	1.4	0.6	641.0	0	0.0	0.02	13.7
0.02	0.02	1.5	0.5	534.2	0	0.0	0.02	13.7
0.02	0.02	1.6	0.4	427.4	0	0.0	0.02	13.7
0.02	0.02	1.7	0.3	320.5	0	0.0	0.02	13.7
0.02	0.02	1.8	0.2	213.7	0	0.0	0.02	13.7
0.02	0.02	1.9	0.1	106.8	0	0.0	0.02	13.7
0.02	0.02	0.8	0	0.0	1.2	1345.3	0.02	13.7
0.02	0.02	0.9	0	0.0	1.1	1233.2	0.02	13.7
0.02	0.02	1	0	0.0	1	1121.1	0.02	13.7
0.02	0.02	1.1	0	0.0	0.9	1009.0	0.02	13.7
0.02	0.02	1.2	0	0.0	0.8	896.9	0.02	13.7
0.02	0.02	1.3	0	0.0	0.7	784.8	0.02	13.7
0.02	0.02	1.4	0	0.0	0.6	672.6	0.02	13.7
0.02	0.02	1.5	0	0.0	0.5	560.5	0.02	13.7
0.02	0.02	1.6	0	0.0	0.4	448.4	0.02	13.7
0.02	0.02	1.7	0	0.0	0.3	336.3	0.02	13.7
0.02	0.02	1.8	0	0.0	0.2	224.2	0.02	13.7
0.02	0.02	1.9	0	0.0	0.1	112.1	0.02	13.7
0.02	0.02	0.8	0.6	641.0	0.6	672.6	0.02	13.7
0.02	0.02	0.9	0.55	587.6	0.55	616.6	0.02	13.7
0.02	0.02	1	0.5	534.2	0.5	560.5	0.02	13.7
0.02	0.02	1.1	0.45	480.8	0.45	504.5	0.02	13.7
0.02	0.02	1.2	0.4	427.4	0.4	448.4	0.02	13.7
0.02	0.02	1.3	0.35	373.9	0.35	392.4	0.02	13.7
0.02	0.02	1.4	0.3	320.5	0.3	336.3	0.02	13.7
0.02	0.02	1.5	0.25	267.1	0.25	280.3	0.02	13.7
0.02	0.02	1.6	0.2	213.7	0.2	224.2	0.02	13.7
0.02	0.02	1.7	0.15	160.3	0.15	168.2	0.02	13.7
0.02	0.02	1.8	0.1	106.8	0.1	112.1	0.02	13.7
0.02	0.02	1.9	0.05	53.4	0.05	56.1	0.02	13.7

Through NMR studies, both the oligomers (from the extracted material) and the polymers contained monomers whose molar ratios reflected the molar ratios of the monomers in the starting material (Table 2-2, Table 2-3).

Table 2-2. Ratio of Monomers Incorporated into Oligomers of the Extracted Material[‡]

Weight Ratio of Monomers		**Theoretical Ratio of Monomers Incorporated into Polymer**		**Measured Ratio of Monomers Incorporated into Oligomer**		**Relative Integrations**	
%wt ACR	%wt BMA	ACR	BMA	ACR	BMA	ACR	BMA
60	40	1.00	3.63	1.00	1.88	51.80	18.87
80	20	1.00	1.36	1.00	2.27	64.67	27.94

[‡] To see the constitution of the crosslinked polymer, please see Table 2-4.

Table 2-3. Ratio of Monomers Incorporated into Polymers[§]

Weight Ratio of Monomers			**Theoretical Ratio of Monomers Incorporated into Polymer**			**Measured Ratio of Monomers Incorporated into Polymer**		
%wt ACR	%wt MMA	%wt BMA	ACR	MMA	BMA	ACR	MMA	BMA
40	60	0	1.00	11.61	0.00	1.00	13.39	0.00
40	30	30	1.00	5.81	4.09	1.00	7.42	8.09
40	0	60	1.00	0.00	8.18	1.00	0.00	6.84
60	40	0	1.00	5.16	0.00	1.00	4.56	0.00
60	20	20	1.00	2.58	1.82	1.00	4.53	3.02
60	0	40	1.00	0.00	3.63	1.00	0.00	5.64
80	20	0	1.00	1.94	0.00	1.00	3.17	0.00
80	10	10	1.00	0.97	0.68	1.00	2.33	1.00
80	0	20	1.00	0.00	1.36	1.00	0.00	2.29

Continued from Above

Weight Ratio of Monomers			**Relative Integrations**[**]		
%wt ACR	%wt MMA	%wt BMA	ACR	MMA	BMA
40	60	0	21.00	40.18	-
40	30	30	21.00	22.25	32.34
40	0	60	21.00	-	27.36
60	40	0	21.00	13.67	-
60	20	20	21.00	9.05	18.10
60	0	40	21.00	-	22.54
80	20	0	21.00	9.52	-
80	10	10	21.00	7.49	3.83
80	0	20	21.00	-	9.14

[§] To see the constitution of the oligomers from extracted from select samples, please see Table 2-3.

2.7.2.11 Synthesis of hPEG-MMA-BMA polymers

The synthesis of hPEG-MMA-BMA polymers were similar to the general procedure above except that hPEG was used instead of ACR.

Table 2-4. Formulation for hPEG-MMA-BMA Polymers

CQ (g)	EDB (g)	hPEG (g)	MMA (g)	MMA (uL)	BMA (g)	BMA (uL)	DEGDA (g)	DEGDA (µL)
0.02	0.02	1.6	0.4	427.4	0	0.0	0.02	13.7
0.02	0.02	1.2	0.8	854.7	0	0.0	0.02	13.7
0.02	0.02	0.8	1.2	1282.1	0	0.0	0.02	13.7
0.02	0.02	0.4	1.6	1709.4	0	0.0	0.02	13.7
0.02	0.02	0	2	2136.8	0	0.0	0.02	13.7
0.02	0.02	1.6	0	0.0	0.4	448.4	0.02	13.7
0.02	0.02	1.2	0	0.0	0.8	896.9	0.02	13.7
0.02	0.02	0.8	0	0.0	1.2	1345.3	0.02	13.7
0.02	0.02	0.4	0	0.0	1.6	1793.7	0.02	13.7
0.02	0.02	0	0	0.0	4	4484.3	0.02	13.7
0.02	0.02	1.6	0.2	213.7	0.2	224.2	0.02	13.7
0.02	0.02	1.2	0.4	427.4	0.4	448.4	0.02	13.7
0.02	0.02	0.8	0.6	641.0	0.6	672.6	0.02	13.7
0.02	0.02	0.4	0.8	854.7	0.8	896.9	0.02	13.7
0.02	0.02	0	1	1068.4	1	1121.1	0.02	13.7

2.7.2.12 Synthesis of oPEG-MMA-BMA polymers

The synthesis of oPEG-MMA-BMA polymers was essentially identical to that of ACR-containing materials. The main difference was that oPEG was used instead of ACR.

Table 2-5. Formulation for oPEG-MMA-BMA Polymers

CQ (g)	EDB (g)	oPEG (g)	MMA (g)	MMA (uL)	BMA (g)	BMA (uL)	DEGDA (g)	DEGDA (µL)
0.02	0.02	2	0	0.0	0	0.0	0.02	13.7
0.02	0.02	1.2	0.8	854.7	0	0.0	0.02	13.7
0.02	0.02	0.6	1.4	1495.7	0	0.0	0.02	13.7
0.02	0.02	0	2	2136.8	0	0.0	0.02	13.7
0.02	0.02	2	0	0.0	0	0.0	0.02	13.7
0.02	0.02	1.2	0	0.0	0.8	896.9	0.02	13.7
0.02	0.02	0.6	0	0.0	1.4	1569.5	0.02	13.7
0.02	0.02	0	0	0.0	2	2242.2	0.02	13.7
0.02	0.02	2	0	0.0	0	0.0	0.02	13.7
0.02	0.02	1.2	0.4	427.4	0.4	448.4	0.02	13.7
0.02	0.02	0.6	0.7	747.9	0.7	784.8	0.02	13.7
0.02	0.02	0	1	1068.4	1	1121.1	0.02	13.7

CHAPTER 3: Tunable, Antibacterial Activity of Silicone Polyether Surfactants[††]

3.1 Abstract

Silicone surfactants are used in a variety of applications, however, limited data is available on the relationship between surfactant structure and biological activity. A series of seven nonionic, silicone polyether surfactants with known structures was tested for *in vitro* antibacterial activity against *Escherichia coli* BL21. The compounds varied in their hydrophobic head, comprised of branched silicone structures with 3-10 siloxane linkages and, in two cases, phenyl substitution, and hydrophilic tail of 8-44 poly(ethylene glycol) units. The surfactants were tested at three concentrations: below, at, and above their Critical Micelle Concentrations (CMC) against 5 concentrations of *E. coli* BL21 in a three-step assay comprised of a 14- 24 h turbidometric screen, a live-dead stain and viable colony counts. The bacterial concentration had little effect on antibacterial activity. For most of the surfactants, antibacterial activity was higher at concentrations above the CMC. Surfactants with smaller silicone head groups had as much as 4 times the

---

[††] This chapter is taken from M. F. Khan, L. Zepeda-Velazquez and M. A. Brook, *Colloids and Surfaces B: Biointerfaces*, **2015**, *132*, 216- 224, and is reproduced by the permission of Elsevier. Zepeda-Velazquez performed the CMC experiments, while Khan developed all experimentation, and conducted biological work and analyses. Khan wrote the manuscript with additions, edits and guidance from Brook.

bioactivity of surfactants with larger groups, with the smallest hydrophobe exhibiting potency equivalent to sodium dodecyl sulfate (SDS). Smaller PEG chains were similarly associated with higher potency. These data link lower micelle stability and enhanced permeability of smaller silicone head groups to antibacterial activity. The results demonstrate that simple manipulation of nonionic silicone polyether structure leads to significant changes in antibacterial activity.

3.2 Introduction

Silicone surfactants find applications in areas ranging from polyurethane foam stabilization[1] to facilitating delivery of agricultural active ingredients,[2] including herbicides.[3] Agricultural adjuvants, **1**, known colloquially as superwetters, are low molecular weight compounds comprised of a trisiloxane head group and low molecular weight oligomeric poly(ethylene glycols)(PEG) of low polydispersity index: different manufacturers place different chemical groups at the PEG terminus. By contrast, higher molecular weight silicone surfactants, such as dimethicone copolyol (DC3225C) **2** and related rake, AB, or ABA block copolymers are complex oligomeric or polymeric materials with broad molecular weight distributions (Figure 3-1). The combination of low surface energy and high mobility of the silicone constituents gives these surfactants unusual properties not possessed by organic derivatives.

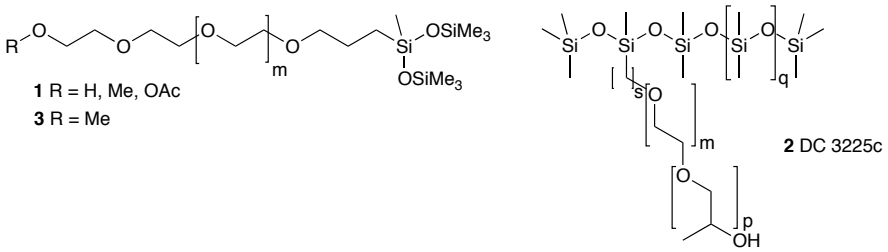

Figure 3-1. Structures of superwetters and a rake silicone surfactant

It is known that some silicones, including superwetters, exhibit biological activity. Several studies have reported the toxicity of superwetters to fruit fly larvae,[4] some aphids,[5-7] citrus leafminers,[8] and armyworm larvae,[4, 9] among others. An interesting comparison of three related silicone surfactants showed that spider mites responded quite differently to different surfactant chemical structures. The superwetter with the smallest hydrophobic head group of the three siloxane polyalkylenoxide copolymers, Silwet L-77, **3** was highly toxic, while L-7607 was less so, and L-7200 was nontoxic (the structures of the latter two compounds are not publicly available, but the authors rely on the description in the paper confirming they have larger, hydrophobic head groups).[10] Enhanced biological activity was related to the surface activity: lower surface activity surfactants with larger head groups were less toxic to the mites.

This structure-function relationship for silicone surfactants has not been examined in detail, but is important to study, both because the materials are so widely used in commerce and because the little available information suggests the biological activity is tunable. One application that could benefit from surfactants with species-specific potency is the development of antibacterial materials (substances that kill bacteria or inhibit their

growth)[11] for hospitals. Death caused by the increasing prevalence of *Clostridium difficile* and *Methicillin-resistant Staphylococcus aureus* (*MRSA*) in hospitals,[12] for example, is an important challenge of the 21st century. The issue is caused, in part, by the overuse of broad-spectrum antimicrobials in surface disinfection protocols,[13] which can lead to transferrable resistance from non-target bacteria to problematic analogues.[14,15] Hence, compounds like Silwet L-77 that have shown selective toxicity to biological organisms may be promising lead candidates for antibacterials, particularly on surfaces.

Recently, we reported the synthesis of a series of closely related silicone surfactants.[16] The hydrophilic tails were methyl-terminated, low polydispersity $(PEG)_{44}$ or $(PEG)_{15}$ polyethers. However, the silicone head groups varied in size, number of silicone groups and number of phenyl groups. We were interested in exploring the changes in biological activity that accompanied the structural and surface activity differences between the surfactants against *Escherichia coli* (*E. coli*). This bacterium serves as a convenient material for a preliminary assessment of bioactivity. Once aspects of the biological activity of these surfactants are determined, then applications can be considered. Surfactants that do not significantly affect organisms can be considered for use as formulations aids. By contrast, those that are toxic to bacteria might have utility in cleaning/disinfecting protocols, but only after their toxicity to mammalian cells is determined. A commercial superwetting material **ACR-008 UP** (Figure 3-2) was used as a positive control.

3.3 Experimental section

3.3.1 Materials

Compounds **Si10-PEG44**, **Si4Ph6-PEG44**, **Si7-PEG15**, **Si7-PEG44**, **Si4Ph3-PEG15**, **Si4Ph3-PEG44** and **Si4-PEG44** (nomenclature: **Si*X***, where **X** is the number of siloxane units; if Si phenyl groups are present their number is indicated with **Ph*Y***, **Y** = 3,6; **PEG*ZZ***, where **ZZ** is the number of OCH_2CH_2 units in the surfactant) were prepared following the procedure of Grande et al.[16] Siltech Corp provided **ACR-008 UP**. These surfactants were used as received. Poly(ethylene glycol) methyl ether (PEG) of ~M_n 2,000, and SDS were purchased from Sigma Aldrich and Bioshop Inc., respectively. Sodium phosphate dibasic heptahydrate ($Na_2HPO_4 \cdot 7H_2O$), sodium phosphate monobasic ($NaH_2PO_4 \cdot H_2O$) and sodium chloride (NaCl) were purchased from Fisher Scientific, EMD Chemicals Inc. and Caledon Laboratories Ltd. respectively. *Escherichia coli* (*E. coli*) BL21(DE3)pLyS was obtained from the Promega Corporation. Bacto ™ yeast extract, Difco ™ granulated agar, and Bacto ™ tryptonewere purchased from Becton, Dickinson and Company (BD). A live-dead *Bac*light™ Bacterial Viability kit (L-7012) was acquired from Invitrogen's Life Technologies.

3.3.2 Stock reagents

Luria-Bertani (LB) agar plates were created using 10 g of tryptone, 5 g of yeast extract, 10 g of NaCl, 15 g of agar and 1 L of deionized water (dH_2O), in accordance with accepted protocols.[17] Note, no antibiotics were added to the mixture since the general

antibacterial activity of surfactants was being tested. Fresh plates were made periodically - typically one day before the start of antibacterial testing - and sealed and stored in their original packing at 4 °C until needed. One litre stock solutions each of LB media (same recipe as for agar plates minus the agar) and 0.9% PBS (2.21 g of $NaH_2PO_4 \cdot H_2O$, 11.26 g of $Na_2HPO_4 \cdot 7H_2O$, 9 g of NaCl, 1 L dH_2O [pH 7.4]) were made, sealed, autoclaved and stored at room temperature. The sterility of all materials, including pipette tips and microtubes, was maintained throughout, with all work conducted aseptically in a biosafety cabinet (BSC).

3.3.3 Microplate set-up

In scaling down from conventional microbiological practices to 96-well plates, optimization of assay parameters and instrument settings was critical to ensure data quality, reliability and reproducibility.[18] The variables optimized for *E. coli* growth in a clear, TC-treated 96-well microplate using the TECAN Infinite® M200 PRO multimode reader plate reader included agitation, headspace and evaporation (Appendix, section 3.9). Based on the optimization data, a 50% working volume in a lid-covered 96-well microplate agitated at amplitude 3 of the plate reader was selected for use. The working volume dictated the individual well compositions (5 µL of *E. coli* suspension, 87.5 µL of LB media, and 92.5 µL of PBS + surfactant (controls lacked a surfactant)). Increasing surfactant concentrations (with positive and negative controls) along the abscissa and decreasing *E. coli* concentrations along the ordinate of each plate (Supporting Information) were used to determine the effect of varying surfactant and *E. coli*

concentration on antibacterial activity (two additional replicates of the test zone were accommodated in each plate per surfactant. A total volume of 2 mL was required for each surfactant at each concentration to permit these multiple experiments to be performed.

3.3.4 Surfactant solutions and CMC determination

Two parallel series of surfactant candidates were used for antibacterial testing (Figure 3-2). Solutions of each surfactant were prepared in *HPLC* grade water (Fisher UK). Solutions were prepared to obtain final concentrations within the range of 0.0005 to 4 mM. Surfactants were weighed into polyethylene cups and dissolved in water on a shaker. Serial dilutions afforded solutions within the desired concentration range. CMC data for these surfactants were acquired using a ThermoCahn Radian Series 300 tensiometer fitted with a platinum du Noüy ring (bolded values) and the standard pendant drop method.[16] Surface tension measurements were performed in triplicate for each surfactant solution and the du Noüy ring was cleaned between measurements by heating to white-hot in a flame. Static critical micelle concentrations were determined by plotting average surface tension against the logarithm of surfactant concentration. Data were fitted using linear regression analysis in Microsoft Excel and the intercept between curves plotted before and after micelle formation (as evident by a change in surface tension) was taken to be the critical micelle concentration.

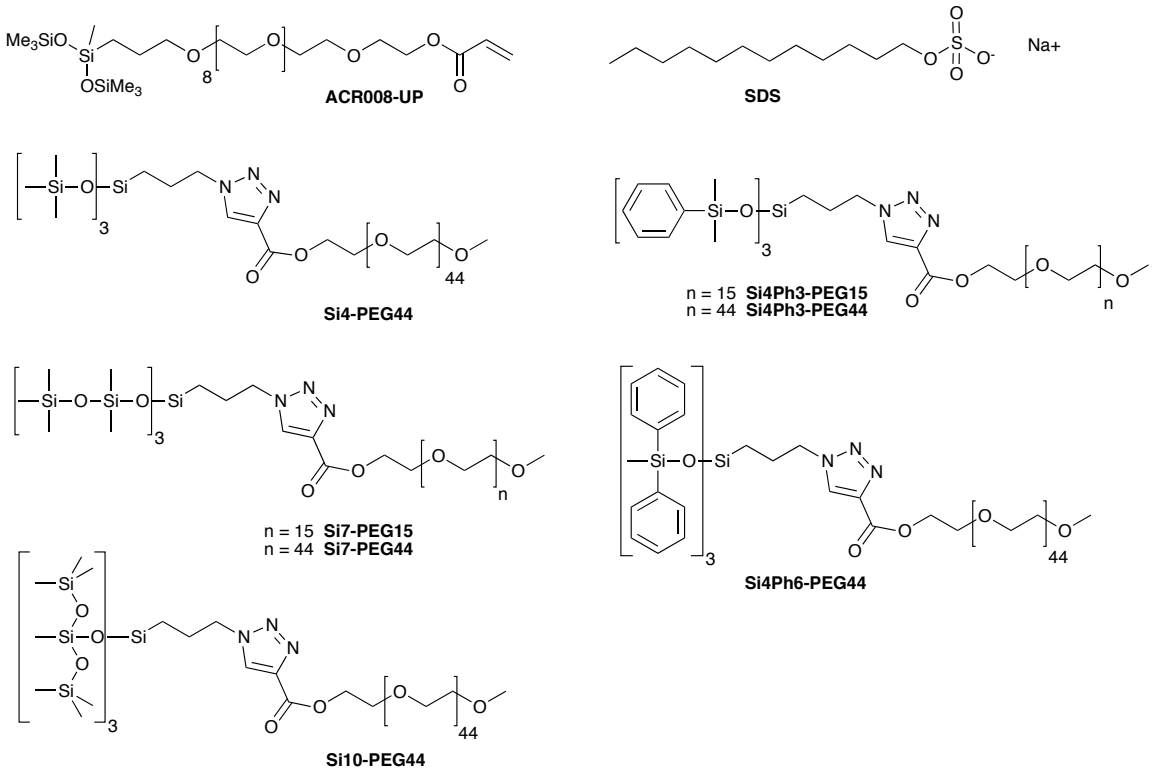

Figure 3-2. Nonionic silicone polyether surfactants screened for biocidal behavior

Toxicity tests were performed at concentrations both below (isolated surfactant molecules), at, and above (surfactant aggregates) the critical micelle concentrations (CMC[19, 20]). The CMC values, 3D Hydrophilic-Lipophilic Balance (HLB) values, along with the calculated masses needed for each surfactant to be at its CMC in 2 mL of autoclaved Phosphate Buffered Saline (PBS), are indicated in Table 3-1. The weight/volume percents (w/v %) thus acquired were used to select weight percentages

needed for each surfactant to be below or above its CMC (0.001 and 2.5 w/v % respectively) (Appendix, Table 3-2).

Table 3-1. Physical characteristics and quantities of surfactants required for antibacterial testing.

Cmpd	**MW (g/mol)**	**3D HLBs [21]**	**CMC (M)**	**W/V% at CMC**	**Moles (<CMC)[a]**	**Moles (at CMC)**	**Moles (>CMC) ***
Si10-PEG44	2891.15	(13.92, 0.95)	**5.0×10^{-5}**	0.01	6.9×10^{-9}	1.0×10^{-7}	1.7×10^{-5}
Si4Ph6-PEG44	2818.65	(14.29, 4.25)	8.3×10^{-5}	0.024	7.1×10^{-9}	1.6×10^{-7}	1.8×10^{-5}
Si7-PEG15	1045.00	(10.58, 1.97)	5.0×10^{-7}	5.2×10^{-5}	--	1.0×10^{-9}	4.8×10^{-5}
Si7-PEG44	2668.68	(15.08, 1.02)	0.9×10^{-3}	0.24	7.5×10^{-9}	1.8×10^{-6}	1.9×10^{-5}
Si4Ph3-PEG15	1281.00	(10.88, 5.45)	7.2×10^{-5}	0.009	1.6×10^{-8}	1.4×10^{-7}	3.9×10^{-5}
Si4Ph3-PEG44	2632.43	(15.31, 2.80)	4.0×10^{-5}	0.01	7.6×10^{-9}	8.0×10^{-5}	1.9×10^{-5}
Si4-PEG44	2446.22	(16.46, 1.12)	1.2×10^{-3}	0.29	8.2×10^{-9}	2.4×10^{-6}	2.1×10^{-5}
ACR008 UP	686.00	(12.0, 5.58)	1.5×10^{-4}	0.001	2.9×10^{-8}	2.9×10^{-7}	7.3×10^{-5}

[a] The weight percentages of surfactants used at <CMC and >CMC were 0.001 and 2.5 w w/v % respectively, while the moles at each concentration are indicative of the final amounts of surfactant in contact with *E. coli.*

3.3.5 *E. coli* BL21 solutions

A glycerol-containing *E. coli* stock solution was brought to room temperature before 50 µL were streaked onto an agar plate and incubated at 37 °C overnight. Two to three colonies from this plate were aseptically transferred into 5 mL of autoclaved LB media, and the tube was incubated at 37 °C for ~ 12 h in a MaxQ8000 Orbital shaker set at 250 rpm. Subsequently, 50 µL of the overnight growth was plated and incubated while the rest was used to create diluted solutions of *E. coli* (1 mL each of undiluted overnight culture, 1/50, 1/100, 1/200 and 1/500 of the overnight suspension in graduated microtubes using fresh LB media. Once prepared, the tubes were placed on ice to retard *E. coli* growth during microplate set-up. The OD_{670} of each was obtained using the TECAN Infinite M200 plate reader so that subsequent preparations of *E. coli* could be adjusted to the same optical density. (The entire process was repeated three times to obtain an average of the starting *E. coli* concentration, which was 2×10^9 cfu/mL). From each of the 1/50, 1/100, 1/200 and 1/500 solutions, 5 µL was used in the appropriate well according to the microplate setup described above. Since each well already contained 180 µL of other solutions (PBS + LB media) the bacteria underwent an additional 1/36 dilution. The actual concentrations of bacteria exposed to the surfactants were therefore calculated by applying a multiple of the dilution factors (e.g. 1/50 x 1/36) to 2×10^9 cfu/mL to yield 1×10^6 cfu/mL, 5×10^5 cfu/mL, 2.7×10^5 cfu/mL and 1×10^5 cfu/mL. Fresh 1 mL solutions of *E. coli* were used for each plate.

3.3.6 Controls

A 0.1 w/v % stock solution of SDS in autoclaved PBS was used as a positive control to gauge the efficacy of each surfactant as a potential antibacterial agent: SDS is a highly potent anionic surfactant known to exhibit antibacterial activity[22, 23] at concentrations ≥ 0.1 %.[24] Negative controls included the use of 0.1% poly(ethylene glycol) methyl ether (PEG) (i.e., the backbone of the surfactants minus the 'active' silicone head group), and *E. coli* growing in the absence of any treatment.

3.3.7 Live-Dead stain

The stain was prepared only when needed in a dark BSC, given its susceptibility to photobleaching,[25] and in the exact amounts required based on the 1:1 ratio of stain: bacteria suspension recommended by the manufacturer for reliable fluorescence readings in a microplate.[25] Briefly, the component dyes (SYTO 9 dye, 3.34 mM (25.2 µL) and propidium iodide, 20 mM (25.2 µL) were thawed from -20 °C (storage) to room temperature, mixed in a 2 mL microtube, then transferred to filter-sterilized dH_2O in a borosilicate glass culture tube for a final volume of 8.4 mL. The tube was wrapped in foil to further prevent photodegradation prior to use.

3.3.8 Protocol for screening antibacterial activity

Testing of biocidal activity for each surfactant was a 3-step process that is detailed below and summarized diagrammatically in the Appendix, Figure 3-12.

3.3.8.1 Turbidometric screen: growth in the presence of treatment:

The prepared solutions of *E. coli,* surfactants and controls were used to fill the microplate as shown in the Appendix, Figure 3-11. The plate was then placed in the M200 plate reader for a 14-20 h incubation period (37 °C, multiple reads/well (3 x 3), orbital shaking at amplitude 3 with 100 ms of settle time prior to OD_{670} measurements every 30 min). After incubation, the plate was placed on ice. The contents of each of the 90-96 wells (depending on the surfactant used) were transferred into correspondingly labeled 2.0 mL flat-top microtubes and centrifuged at 5000 g for 5 min. The supernatant was discarded and the pellet was resuspended with gentle vortexing (5-6 s, speed 2) in 185 µL of autoclaved PBS. After an additional wash step (centrifugation and resuspension), the tubes were placed on ice in preparation for the subsequent steps.

3.3.8.2 Live Dead stain after treatment removal

Upon preparation of the stain (as described above), 92.5 µL from each of the tubes from step 1 were transferred into the corresponding wells of a fresh BD Falcon 96-well, clear-bottom black plate. A fresh pipette tip was used to add 92.5 µL of stain to each well followed by mixing via thrice forward pipetting. Care was taken to work in a dark BSC. Once all the wells had received the dye, the microplate was covered with its lid and aluminum foil for 15 min of incubation at RTP. The bottom-read fluorescence intensity from each well was measured after gain optimization in the same Infinite® M200 PRO plate reader with an excitation wavelength of 485 nm and emission wavelengths of 530

nm (live) then 630 nm (dead). The ratio of live:dead fluorescence counts was plotted (Figure 3-3- Figure 3-6).

3.3.8.3 Plating the treatment after removal to determine viable concentrations

For the first three surfactants tested (**Si10-PEG44**, **Si7-PEG44**, **Si4-PEG44**), 10 μL of the remaining *E. coli* in PBS from the microtubes used in step 2 were serially diluted in fresh autoclaved tubes by 10^{-4} and 10^{-6} using PBS. After vortexing the tube contents (15 s, speed 2), 50 μL of the 10^{-4} and 10^{-6} dilutions for each of the 90-96 wells was spread onto pre-prepared Petri-dishes of LB agar. The plates were incubated at 37 °C for ~ 12 h before being photographed and refrigerated at 4 °C. Colony counts were obtained from the images thus obtained, while counts of colonies <20 or >200 were not included in the final analyses. Based on these preliminary results, for subsequent surfactants only 10 μL of 10^{-5} dilutions were plated, with half a Petri-dish/well, since 10^{-5} dilutions were deemed to produce an adequate number of countable colonies. For these plates, colonies < 5 and >200 were not analyzed. The 3-step process was repeated for each of the surfactants tested.

3.4 Results

The 3D HLB (hydrophilic-lipophilic balance) values[16, 21] of the surfactants tested ranged from (10.88, 5.45) for **Si4Ph3-PEG15** to (16.46, 1.12) for **Si4-PEG44** (the first number refers to the weight fraction of the surfactant that is water soluble, and most closely correlates with traditional HLB values). For comparison, the non-ionic surfactant

Tween® 80 (polyoxyethylene sorbitan monooleate) has an HLB of 15.0). Such values suggest the surfactants should have good solubility in aqueous solutions. Experimentally, each surfactant (most of which were solid at room temperature) required a 15-90 min dissolution/dispersion time in PBS, with higher dissolution/dispersion times required for surfactants with larger hydrophobic head groups. For example, **Si10-PEG44** required more time with vortexing to achieve a homogenous solution than **Si4-PEG44**. The dispersions formed from surfactants above their CMCs were typically milky-white and did not phase separate after 30 min of sitting once stirring was stopped.

E. coli at concentrations ranging from 1.0×10^5 to 2×10^9 cfu/mL were exposed to surfactant solutions below, at or above their CMC values, respectively. Results from each step of the assay are shown for a sample surfactant (**Si7-PEG44**) in Figure 3-3 (for raw data in this format for the remaining surfactants, see Appendix, section 3.9.4). The primary analysis of surfactant activity was based on the live-dead stain data, which provided information both about the presence/ absence of antibacterial activity and its nature (inhibitory/ lethal).

Several features about the response of the *E. coli* to the surfactants may be seen from Figure 3-3. We examine the effect of bacteria concentration and of surfactant concentration first, and then consider the specific responses of *E. coli* to specific surfactants.

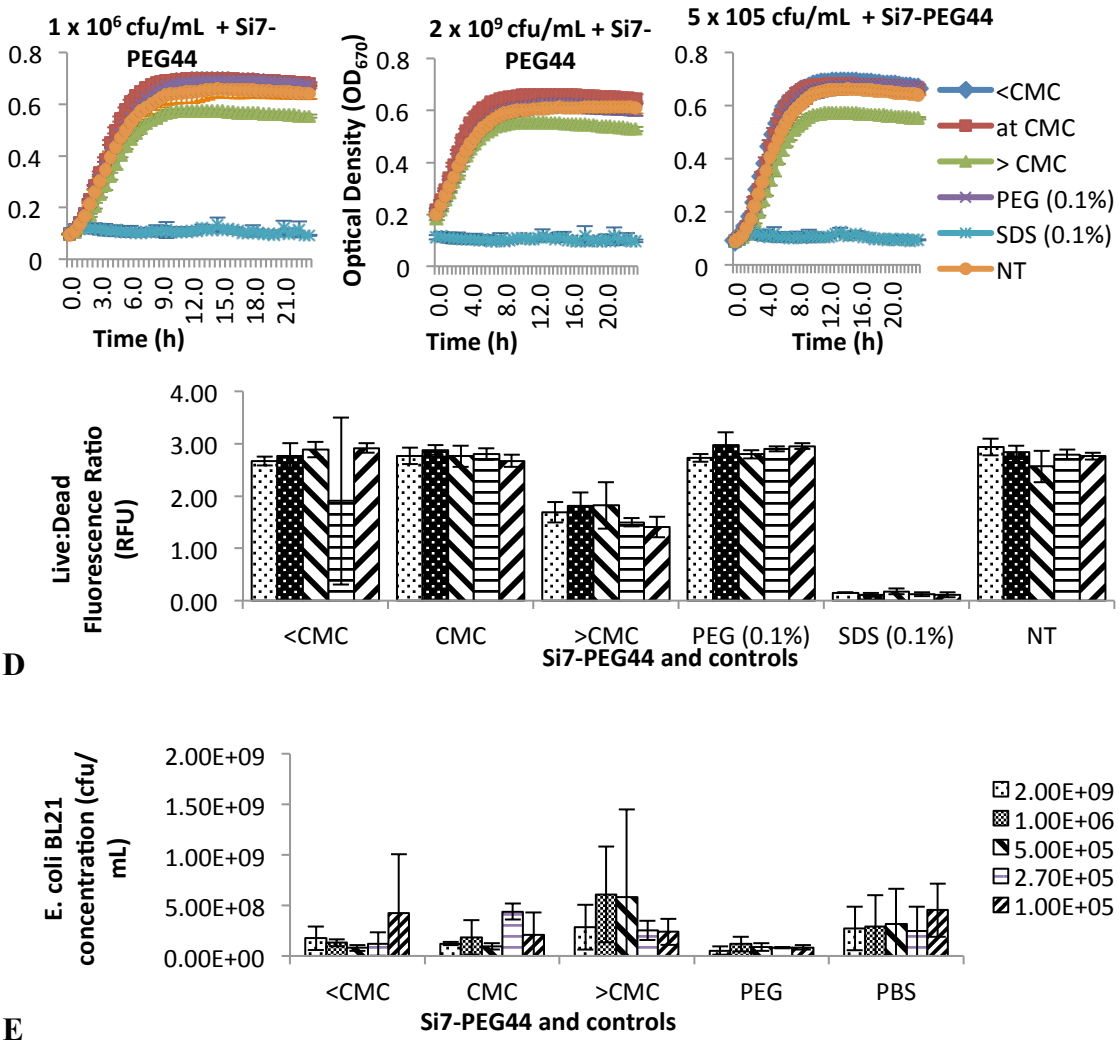

Figure 3-3. A-C Growth curves of *E. coli* BL21 over ~24 hours in the presence of **Si7-PEG44** at three different bacteria concentrations. Graph titles indicate the differences in starting concentration of *E. coli* used (for 1/200: 2.7 x 10^5 cfu/mL and 1/500: 1.0 x 10^5 cfu/mL, see Appendix, section 3.9.4), while the error bars represent standard deviation from triplicate measurements. (D) Fluorescence Live:Dead ratios of *E. coli* BL21 in response to **Si7-PEG44** and controls (fluorescence values are uncorrected). (E) Results of the colony counts produced after treatment removal and growth of *E. coli* on LB agar plates. In each graph, the bars represent standard deviation around the mean of triplicate measurements.

There was essentially no relationship between the response to a given surfactant and bacterial concentrations over several log ranges. This is clearly seen from Figure 3-3, where the trends produced by the different concentrations of surfactant within each category of *E. coli* concentration were the same for all concentrations of *E. coli.* As a consequence, subsequent figures were only plotted for the effect seen at 1 x 10^6 cfu/mL (for the plot of other surfactants, see Appendix, section 3.9.4).

A concentration-dependent effect on *E. coli* viability was observed for each tested surfactant. While there was little difference in *E. coli* viability between <CMC and at CMC relative to the controls, >CMC showed clear bactericidal activity in comparison (Figure 3-4). For example, **Si10-PEG44** had identical LDRs of 3.7 below and at the CMC, but 3.0 above the CMC: **Si7-PEG44** was 2.8 at and below the CMC and 1.7 above the CMC. We consider the origins of this effect below.

A small subset of surfactants was compared in which there were no **Si7-PEG44**, one **Si4Ph3-PEG44** or two phenyl groups **Si4Ph6-PEG44**. The LDRs of the phenyl-containing surfactants were relatively invariant with surfactant concentration. However, the presence of the phenyl group was accompanied by a more potent biological activity when compared with analogous compound **Si7-PEG44** (with respect to molecular weight). The most antibacterial of these surfactants, **Si4Ph6-PEG44** with 2 phenyl rings, was still only half as effective as SDS (Figure 3-5, Table 3-1).

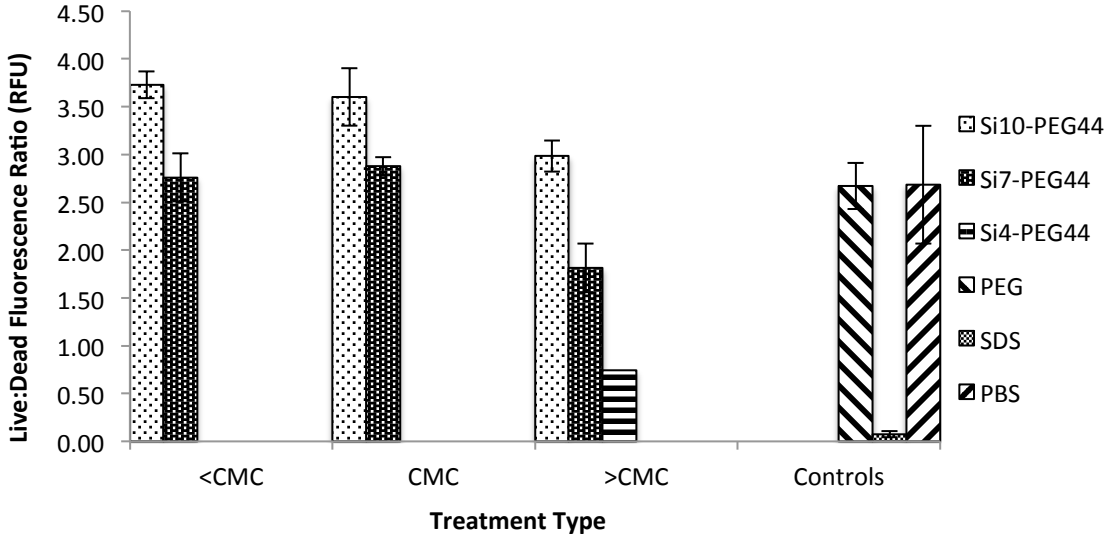

Figure 3-4. : Fluorescence Live:Dead ratios of *E. coli* BL21 in response to surfactants with varying hydrophobic head sizes (**Si10-PEG44** > **Si7-PEG44** > **Si4-PEG44** seen above the graph). The surfactant concentrations <CMC and >CMC correspond to 0.001 and 2.5 w/v % respectively, while at CMC concentrations for **Si10-PEG44**, **Si7-PEG44** and **Si4-PEG44** are 0.01, 5.2 x 10^5 and 0.29 w/v % respectively. Errors bars represent the standard deviation (n=3), while the plotted fluorescence counts are uncorrected.

Little antibacterial activity was observed for **ACR-008 UP**, bearing the smallest of the silicone head groups tested, at <CMC and at the CMC: at these concentrations the observed LDRs were very similar and comparable to that of PEG and No Treatment (i.e., PBS) (Figure 3-6.A). However, remarkably low LDRs were seen >CMC (<0.08) that were almost identical to those of SDS (<0.06). The LDR for **ACR-008 UP** were the lowest achieved by any surfactant in the series of compounds tested for antibacterial activity, and the most similar to that of SDS, making **ACR-008 UP** a potent bacteriocide by comparison.

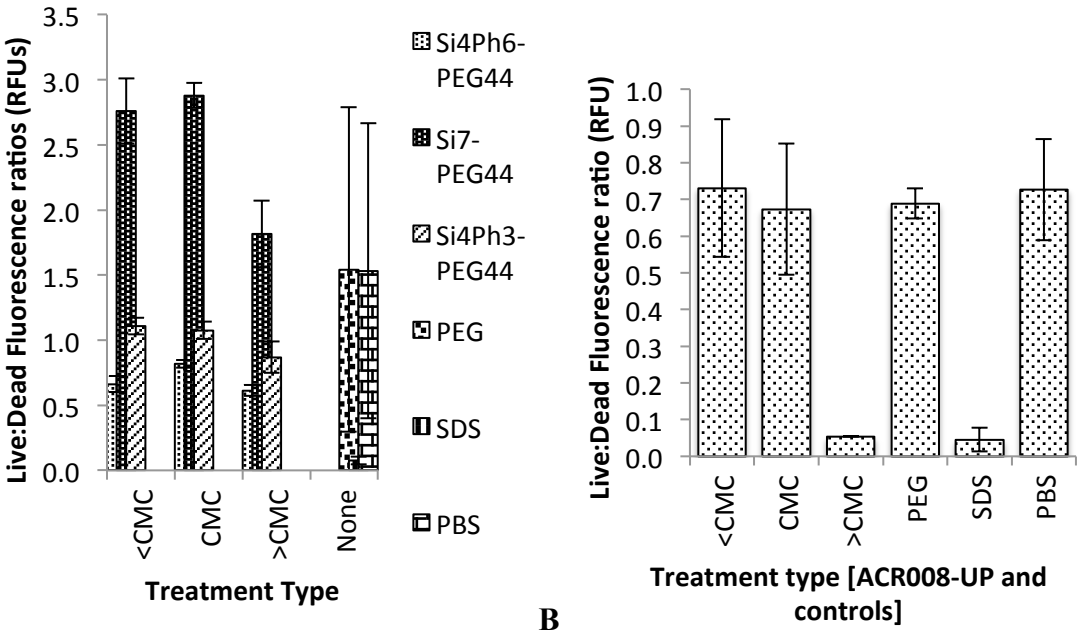

Figure 3-5. Fluorescence Live:Dead ratios of *E. coli* BL21 in response to: A: increasing phenyl content of the hydrophobe and, B: **ACR-008 UP**, For each graph, the concentrations <CMC and >CMC correspond to 0.001 and 2.5 w/v %. Errors bars represent the standard deviation (n=3), while the plotted fluorescence counts are uncorrected.

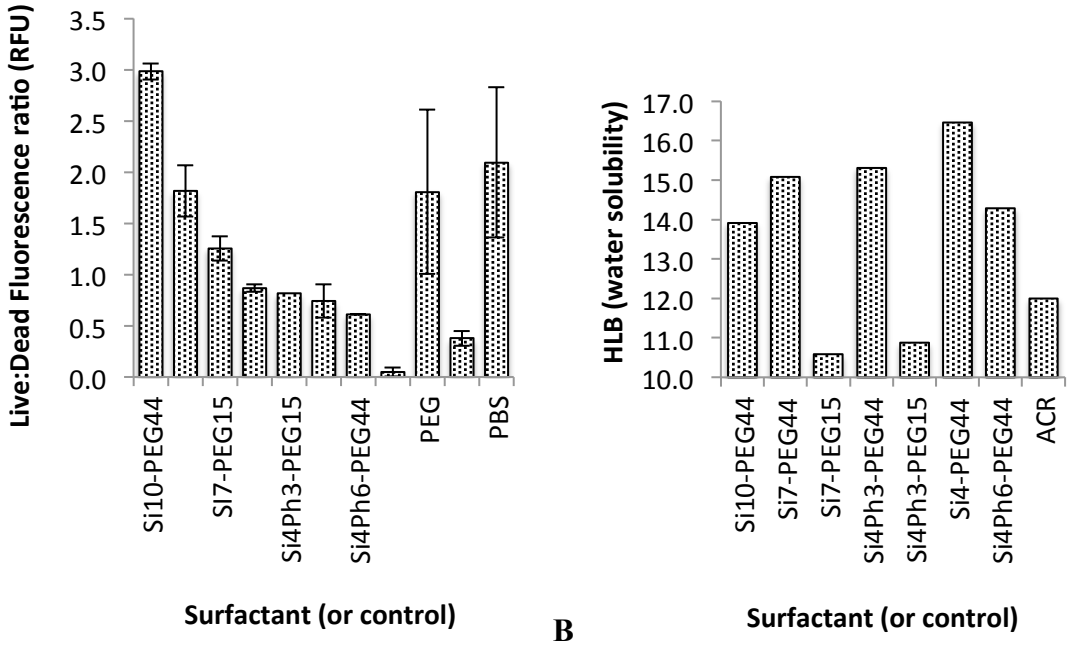

Figure 3-6. A: Live-dead fluorescence ratios of all surfactants at >CMC against 10^6 cfu/mL *E. coli.* The plotted fluorescence counts are uncorrected. B: The 3D HLB (water solubility number) for surfactants.

3.5 Discussion

Surfactants can be potent, generic antibacterial agents or they can have species-selective bactericidal activity. A notable example are the surfactants produced from coupling hydrophilic, tobramycin (an aminoglycoside antibiotic) to linear aliphatic chains, because manipulation of their chemical structures allows killing of gram-positive pathogens as well as the usual gram-negative targets of tobramycin alone.[26] Manipulation of the link between antibiotic and carbon chain can further control its antibacterial potency; compounds with thioether links seem particularly potent,[26] likely because they enhance the mechanism by which surfactants damage cells (both eukaryotic and prokaryotic).

In general, surfactant toxicity is a result of destabilizing effects on cell membranes for colloidal reasons. In brief, surface-active molecules such as surfactants can partition into bilayers and disrupt the self-assembly of molecules found therein (e.g., protein-lipid interactions and lipid-lipid interactions). As a consequence, membrane fluidity is increased, which allows for better exchange of surfactant molecules between membrane and solution, some of which take membrane proteins and lipids with them into solution to form mixed micelles. The leakage of cellular contents through the 'holes' thus created in the bacterial membrane, along with the rapid loss of potential transport channels, receptors and/or enzymes from lipid rafts[27] causes cell death. Hence, surfactants are common lysing agents in research laboratories, with anionic (sodium dodecyl sulfate, SDS) or non-ionic (Tween 80) surfactants as prime examples of surface-active molecules that cause bacterial lysis through intercalation.

Since the function of molecules in general is tightly linked to their chemical structure, and since there exist differences between prokaryotic and eukaryotic cells, not all surfactants that are active against one cell type will be active against another. Hence, while some silicone polyether surfactants described herein exhibit moderate to high toxicity against the bacterium tested, for example, **Si10-PEG44** and **ACR-008 UP**, respectively, their toxicity to eukaryotic, mammalian cells is yet unknown. This is key when considering possible applications. If extended contact between surfactant and patients/other health care personnel is expected, for example, then the surfactants need also be subjected to toxicity studies against relevant mammalian cells lines. With an appropriate toxicity profile, these surfactants could have efficacy in cleaning applications. As with all

antibacterials, care must be taken to ensure the most effectively tailored surfactant concentration is used, at the right concentration and possibly in conjunction with other efficacious compounds. These parameters need to be identified in the lab prior to use, since use of sub-optimal concentrations that kill less than the desired amount of bacteria can facilitate the development of resistant variants. Those surfactants that had little efficacy against bacteria may still be useful as formulation aids in topical and internal delivery systems. As with the more bacteriotoxic materials, further testing is warranted.

In addition to considering the bioactivity of these surfactants, their application would require an assessment of environmental safety. Fortunately, both constituents of the silicone surfactants have an excellent record for degradation in the environment, biologically[28] and through chemical processes. Silicone polymers readily depolymerize in soil, and are further degraded over long time periods to sand, water and CO_2.[29] Polyethers undergo both biological and environmental oxidation that converts ethers to esters, which subsequently undergo hydrolysis to glycolic acids.[30]

Bacterial resistance to antibiotics develops from the complexity of coping mechanisms that microbes have evolved. *Staphylococcus aureaus,* for example, has efflux pumps that can remove quaternary ammonium (QA) surfactants from the membrane core at concentrations less than the minimum inhibitory concentratin (MIC).[31] Gram-negative bacteria like *E. coli* possess similar protective pumps (e.g., ACrAB) that combat stress from surfactants like bile salts,[32,33] while cells grown repeatedly in high concentrations of SDS (5 %) changed their protein composition to produce 4 out of the 19 known detergent-stress proteins used to resist SDS at an increased rate of synthesis (from 3 to

11.8-fold).[34] To circumvent these types of defenses, the surfactant concentration has to be above the defendable threshold for bacteria to be effective, irrespective of the specific mode of action for antibacterial activity. Cell membranes are comprised of surface-active molecules. It is therefore challenging for bacteria to protect against exposure to surfactants (that are also surface active) without affecting the stability of the native membrane.

In the case of the silicone polyether surfactants tested, greater antibacterial activity was observed at concentrations above their CMCs for five of the eight (**Si10-PEG44**, **Si7-PEG15**, **Si7-PEG44**, **Si4-PEG44**, and **ACR-008 UP**). This fact is in good accordance with the literature, and consistent with a non-specific mode of interaction between bacterium and surfactant. That is, at surfactant concentrations above the CMC, bacterial cell membranes become saturated with enough surfactant monomers to cause cell lysis. The absence of a difference in LDRs with different concentrations of **Si4Ph6-PEG44**, **Si4Ph3-PEG15** and **Si4Ph3-PEG44**, respectively (i.e., activity even at concentrations below their CMCs), indicates that there are other factors at play in these cases, which may be affiliated with rigidity, ability of the phenyl groups to pi-stack with each other or intercalate with cell membrane constituents. Further experimentation with additional structures is required to better understand these issues.

It is not straightforward to pick apart differences in anti-bacterial activity based on PEG chain length vs. the nature of the silicone head group in the silicone surfactants under consideration. However, three pairs of compounds permit the role of PEG chain size to be examined to some degree. There is a slightly enhanced antibacterial activity of **Si4Ph3-**

PEG15 (0.8) when compared to its more hydrophilic counterpart **Si4Ph3-PEG44** (0.85). A more striking difference with the same trend can be seen with **Si7-PEG15** (1.25) in comparison to **Si7-PEG44** (1.8). The last comparison is made between the excellent biocidal activity of **ACR-008 UP** with the shorter PEG chain (0.05) and **Si4-PEG44** (0.75), which has a longer PEG chain, but only a slightly larger hydrophobic head group. These observations may be explained by examining the reported role of PEG in influencing the biological activity of compounds.

In vitro assays show that functionalizing the surfaces of silicone elastomers with PEG can partly silence the response of various cells to the presence of an otherwise synthetic, hydrophobic surface.[35-40] PEG stabilizes the interface by providing a flexible, hydrated surface without any attractive binding sites for cellular surfaces. This strategy is exploited in drug delivery applications, in which pegylation of delivery vehicles or the drugs themselves is used to extend the longevity of bioactive species in vivo.[41] Such effects are also conveyed by PEG-containing surfactants. For example, the hemolytic activity of a nonionic surfactant decreases with increasing PEG length.[42] This observation is analogous to detergent-induced bacteriolysis, since red blood cells are a commonly used model for the study of amphiphilic drugs that exhibit similar mechanisms of action for bilayer perturbation and solubilization.[43] Above the CMC, silicone surfactant micelles will present analogous hydrophilic coronas that, with increasing PEG size, will be less predisposed to display any hydrophobic groups. Interaction with cells will thus increasingly be disfavored with longer PEG chains, which protect the hydrophobic core of the micelle, prevent membrane integration of the surfactant via steric hindrance and

interference with the hydrophobic-hydrophobic interactions between surfactant and membrane. Based on these published reports, the PEG chains of the silicone surfactants may be affecting the interaction between micelles and the bacterial surface; longer PEG chains in the silicone polyether surfactants may form larger coronas around the hydrophobic head, thereby limiting the 'delivery' of surfactants from the solution to the membrane for integration or exchange.[44]

Altering the PEG chain length of any surfactant also alters its HLB. This has a reportedly significant affect on antibacterial activity, with moderately soluble surfactants (HLBs 12-14 on a scale of 20) described as most potent.[45] Though the exact biocidal mechanism resulting from HLB changes is unclear, moderately high HLBs may be desirable for facilitating solubilization of membrane lipids and proteins *after* surfactant integration into the membrane (large PEG chains would have greater affinity for the external aqueous environment than the hydrophobic core of the membrane). In the case of the silicone surfactants under consideration, however, the water solubility number of the 3D HLB does not correlate with LDR (Figure 3-6.B).

The efficiency of intercalation of cellular membranes also relies upon the structure of the hydrophobic head. Nonionic surfactants solubilize bilayers via hydrophobicity-dependent membrane integration,[46] particularly in the lipid portion.[44] Not surprisingly, therefore, the nature of the silicone hydrophobe had a profound effect on antibacterial activity of the surfactants. Hydrophobic groups in organic surfactants are normally linear alkyl or arylalkyl groups. By contrast, the methylsilicones here are highly branched, three-dimensional objects. Larger silicone head groups were associated with lower activity

(Figure 3-6). The stability of the micelle (equilibrium constant for loss of molecules from the micelle) will increase with larger hydrophobes, with which presentation to water is disadvantageous. Perhaps more importantly, larger groups will intercalate less effectively into a cell membrane comprised of biological surfactants with linear alkyl hydrophobic residues: the 'fit' is inefficient.

The results from the phenylsilicone surfactants were unexpected. The packing of phenyl groups within the micelle core should act to diminish the ability of the surfactants to diffuse away from the micelle,[47, 48] and the presence of rigid, phenyl groups was expected to render these materials less able to interact with cell membranes, leading to a lower antibacterial activity. That was true for the monophenyl-substituted surfactant **Si4Ph3-PEG15**. However, the diphenyl analogue **Si4Ph6-PEG44** did not follow the trend. We currently do not have an explanation for the higher than expected antibacterial activity of **Si4Ph6-PEG44**. As is well known, very small structural differences can significantly affect biological activity. For example, the small silicone 2,6-*cis*-diphenylhexamethylcyclotetrasiloxane (*cis*-$DD^{Ph}DD^{Ph}$) is knows to be an estrogen mimic, while other isomers including the *trans* analogue are not.[49, 50] Additional members of the library will be made to probe this interesting outcome.

As noted above, most silicones are ill-defined mixtures of materials. This work demonstrates, unsurprisingly, that silicone surfactant structure affects function. Significant differences in antibacterial activity were associated with both the size of silicone head group and PEG tail, but these differences were not represented by the commonly used HLB parameter. Smaller silicone head groups and PEG tails were

associated with higher antibacterial activity. These characteristics can be affiliated with efficiency of delivery of the surfactant from a micelle to the bacterial cell membranes. Micelles derived from larger silicone groups, which will more strongly affiliate, are more stable. Similarly, larger PEG chains provide a more difficult-to-disrupt corona on the micelle. By contrast, micelles derived from surfactants with smaller silicone head groups and PEG tails can more easily deliver the surfactant to the cell membrane where, because of their small size – more comparable to the biological constituents of the membrane – they more easily intercalate, disrupting the membrane.

Some of the surfactants have antibacterial activity typical of active organic surfactants and may be considered for disinfection applications. However, some of the surfactants have less than a log-reduction (SI) against the convenient biological target of E coli BL21(DE3)pLyS (much less than some other commonly used antibacterials). These results demonstrate it is possible to create explicit silicone surfactants with tunable surface activity and antibacterial properties, and provide some guidelines into the design of practically useful compounds. Depending on the specific application, it may be beneficial to kill biological entities,[51] or to provide a level of surface activity without significantly compromising the cell, for example, in formulations involving delivery of bioactives. Further assessment of the biological activity, particularly for the most bacteriotoxic compound is warranted so that the generality of the activity can be assessed for bacteria, and also mammalian cells.

3.6 Conclusion

Smaller silicone head groups and smaller hydrophilic tails were associated with higher antibacterial activity in a group of low molecular weight silicone surfactants. In general, the biological activity was higher above the surfactant CMC. These data support a model in which micelles more effectively deliver surfactants to the bacterial cell membrane than low concentration surfactant solutions. Both longer hydrophilic tails and larger hydrophobic heads are affiliated with more stable micelles that are less able to approach a bacteria surface and less able to delivery surfactant molecules into the cell membrane. Larger branched silicone head groups, with lower surface energy than the alkyl groups within the membrane, will intercalate less effectively for both colloidal and structural reasons. It is therefore possible to tune surfactant structure to manipulate both surface and antibacterial activity.

3.7 Acknowledgements

We acknowledge with gratitude the financial support of the Natural Sciences and Engineering Research Council of Canada (NSERC) and Sentinel: NSERC Research Network on Bioactive Paper. The authors would like to thank Siltech for the provision of **ACR-008 UP**, Ms. Dawn White and Dr. Erica Forsberg for their timely support and expertise, and Dr. John Grande for synthesizing the silicone polyethers.

3.8 References

1. X. D. Zhang, C. W. Macosko, H. T. Davis, A. D. Nikolov and D. T. Wasan, *Journal of Colloid and Interface Science*, 1999, **215**, 270-279.
2. *US Patent 5,558,806 Pat.,* Sep. 24, 1996.
3. R. D. Buick, G. D. Buchan and R. J. Field, *Pesticide Science*, 1993, **38**, 227-235.
4. M. F. Purcell and W. J. Schroeder, *J. Econ. Entomol.*, 1996, **89**, 1566-1570.
5. T. IMAI, S. TSUCHIYA, K. MORITA and T. FUJIMORI, *Appl. Entomol. Zool*, 1994, **29**, 389-393.
6. T. Imai, S. Tsuchiya and T. Fujimori, *Appl. Entomol. Zool.*, 1995, **30**, 380-382.
7. B. W. Wood, W. L. Tedders and J. Taylor, *HortScience*, 1997, **32**, 1074-1076.
8. J. P. Shapiro, W. J. Schroeder and P. A. Stansly, *Florida Entomologist*, 1998, 201-210.
9. L. Chandler, *Arthr. Manag. Tests*, 1995, **20**, 353-354.
10. R. S. Cowles, E. A. Cowles, A. M. McDermott and D. Ramoutar, *J. Econ. Entomol.*, 2000, **93**, 180-188.
11. A. J. O'Neill and I. Chopra, *Expert Opinion on Investigational Drugs*, 2004, **13**, 1045-1063.
12. H. Hanberger, S. Walther, M. Leone, P. S. Barie, J. Rello, J. Lipman, J. C. Marshall, A. Anzueto, Y. Sakr, P. Pickkers, P. Felleiter, M. Engoren and J.-L. Vincent, *International journal of antimicrobial agents*, 2011, **38**, 331-335.
13. T. C. Penna, P. G. Mazzola and A. M. S. Martins, *BMC Infectious Diseases*, 2001, **1**, 16.
14. D. J. Hoban, *Clinical Cornerstone*, 2003, **5, Supplement 3**, S12-S20.
15. C. M. Yates, D. J. Shaw, A. J. Roe, M. E. J. Woolhouse and S. G. B. Amyes, *Biology Letters*, 2006, **2**, 463-465.
16. F. Gonzaga, J. B. Grande and M. A. Brook, *Chemistry – A European Journal*, 2012, **18**, 1536-1541.
17. M. F. Khan, Masters of Applied Science (MASc), McMaster University, 2013.

18. S. P. Crouch and K. J. Slater, *Drug discovery today*, 2001, **6**, 48-53.

19. H. Wennerström and B. Lindman, *Physics Reports*, 1979, **52**, 1-86.

20. L. L. Schramm, *Surfactants: fundamentals and applications in the petroleum industry*, Cambridge University Press, 2000.

21. A. J. O'Lenick Jr. and J. K. Parkinson, *Cosmet. Toilet.*, 1996, **111**, 37-44.

22. P. V. Gawande, K. LoVetri, N. Yakandawala, T. Romeo, G. G. Zhanel, D. G. Cvitkovitch and S. Madhyastha, *Journal of Applied Microbiology*, 2008, **105**, 986-992.

23. L. Li, S. Molin, L. Yang and S. Ndoni, *International Journal of Molecular Sciences*, 2013, **14**, 3050-3064.

24. V. C. Kramer, K. W. Nickerson, N. V. Hamlett and C. O'Hara, *Canadian Journal of Microbiology*, 1984, **30**, 711-713.

25. M. Probes, *Journal*, 2004.

26. I. M. Herzog, M. Feldman, A. Eldar-Boock, R. Satchi-Fainaro and M. Fridman, *MedChemComm*, 2013, **4**, 120-124.

27. D. López and R. Kolter, *Genes & development*, 2010, **24**, 1893-1902.

28. B. Laubie, E. Bonnafous, V. Desjardin, P. Germain and E. Fleury, *Science of the Total Environment*, 2013, **454**, 199-205.

29. M. A. Brook, in *Silicon in Organic, Organometallic and Polymer Chemistry*, Wiley, New York, 2000, ch. 9, pp. 256-308.

30. F. Kawai and B. Schink, *Critical Reviews in Biotechnology*, 1987, **6**, 273-307.

31. D. A. Rouch, D. S. Cram, D. Di Berardino, T. G. Littlejohn and R. A. Skurray, *Molecular Microbiology*, 1990, **4**, 2051-2062.

32. D. Ma, D. N. Cook, M. Alberti, N. G. Pon, H. Nikaido and J. E. Hearst, *Molecular Microbiology*, 1995, **16**, 45-55.

33. D. Ma, D. N. Cook, J. E. Hearst and H. Nikaido, *Trends in Microbiology*, 1994, **2**, 489-493.

34. M. Adamowicz, P. M. Kelley and K. W. Nickerson, *Journal of bacteriology*, 1991, **173**, 229-233.

35. J. L. Brash, *J. Biomater. Sci. Polym. Ed.*, 2000, **11**, 1135-1146.

36. P. Kingshott and H. J. Griesser, *Curr. Opin. Solid State Mater. Sci.*, 1999, **4**, 403-412.

37. P. Kingshott, H. Thissen and H. J. Griesser, *Biomaterials*, 2002, **23** 2043-2056.

38. L. D. Unsworth, H. Sheardown and J. L. Brash, *Langmuir*, 2008, **24**, 1924-1929.

39. B. J. Klenkler, H. Chen, Y. Chen, M. A. Brook and H. Sheardown, *J. Biomater. Sci.-Polym. Ed.*, 2008, **19**, 1411-1424.

40. H. Chen, M. A. Brook and H. Sheardown, *Biomaterials*, 2004, **25**, 2273-2282.

41. S. M. Ryan, G. Mantovani, X. X. Wang, D. M. Haddleton and D. J. Brayden, *Expert Opin. Drug Deliv.*, 2008, **5**, 371-383.

42. M. P. Vinardell and M. R. Infante, *Comparative Biochemistry and Physiology Part C: Pharmacology, Toxicology and Endocrinology*, 1999, **124**, 117-120.

43. S. Schreier, S. V. P. Malheiros and E. de Paula, *Biochimica et Biophysica Acta (BBA) - Biomembranes*, 2000, **1508**, 210-234.

44. M. le Maire, P. Champeil and J. V. Møller, *Biochimica et Biophysica Acta (BBA)-Biomembranes*, 2000, **1508**, 86-111.

45. R. W. Egan, *Journal of Biological Chemistry*, 1976, **251**, 4442-4447.

46. A. M. Seddon, P. Curnow and P. J. Booth, *Biochem. Biophys. Acta*, 2004, **1666**, 105-117.

47. M. Gradzielski, *Curr. Opin. Colloids Interf. Sci.*, **8**, 337-345.

48. I. Capek, *Adv. Colloid Interface Sci.*, **107**, 125-155.

49. D. R. Bennett and B. Aberg, *Acta Pharmacology and Toxicology (Copenhagen)*, 1975, **36(Suppl 3)**, 5-7.

50. R. R. Le Vier, D. R. Bennett and M. J. Hunter, *Acta Pharmacology and Toxicology (Copenhagen)*, 1975, **36(Suppl 3):**, 68-80.

51. R. Cowles, E. Cowles, A. McDermott and D. Ramoutar, *Journal of economic entomology*, 2000, **93**, 180-188.

52. C. B. Maddox, L. Rasmussen and E. L. White, *Journal of the Association for Laboratory Automation*, 2008, **13**, 168-173.

3.9 Appendix

3.9.1 Process optimization

To determine which set of parameters produce the best growth curve for *E. coli* BL21.

3.9.1.1 Methods

A vial of *E. coli* stock solution (from storage) was thawed and 50 µL were streaked on a pre-made agar plate, and incubated at 37 °C for ~12 h to produce distinct colonies. Three of these were used to inoculate 5 mL of fresh LB media, which was incubated for an additional 12 h at 37 °C and 250 rpm in a MaxQ8000 orbital shaker. The overnight culture was subsequently diluted in 2 mL microtubes using fresh LB media to produce solutions with 1/100th, 1/200th and 1/500th of the original concentration. Once made, the *E. coli* solutions were transferred into a clear BD Falcon 96-well plate in triplicates of 25%, 50% and 75% of the total well volume (92.5 µL, 185 µL, 277.5 µL). The entire process was repeated for each plate used in the experiments listed below, with all experiments conducted at 37 °C:

- Plate + parafilm + no mixing for 10 h with OD_{670} measurements every 30 min using the TECAN infinite M200 plate reader;
- Plate + parafilm + mixing in a MaxQ8000 orbital shaker with OD measurements obtained as above;
- Plate + parafilm + mixing via orbital shaking at amplitude 3 mm directly in the TECAN infinite M200 plate reader with OD measurements obtained from the same;

- Plate + parafilm + mixing at amplitude 6 mm;
- Plate + lid + mixing at amplitude 3 mm.

Parafilm was used as a plate cover for the initial set of experiments due to its reportedly high oxygen permeability.

3.9.1.2 Select results

Based on the observed growth profiles, it was found that the different dilution factors affected the approximate start time of the exponential phases of *E. coli* growth (1/100 = 2.0 h, 1/200 = 2.5 h and 1/500 = 3.0 h), such that the lower the starting concentration of *E. coli* the longer it took begin exponential growth. The same trend was apparent in Figure A2 where the plate was subjected to mixing at 120 rpm. Regardless of the type of mixing (120 rpm, amp 3/6, no mixing), all growth curves began to plateau at 10 h. However, whereas the highest end-O.D. achieved in Figures A1 and A2 was ~0.2-0.4, plates with amplitude 3/6 mixing showed (in most cases) end-O.D.s of ≥1.0, which is more than double the amount seen in plates with no mixing or mixing at 120 rpm. Oddly, no difference was seen between the atypical curves (in terms of shape) of different working volumes in Figure A4, while the working volumes of 25 and 50% had less variance in their measurements (Fig. A3). Additionally, a working volume of 50% with shaking at amplitude 3 had curves that began to plateau 5-6 h after those for a 25% working volume. In general, smoother curves were observed in Figures A3 and A4.

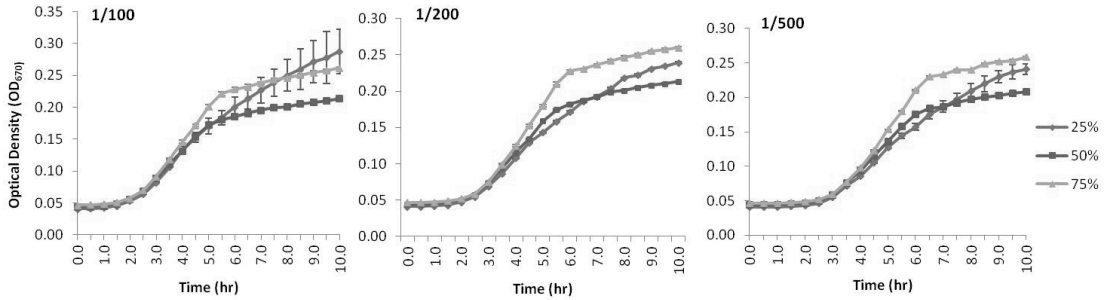

Figure 3-7. Growth profiles of *E. coli* BL21 in a 96-well plate covered in parafilm with **no mixing** (error bars represent standard error (n=3)).

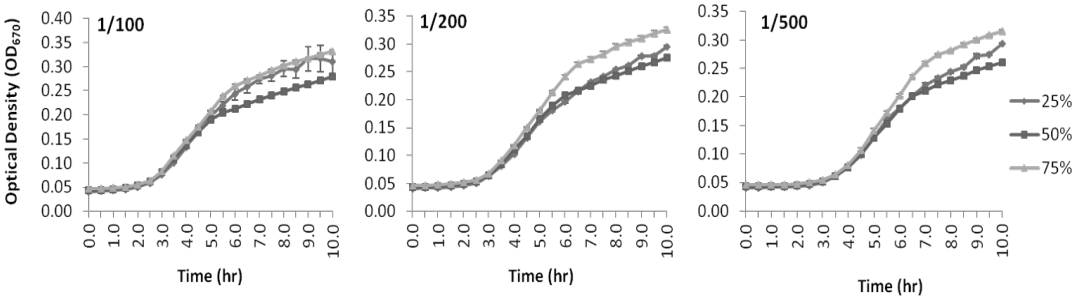

Figure 3-8. Growth profiles of *E. coli* BL21 in a 96-well plate covered in parafilm with **mixing at 120 rpm** in a MaxQ8000 orbital shaker and incubator (error bars represent standard error (n=3)).

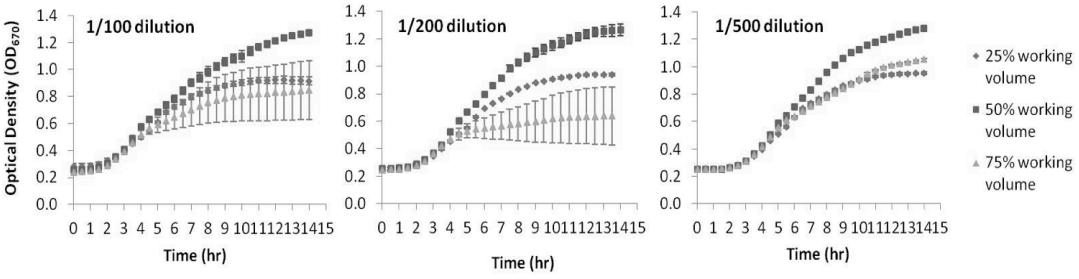

Figure 3-9. Growth profiles of *E. coli* BL21 in a 96-well plate covered in parafilm with **mixing at amplitude 3 mm** of a TECAN Infinite M200 PRO plate reader (error bars represent standard error (n=3)).

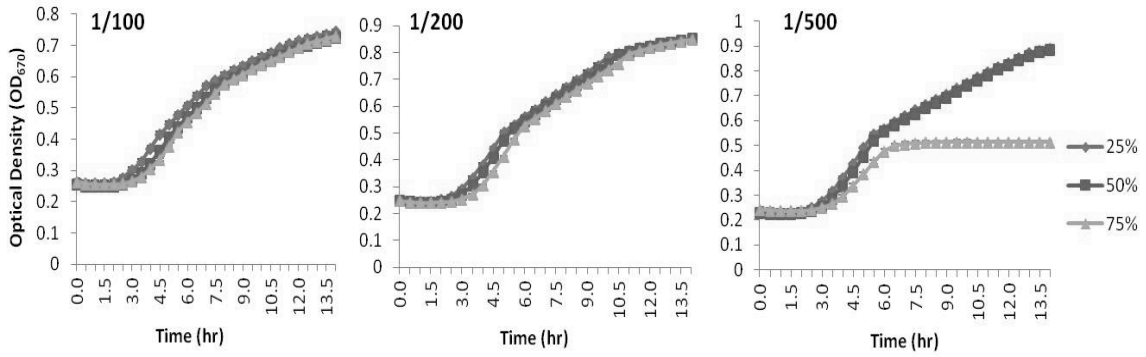

Figure 3-10. Growth profiles of *E. coli* BL21 in a 96-well plate covered in parafilm with **mixing at amplitude 6 mm** of a TECAN Infinite M200 PRO plate reader (error bars represent standard error (n=3)).

In an attempt to discern the cause of high starting O.D.s (~0.25-0.3), a subset of the experiments was repeated with *E. coli* that was diluted to a greater extent than 1/500. Regardless of the starting dilution, however, the O.D. remained high. A lid was used in lieu of parafilm in a subsequent repetition of the work, and the starting O.D. values fell to ~0.07-0.09. A summary of the variables optimized, along with key results, is presented in Table 3-2 below.

Table 3-2. Assay parameters that were optimized prior to antibacterial testing of surfactants.

Variable	Relevance	Parameter	Test conditions	Key observations
Duration of growth curve	Affects length of individual phases of growth, which allows selection of specific points for surfactant addition.	Starting *E. coli* concentration	1/100 dilution 1/200 dilution 1/500 dilution	Little difference observed between growth profiles produced from different starting concentrations.
Agitation	Affects liquid mass transfer coefficients of oxygen	Amplitude (Plate reader) Frequency (MaxQ shaker)	3 mm 6 mm 120 rpm	Best growth profiles achieved by shaking at amplitude 3 in the Tecan plate reader.
Headspace	Affects the exchange of oxygen and carbon dioxide by the media	Working volumes (percentage of total well volume)	25% 50% 75%	50% working volume is ideal since it allows for higher end-ODs and causes less errors in measurement.
Evaporation[‡‡52]	Affects viability of bacteria in samples.	Cover for microplate	Lid	Good growth profiles achievable by both, but lid has consistent thickness that allows detection of low starting ODs

[‡‡] Sample evaporation is a noted concern of assay miniaturization.

3.9.1.3 Discussions and conclusions in brief

Given the smooth growth profiles and high concentrations of *E. coli* (as evident by the high end-O.D. values) achieved in Figure A3, amplitude 3 shaking was selected for use. O.D. values of 1.2-1.4 are not only the norm for good *E. coli* growth in microplates, but they are also needed in protocols that involve IPTG use, for example, since induction should occur at 0.5 and end values of 0.3 (as was the case in Figures A1 and A2) are insufficient. Since the use of IPTG is planned for adhesion experiments on polymers modified with the best of the silicone-polyether surfactants, growth profiles such as those in Figure A3 were deemed best. Out of the curves seen in this Figure, a 50% working volume seemed ideal from a logistical standpoint, since the longer duration of growth provided ample time for completion of perquisite work for the next steps in the antibacterial assay.

Lastly, the high starting O.D. seen for each of the graphs presented above was concerning, since standard dilutions should produce O.D. values of around 0.03 or less, and especially because in the context of this project and the next, low starting O.D.s were required for steps like IPTG addition and Live:Dead stain calibration. The drop in initial O.D.s seen with the use of the lid instead of parafilm suggests that the latter was contributing to the high O.D. values seen originally. As a consequence, all optical density measurements in the experiments with silicone-polyethers were conducted using a lid-covered 96-well plate.

3.9.2 Microplate set-up and sample preparation

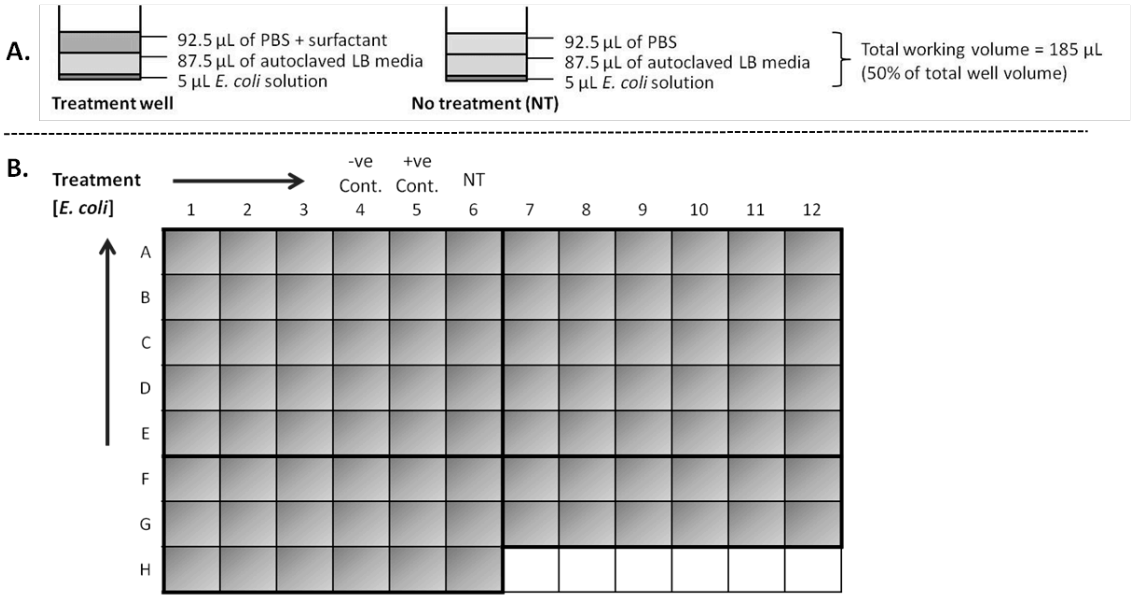

Figure 3-11. Diagrammatic representation of microplate set-up. A) Composition of individual treatment and control wells. B). Overall plate set-up. Bold borders delineate replicates (e.g., n = 1, n =2 etc); green blocks represent wells with *E. coli* growing in the absence of treatment; the direction of arrows indicates increasing concentrations (such that the highest concentration of surfactant is column 3 and repeated in column 9, while the highest concentration of *E. coli* is in row A and repeated in row F); positive and negative controls are denoted as '+ ve Cont.' and '–ve Cont.' respectively.

Note, that according to the microplate set-up, 92.5 µL of the surfactant solution was used with 92.5 µL of additional media, which effectively dilutes the surfactant concentration by half. In anticipation of this, and to ensure *E. coli* interacted with surfactants at, above, or below their CMCs, the masses used to prep 2 mL were double the weight percent amounts needed in a 2 mL solution for each concentration. The masses measured and

used for at CMC solutions of each surfactant are indicated in Table 2 below (masses used for <CMC (0.001 wt% x 2) and >CMC (2.5 wt% x 2) were 0.02 mg and 100 mg respectively).

Table 3-3. Amounts of surfactant used to prepare 2 mL solutions for microplate set-up and antibacterial testing.

Compound Name	**MW (g/mol)**	**CMC (M)**	**Mass (mg) at CMC**
Si10-PEG44	2891.15	5.0×10^{-5}	0.58
Si4Ph6-PEG44	2818.65	8.3×10^{-5}	0.94
Si7-PEG15	1045.00	5.0×10^{-7}	2.10×10^{-3}
Si7-PEG44	2668.68	0.9×10^{-3}	9.6
Si4Ph3-PEG15	1281.00	7.2×10^{-5}	0.36
Si4Ph3-PEG44	2632.43	4.0×10^{-5}	0.42
Si4-PEG44	2446.22	1.2×10^{-3}	11.74
ACR008 UP	686.00	1.5×10^{-4}	0.40

3.9.3 Diagrammatic summary of protocol

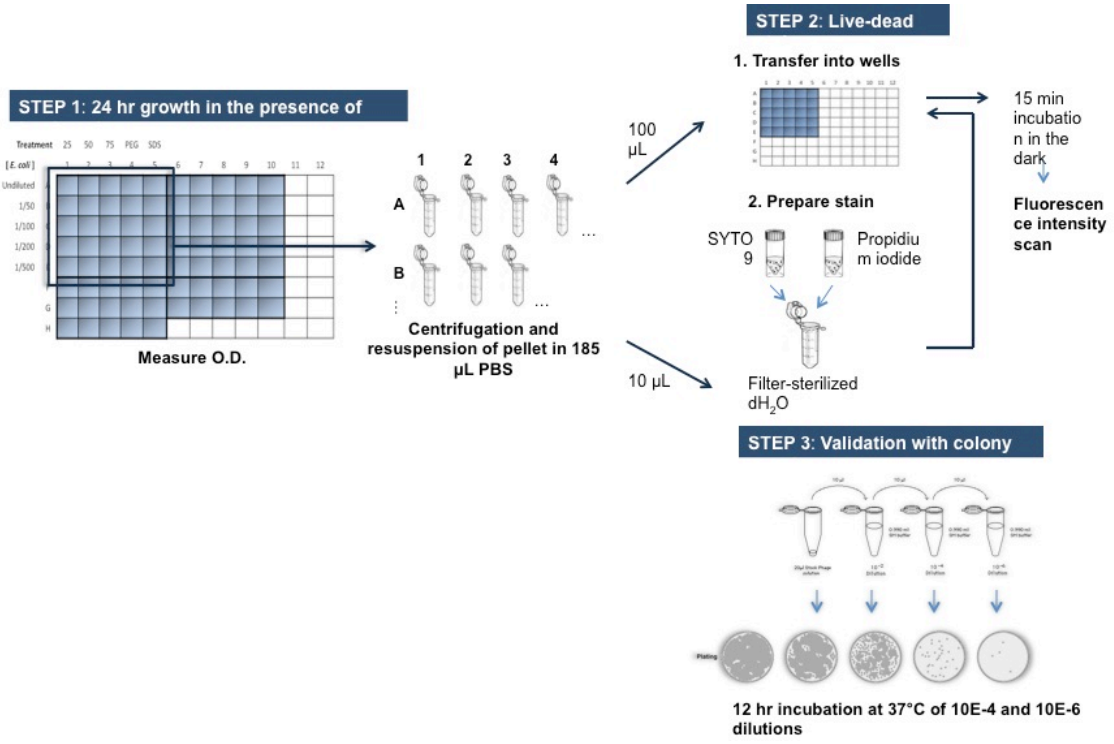

Figure 3-12. Overview of the screening protocol used for the in vitro antibacterial analysis of silicone-poly(oxyethylene) surfactants. Note that for each plate, contents of each of the 96-wells were pipetted into correspondingly labeled tubes, and not just the representative grid shown in the diagram above.

3.9.4 Data for each surfactant tested

3.9.4.1 Si10-PEG44

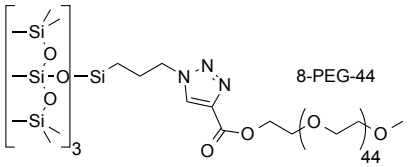

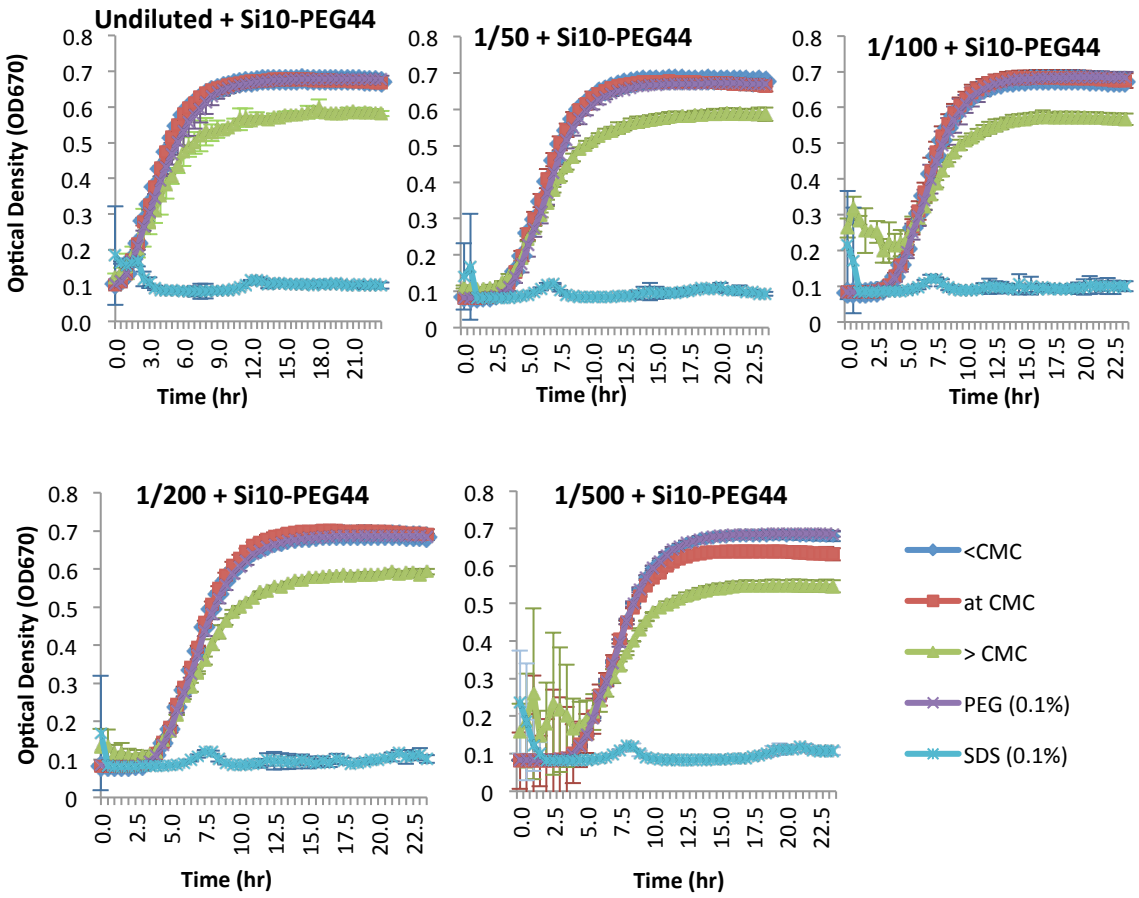

Figure 3-13. Growth curves of *E. coli* BL21 over ~24 hours in the presence of **Si10-PEG44**. Graph titles indicate the differences in starting concentration of *E. coli* used (undiluted: 2 x 10^9 cfu/mL, 1/50: 1 x 10^6 cfu/mL, 1/100: 5 x 10^5 cfu/mL, 1/200: 2.7 x 10^5 cfu/mL, 1/500: 1.0 x 10^5 cfu/mL) while the error bars represent standard deviation from triplicate measurements.

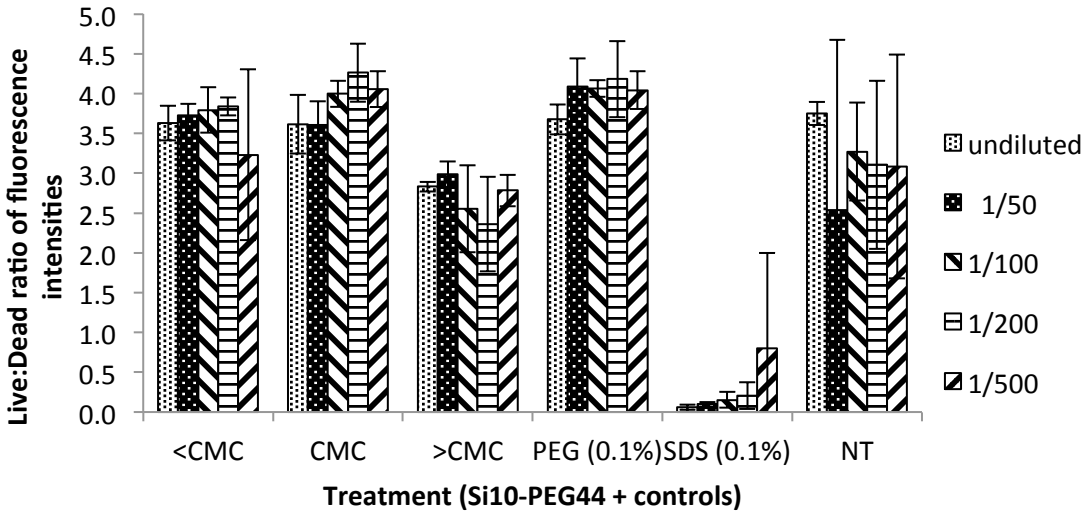

A

B.

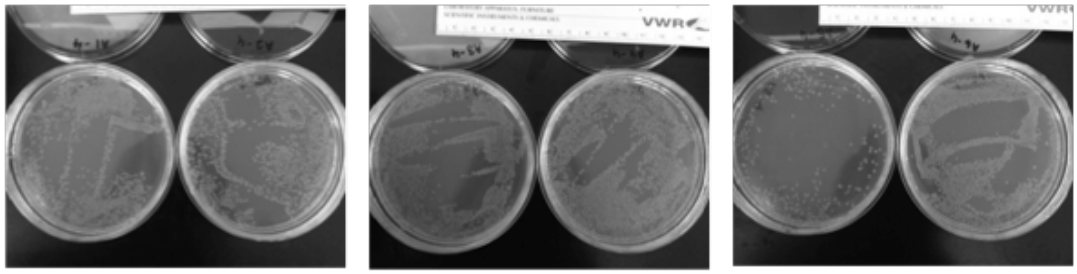

Figure 3-14. **A)** Live:Dead fluorescence ratios of *E. coli* BL21 in response to **Si10-PEG44** and controls (bars represent standard deviation (n=3); fluorescence values are uncorrected). **B)** Photographs of a 10^{-4} dilution of *E. coli* growing on LB agar plates (images were taken after overnight incubation of the plates). In this case, the low dilution factor resulted in colonies that were Too Numerous To Count (TNTC).

3.9.4.2 Si4Ph6-PEG44

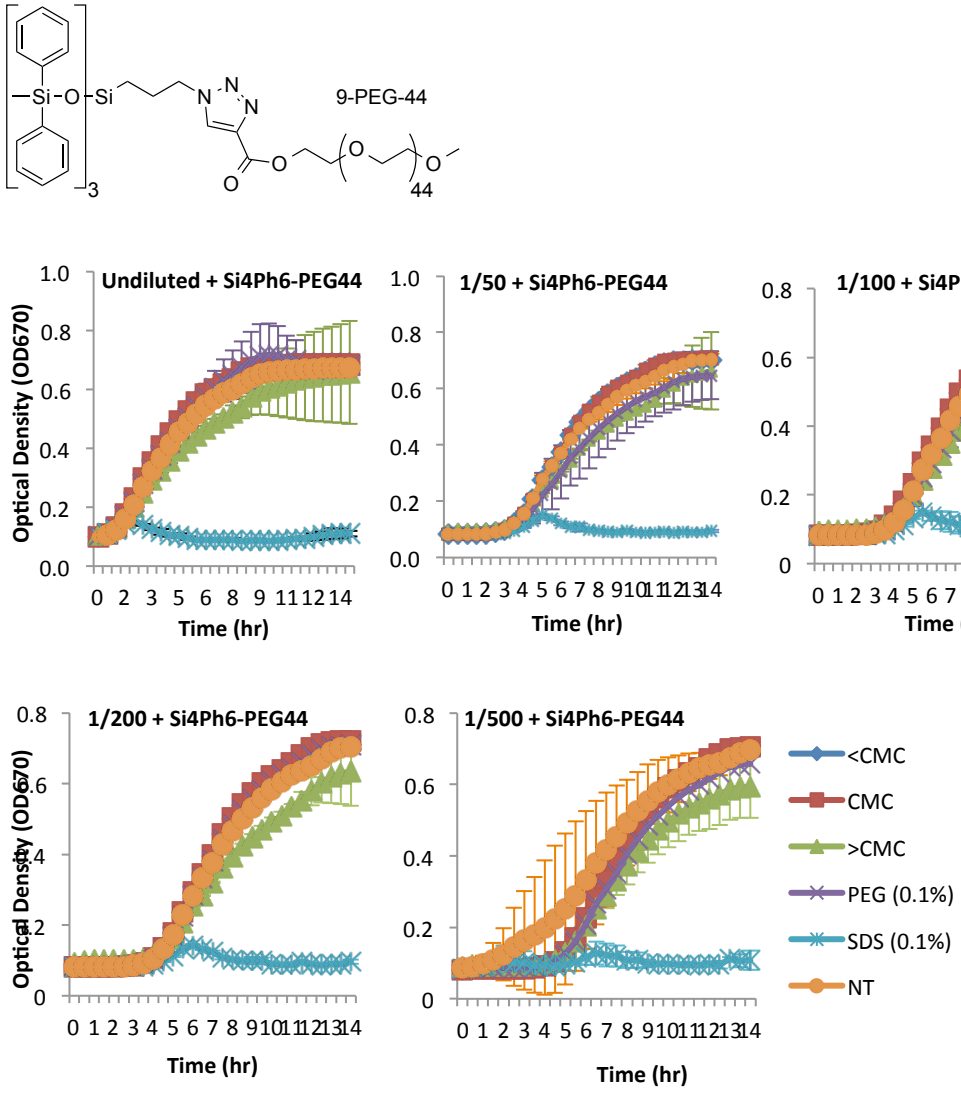

Figure 3-15. Growth curves of *E. coli* BL21 over ~14 hours in the presence of Si4Ph6-PEG44. Graph titles indicate the differences in starting concentration of *E. coli* used (undiluted: 2 x 10^9 cfu/mL, 1/50: 1 x 10^6 cfu/mL, 1/100: 5 x 10^5 cfu/mL, 1/200: 2.7 x 10^5 cfu/mL, 1/500: 1.0 x 10^5 cfu/mL) while the error bars represent standard deviation from triplicate measurements.

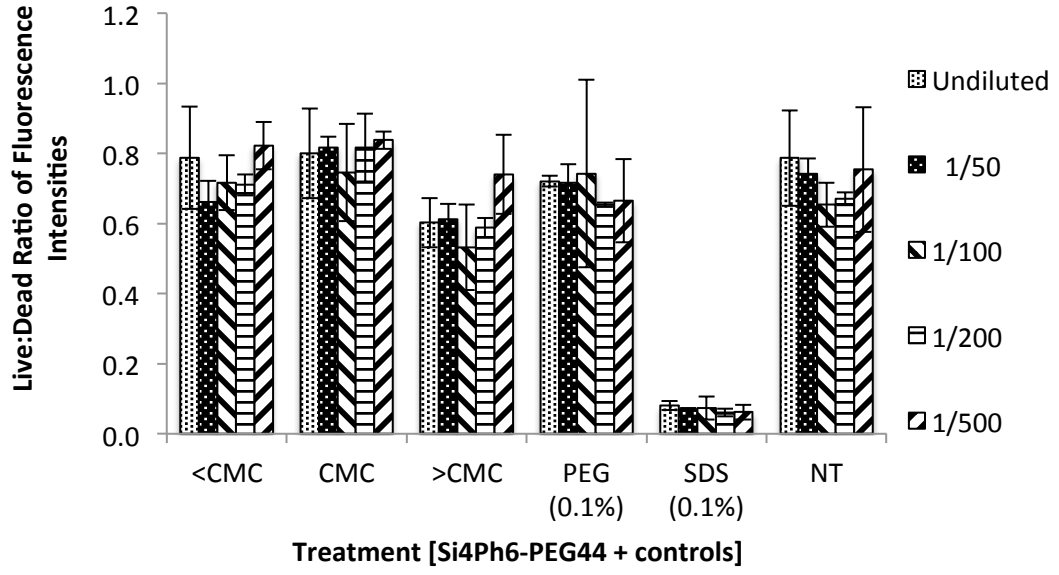

A

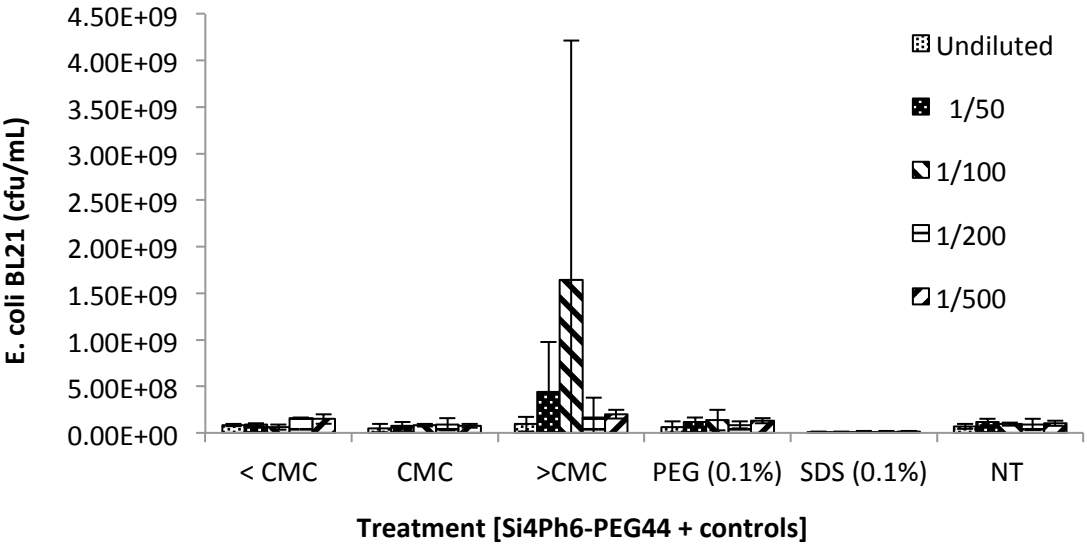

B

Figure 3-16. **A)** Live:Dead fluorescence ratios of *E. coli* BL21 in response to **Si4Ph6-PEG44** and controls (bars represent standard deviation (n=3); fluorescence values are uncorrected). **B)** Results of the colony counts produced after treatment removal and growth of *E. coli* on LB agar plates. In each graph, the bars represent standard deviation around the mean of triplicate measurements.

3.9.4.3 Si7-PEG15

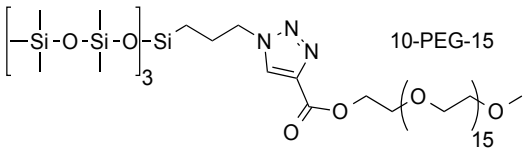

NB: insufficient surfactant to run all three concentrations. Since activity for most surfactants was observed >CMC, the two concentrations selected here were 'at CMC' and '>CMC'. The orange line on the turbidometri graph (Undiluted + 10-PEG-15) is >CMC 10-PEG-15 in the absence of E. coli i.e. the solution was cloudy, milk-coloured suspension with high turbidity to begin with.

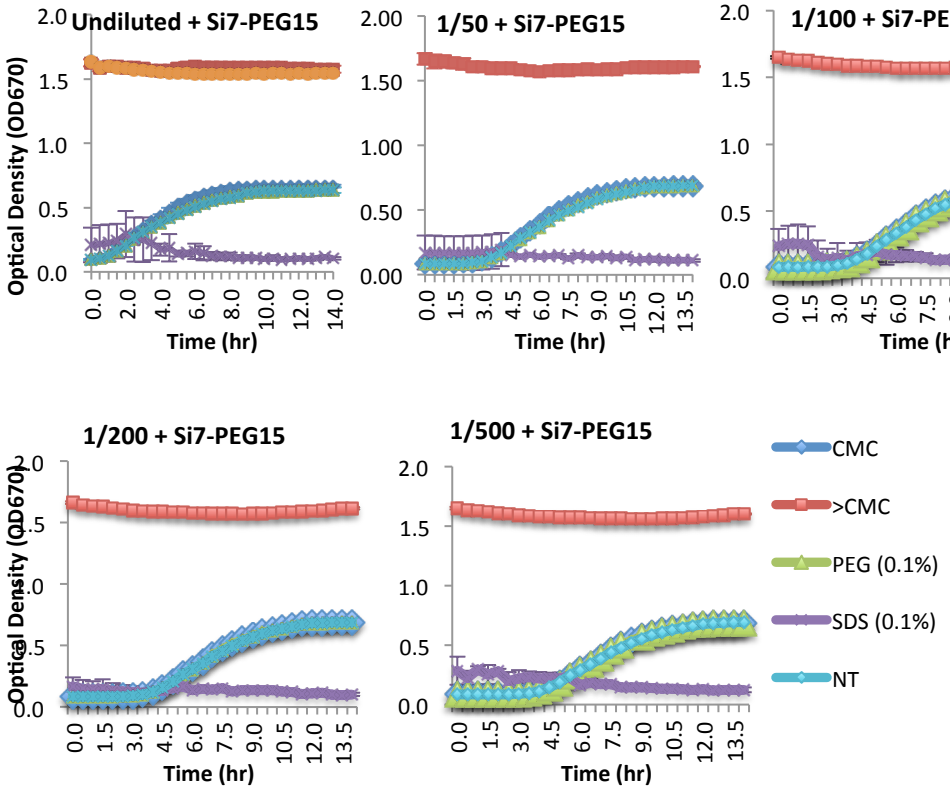

Figure 3-17. Growth curves of *E. coli* BL21 over ~14 hours in the presence of **Si7-PEG15**. Graph titles indicate the differences in starting concentration of *E. coli* used (undiluted: 2 x 10^9 cfu/mL, 1/50: 1 x 10^6 cfu/mL, 1/100: 5 x 10^5 cfu/mL, 1/200: 2.7 x 10^5 cfu/mL, 1/500: 1.0 x 10^5 cfu/mL) while the error bars represent standard deviation from triplicate measurements.

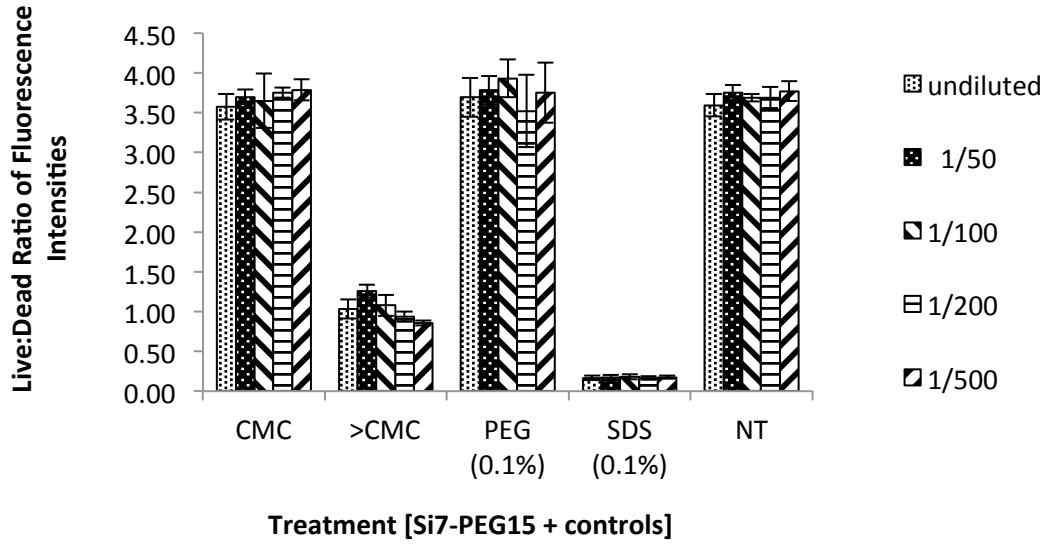

A.

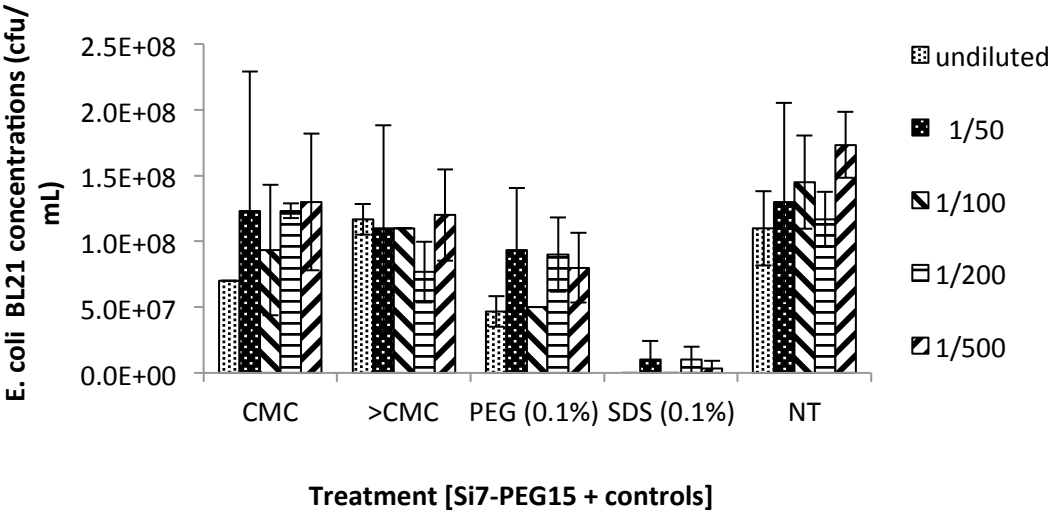

B.

Figure 3-18. **A)** Live:Dead fluorescence ratios of *E. coli* BL21 in response to **Si7-PEG15** and controls (bars represent standard deviation (n=3); fluorescence values are uncorrected). **B)** Results of the colony counts produced after treatment removal and growth of *E. coli* on LB agar plates. In each graph, the bars represent standard deviation around the mean of triplicate measurements.

3.9.4.4 Si7-PEG44

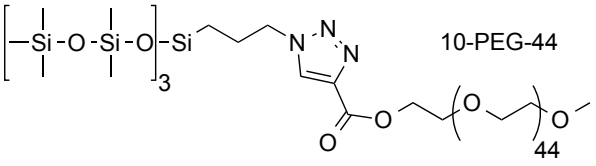

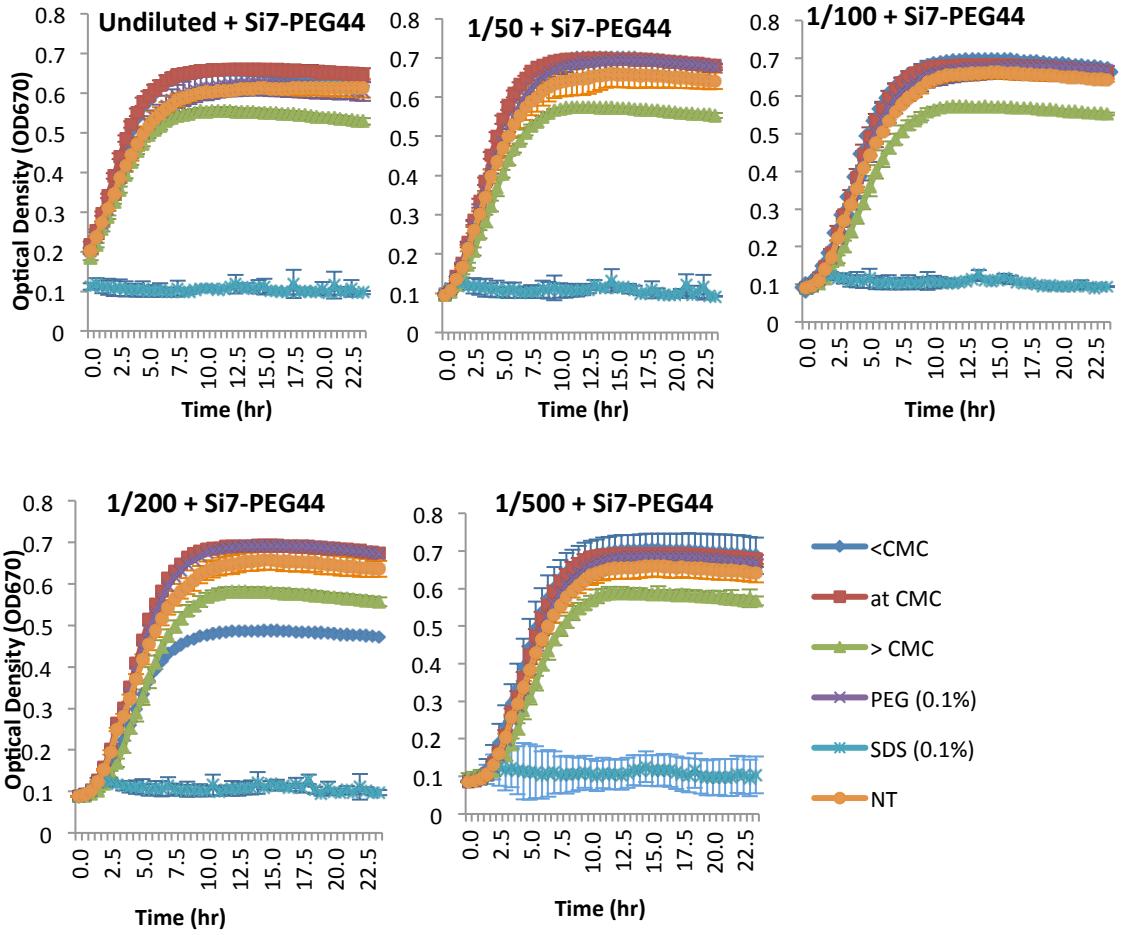

Figure 3-19. Growth curves of *E. coli* BL21 over ~24 hours in the presence of **Si7-PEG44**. Graph titles indicate the differences in starting concentration of *E. coli* used (undiluted: 2 x 10^9 cfu/mL, 1/50: 1 x 10^6 cfu/mL, 1/100: 5 x 10^5 cfu/mL, 1/200: 2.7 x 10^5 cfu/mL, 1/500: 1.0 x 10^5 cfu/mL), while the error bars represent standard deviation from triplicate measurements.

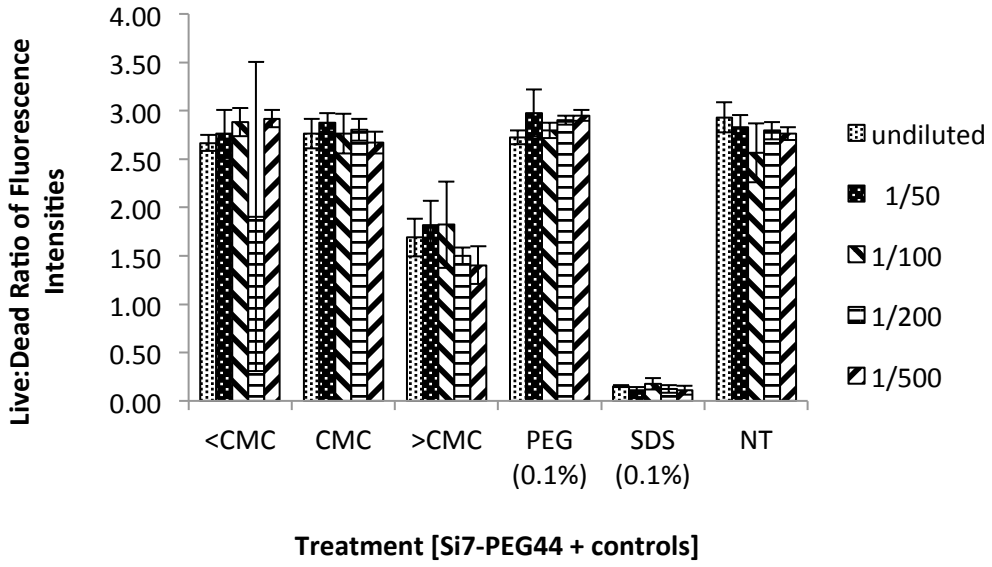

A.

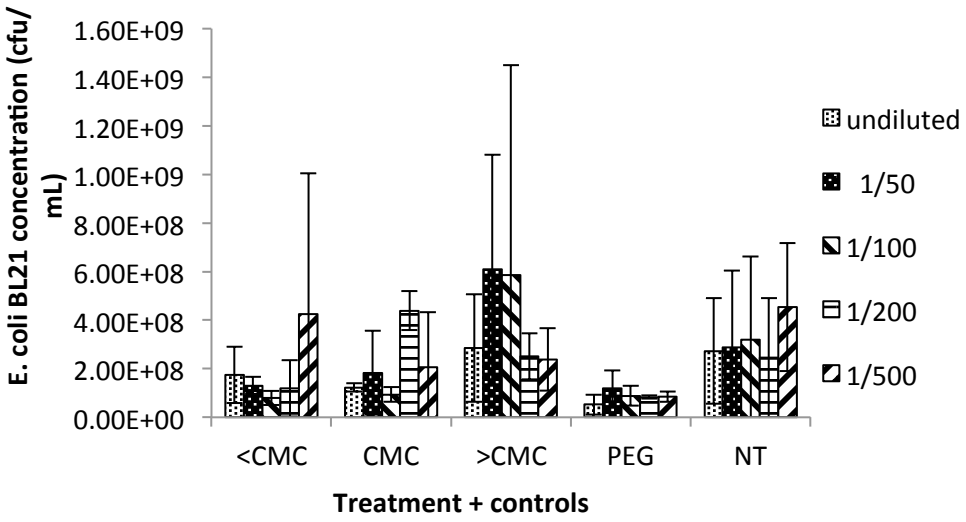

B.

Figure 3-20. **A)** Live:Dead fluorescence ratios of *E. coli* BL21 in response to **Si7-PEG44** and controls (fluorescence values are uncorrected). **B)** Results of the colony counts produced after treatment removal and growth of *E. coli* on LB agar plates. In each graph, the bars represent standard deviation around the mean of triplicate measurements.

3.9.4.5 Si4Ph3-PEG15

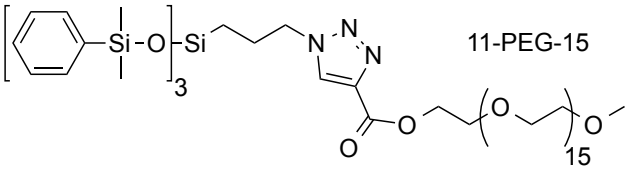

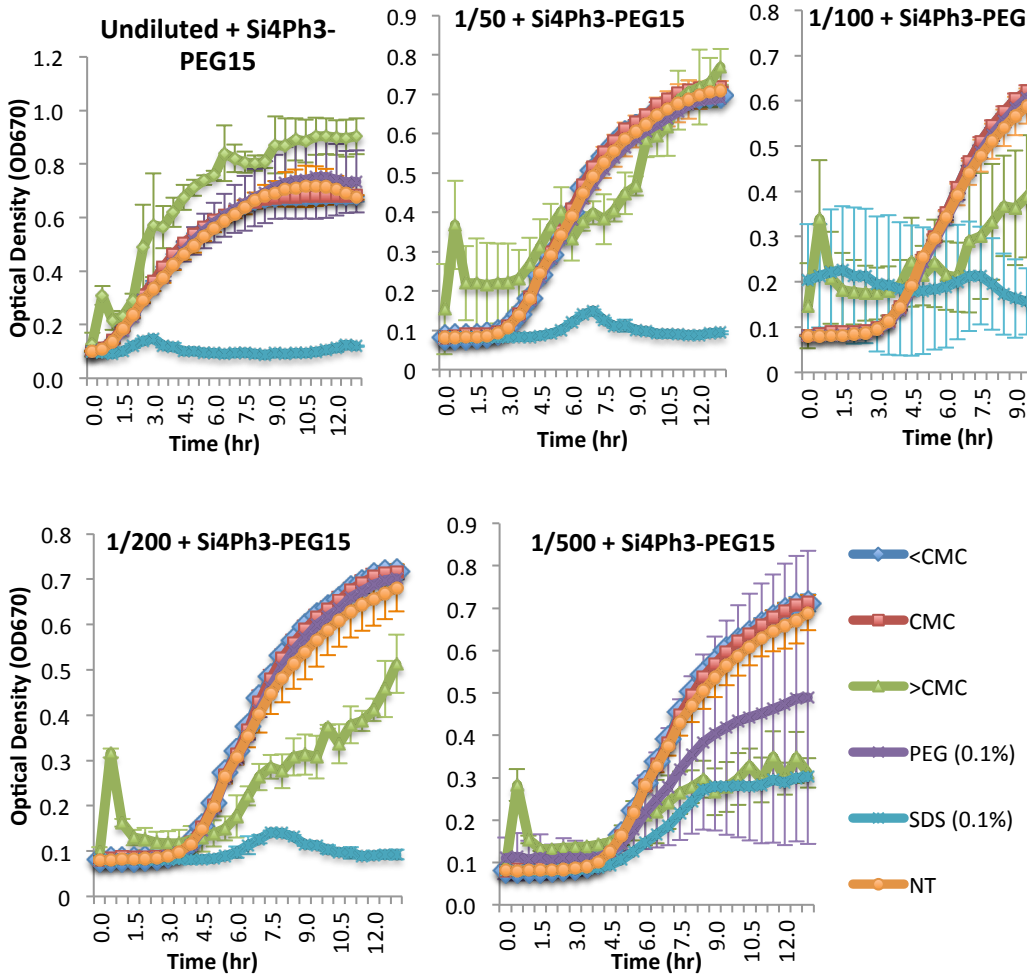

Figure 3-21. Growth curves of *E. coli* BL21 over ~24 hours in the presence of **Si4Ph3-PEG15**. Graph titles indicate the differences in starting concentration of *E. coli* used (undiluted: 2 x 10^9 cfu/mL, 1/50: 1 x 10^6 cfu/mL, 1/100: 5 x 10^5 cfu/mL, 1/200: 2.7 x 10^5 cfu/mL, 1/500: 1.0 x 10^5 cfu/mL), while the error bars represent standard deviation from triplicate measurements.

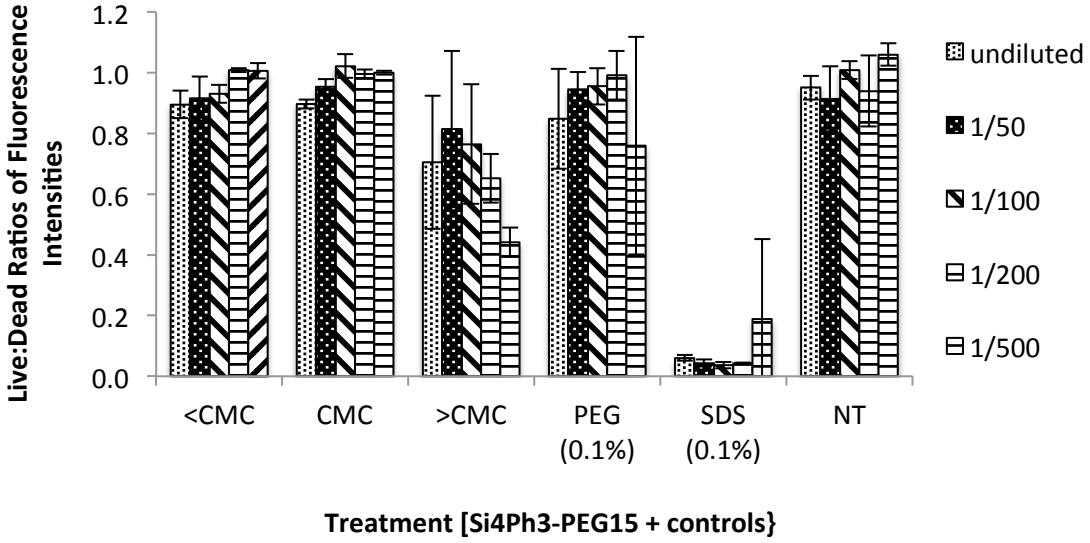

A.

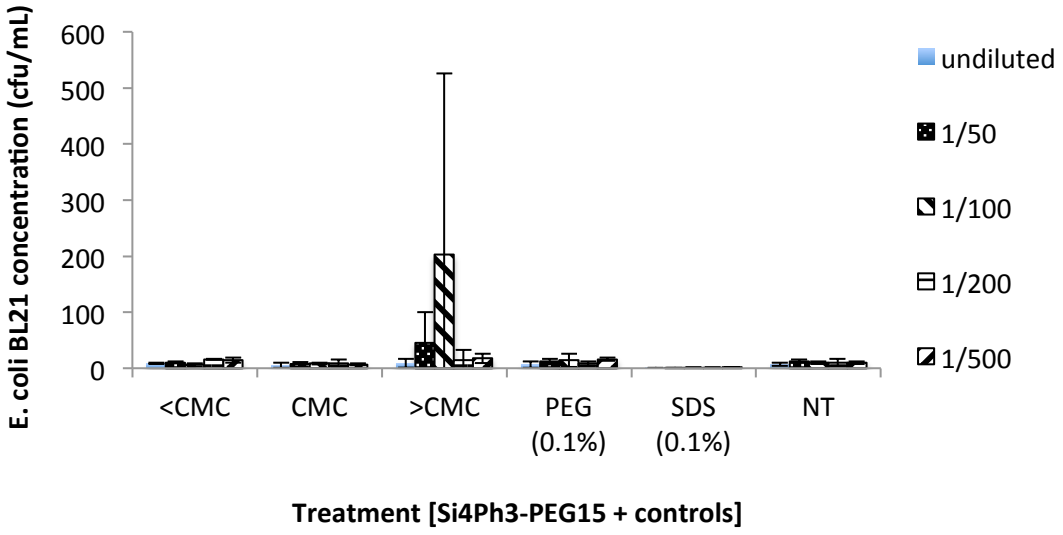

B.

Figure 3-22. **A)** Live:Dead fluorescence ratios of *E. coli* BL21 in response to **Si4Ph3-PEG15** and controls (fluorescence values are uncorrected). **B)** Results of the colony counts produced after treatment removal and growth of *E. coli* on LB agar plates. In each graph, the bars represent standard deviation around the mean of triplicate measurements.

3.9.4.6 Si4Ph3-PEG44

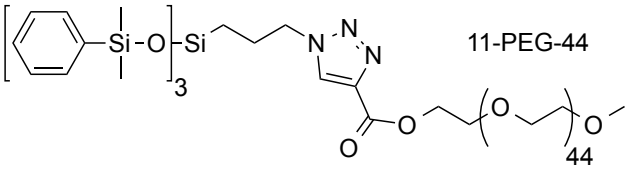

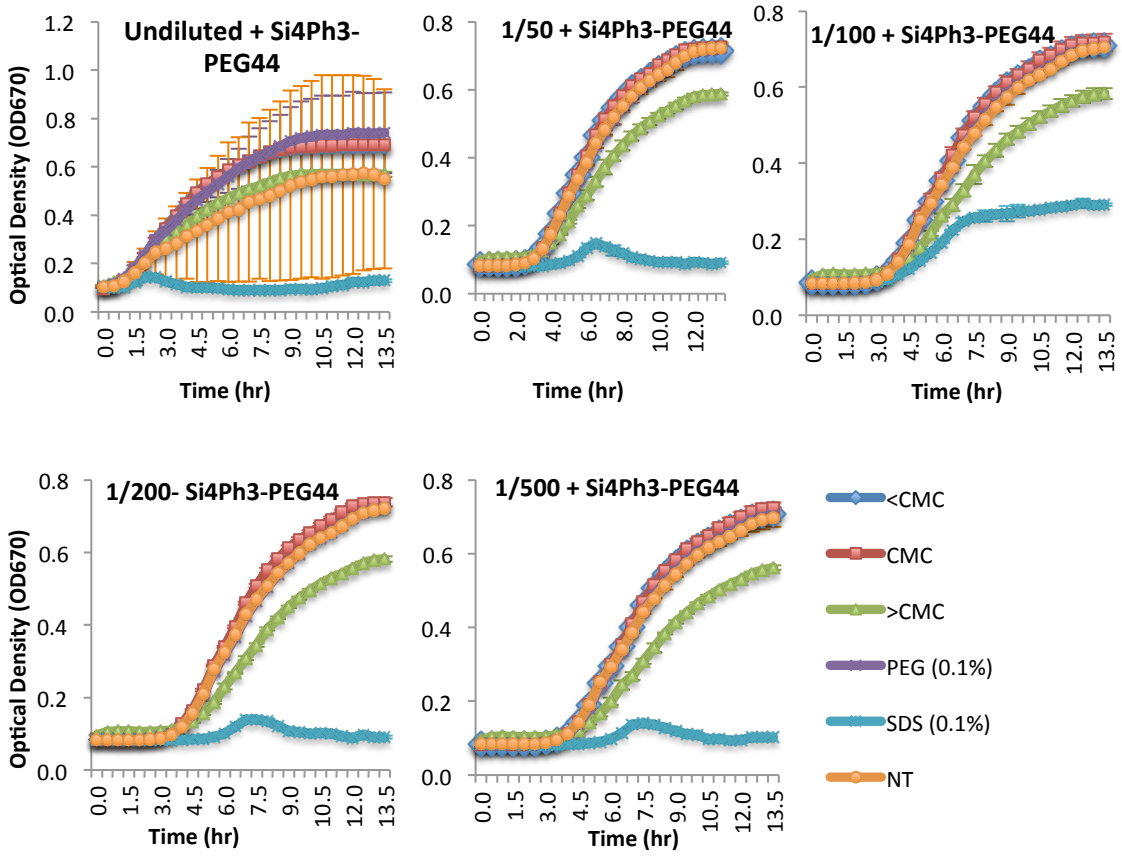

Figure 3-23. Growth curves of *E. coli* BL21 over ~24 hours in the presence of **Si4Ph3-PEG44**. Graph titles indicate the differences in starting concentration of *E. coli* used (undiluted: 2 x 10^9 cfu/mL, 1/50: 1 x 10^6 cfu/mL, 1/100: 5 x 10^5 cfu/mL, 1/200: 2.7 x 10^5 cfu/mL, 1/500: 1.0 x 10^5 cfu/mL), while the error bars represent standard deviation from triplicate measurements.

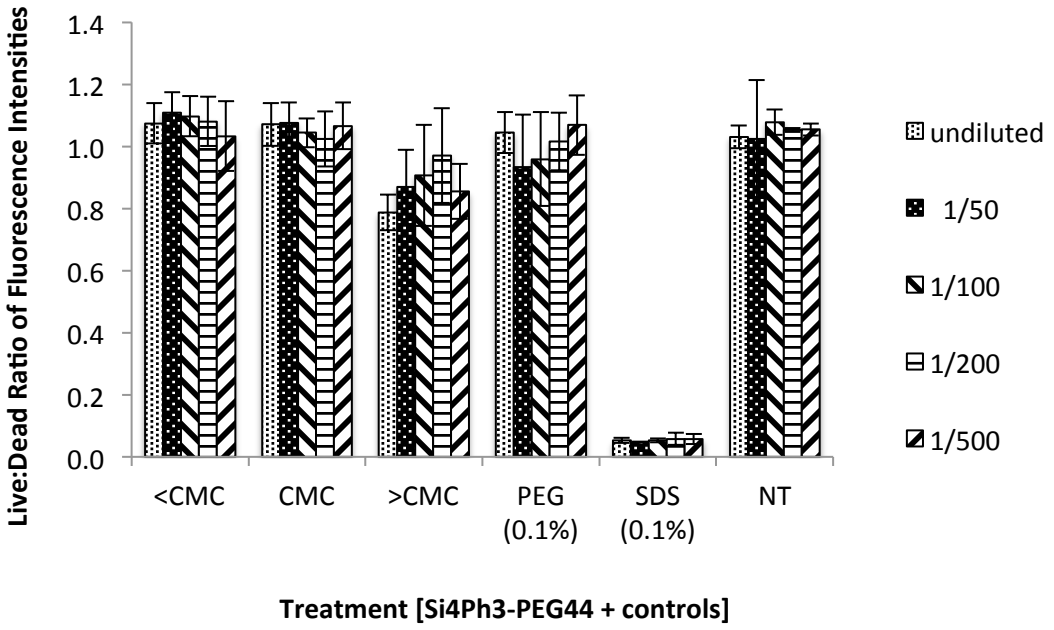

A.

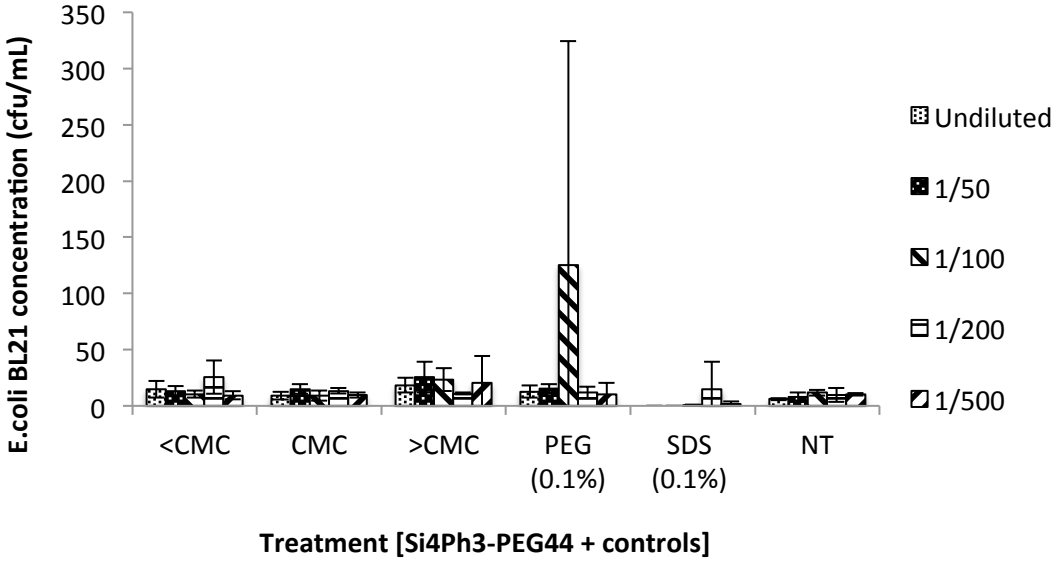

B.

Figure 3-24. **A)** Live:Dead fluorescence ratios of *E. coli* BL21 in response to **Si4Ph3-PEG44** and controls (fluorescence values are uncorrected). **B)** Results of the colony counts produced after treatment removal and growth of *E. coli* on LB agar plates. In each graph, the bars represent standard deviation around the mean of triplicate measurements.

3.9.4.7 Si4-PEG44

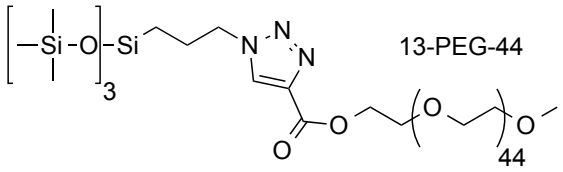

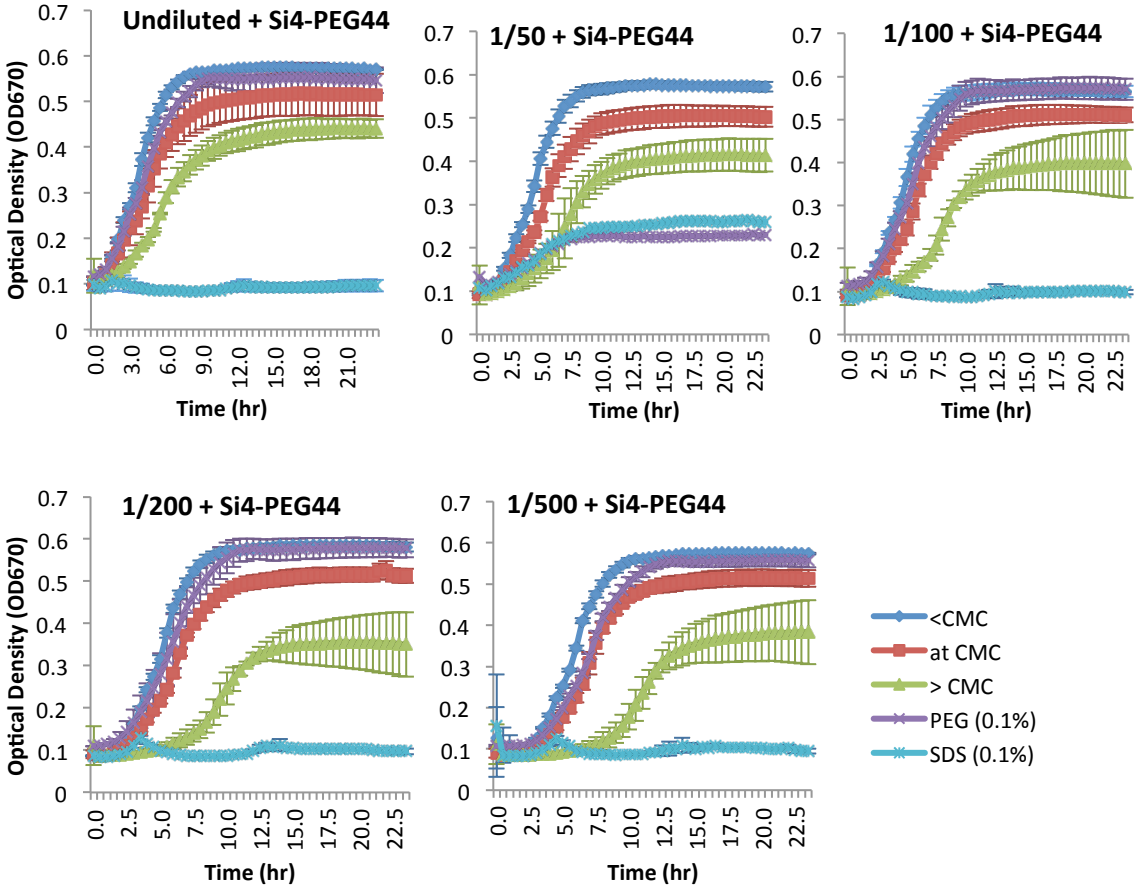

Figure 3-25. Growth curves of *E. coli* BL21 over ~24 hours in the presence of 13-PEG-44 (**Si4-PEG44**). Graph titles indicate the differences in starting concentration of *E. coli* used (undiluted: 2 x 10^9 cfu/mL, 1/50: 1 x 10^6 cfu/mL, 1/100: 5 x 10^5 cfu/mL, 1/200: 2.7 x 10^5 cfu/mL, 1/500: 1.0 x 10^5 cfu/mL), while the error bars represent standard deviation from triplicate measurements.

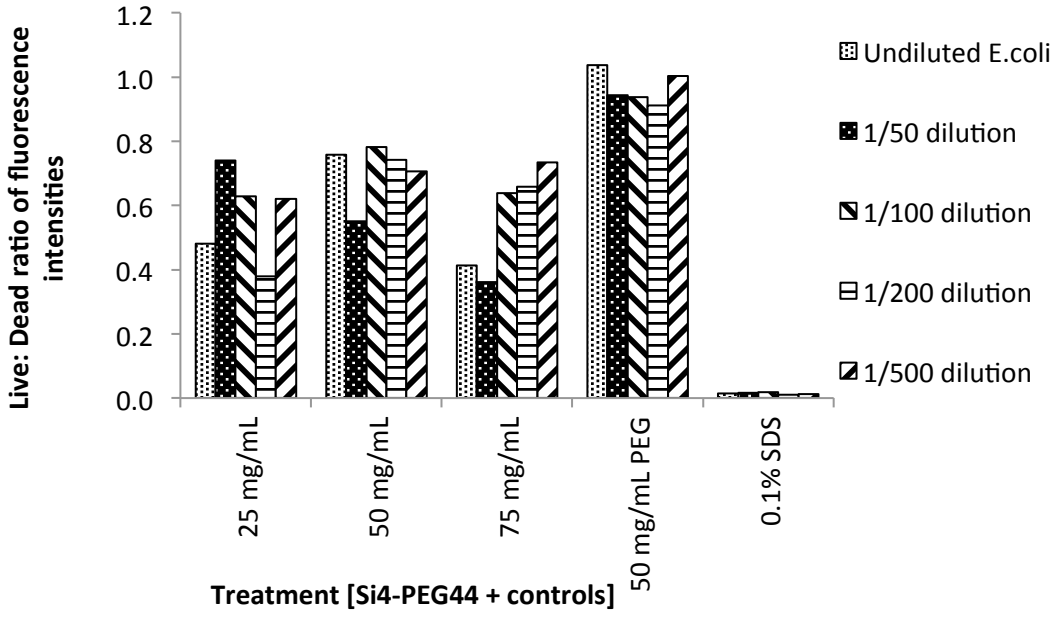

A.

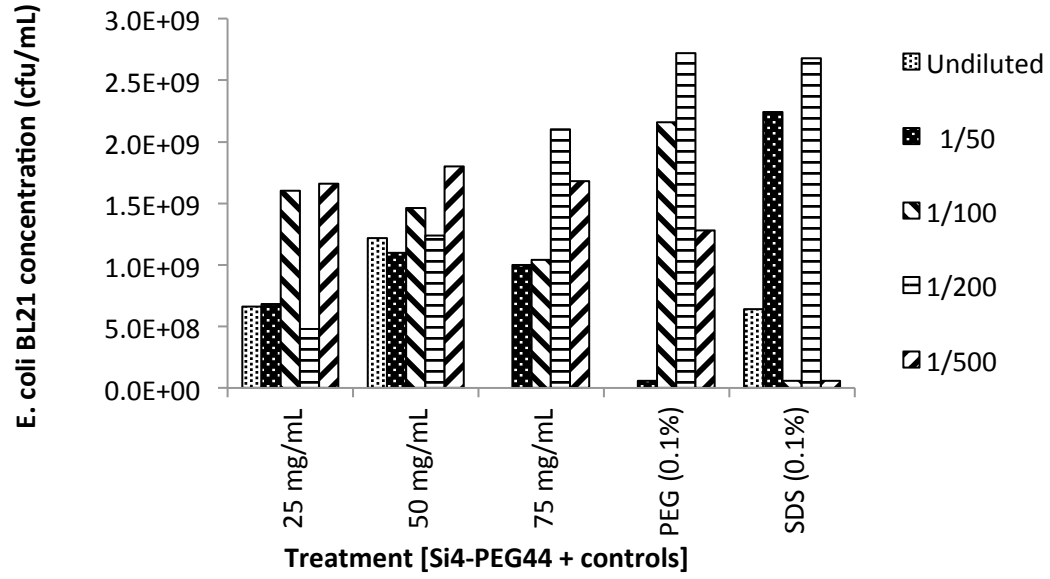

B.

Figure 3-26. **A)** Live:Dead fluorescence ratios of *E. coli* BL21 in response to **Si4-PEG44** and controls (fluorescence values are uncorrected). **B)** Results of the colony counts produced after treatment removal and growth of *E. coli* on LB agar plates.

3.9.4.8 ACR008-UP

NB: Unfortunately due to lab timings, the colony counts for ACR-008 UP could not be conducted.

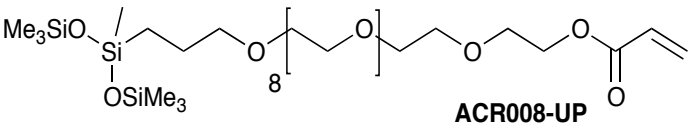

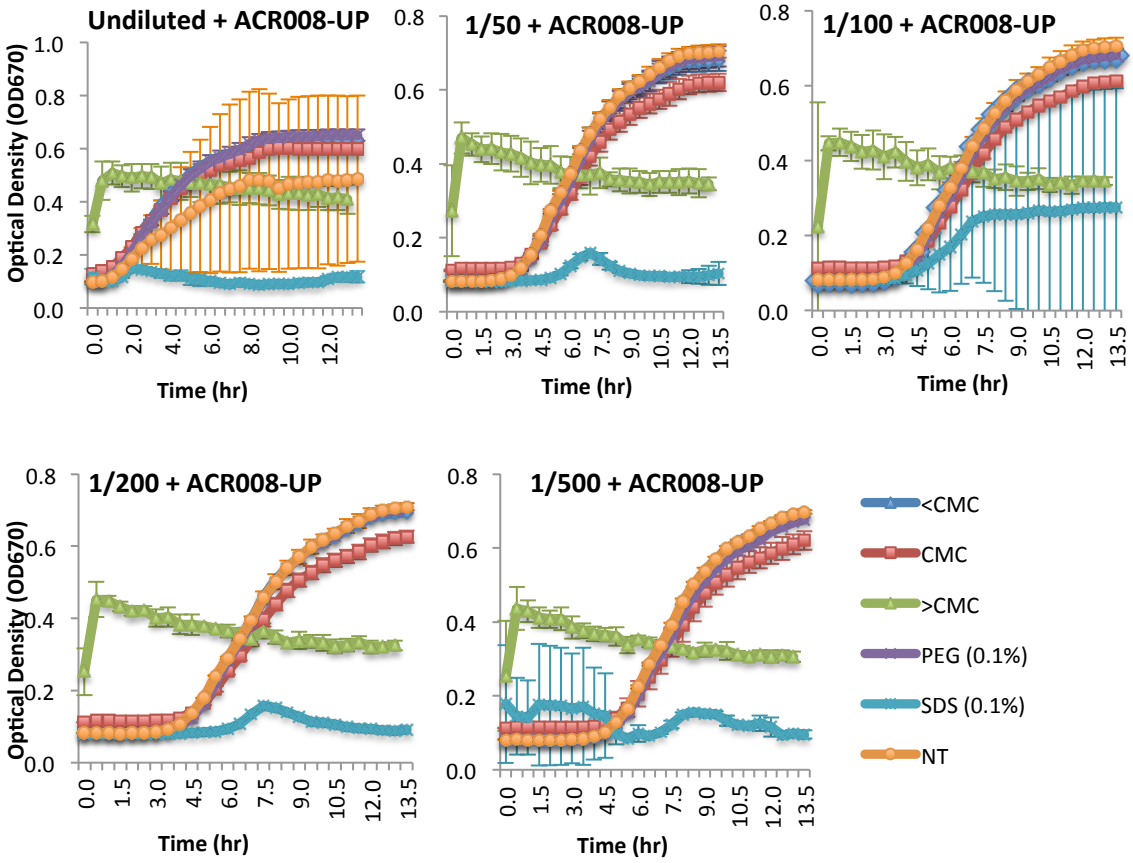

Figure 3-27. Growth curves of *E. coli* BL21 over ~24 hours in the presence of **ACR008-UP**. Graph titles indicate the differences in starting concentration of *E. coli* used (undiluted: 2 x 10^9 cfu/mL, 1/50: 1 x 10^6 cfu/mL, 1/100: 5 x 10^5 cfu/mL, 1/200: 2.7 x 10^5 cfu/mL, 1/500: 1.0 x 10^5 cfu/mL), while the error bars represent standard deviation from triplicate measurements.

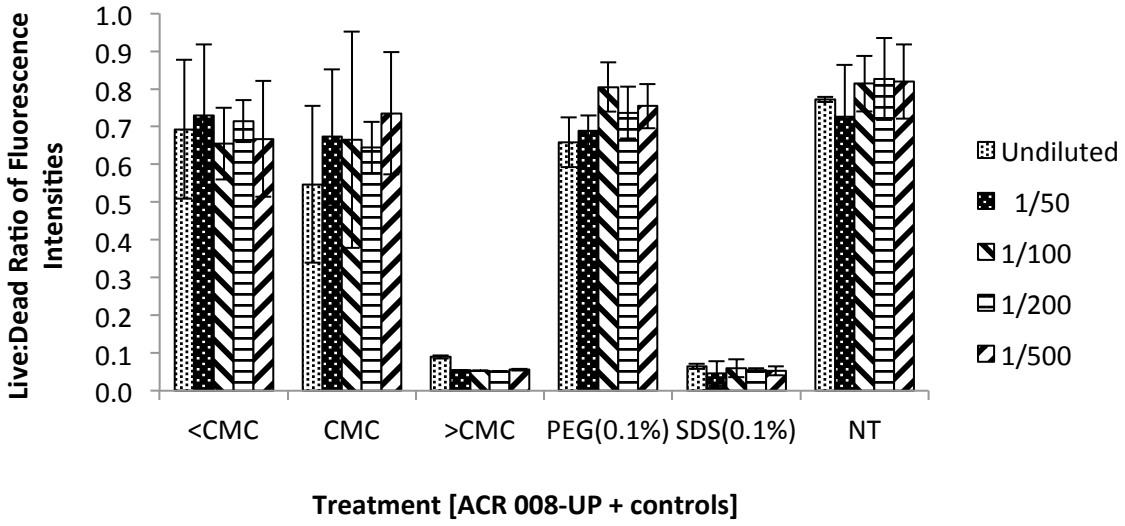

Figure 3-28. Live:Dead fluorescence ratios of *E. coli* BL21 in response to ACR and controls (fluorescence values are uncorrected).

3.9.5 Graphical summary of Live:Dead Ratios (LDRs)

NB: in the context of these experiments, the starting concentration of E. coli BL21 seemed to have little/no effect.

Si7-PEG15 vs. **Si7-PEG44,**

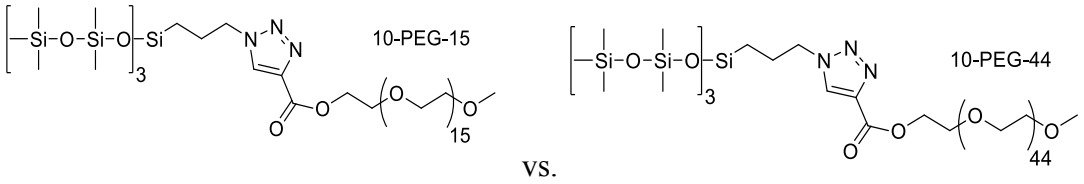

Si4Ph3-PEG15 vs. **Si4Ph3-PEG44**

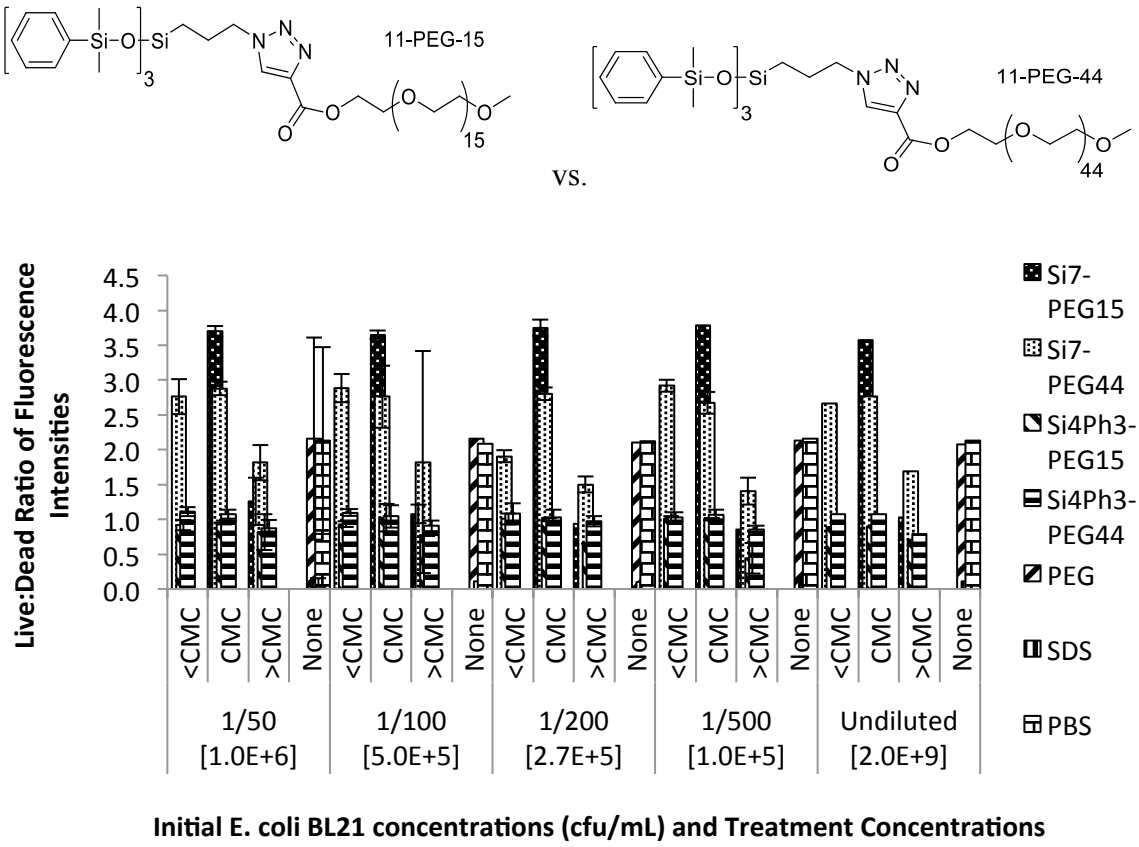

Figure 3-29. Live:Dead fluorescence ratios of *E. coli* BL21 in response to the PEG-chain length: 44 units **Si7-PEG44**, **Si4Ph3-PEG44** shown above vs. 15 units **Si7-PEG44**, **Si4Ph3-PEG44** shown above. The surfactant concentrations <CMC and >CMC correspond to 0.001 and 2.5 w/v % respectively, while the at CMC concentrations for Si7-PEG15, Si7-PEG44, Si4Ph3-PEG15 and Si4Ph3-PEG44 are 0.24, 5.2 x 10^5, 0.009 and 0.01 w/v % respectively. Errors bars represent the standard deviation (n=3), while the plotted fluorescence counts are uncorrected.

CHAPTER 4: Silicone elastomers modified with nonionic silicone polyether surfactants can be cytophobic and non-bactericidal[§§]

4.1 Abstract

The modification of silicone-based biomaterials to produce hydrophilic, wettable interfaces has received much attention. Such a surface might limit biofilm formation without promoting bacterial resistance, since it could prevent adhesion without killing bacteria. Superwetting silicone polyether surfactants, which can promote greater water wicking than their hydrocarbon analogues, may be ideal surface modifiers for such surfaces. Consequently, 18 compounds were rationally synthesized or prepared using PEG backbones and terminal functionalities ranging from linear alkyl chains, to highly branched phenyl-containing hydrophobes. The former showed ~ 4x the antibacterial activity of the latter against gram-negative *Escherichia coli*, and others were similarly potent. These compounds were incorporated into homemade RTV silicone elastomers to yield materials with concentration-dependent transparency (11 – 92 % with 0-20 wt% of

---

[§§] This chapter is taken from a manuscript that is being prepared for submission by M. F. Khan, Y. Chen and M. A. Brook. Chen synthesized then characterized all the surfactants using NMR, before using them to create modified elastomers. Khan measured CMCs of the surfactants, characterized the materials, developed and performed all biological work, and wrote the manuscript with additions, edits and guidance from Brook.

the compound, respectively) and moderate to high hydrophilicity (~20 – 80°). The materials were further tested for contact-killing and cytophobicity to yield two promising anti-adhesive materials: different elastomers containing 0.5- 1 wt% of $(EtO)_3$Si-PEG-laurate and separately $(EtO)_3$Si-PEG-tBS had sessile drop contact angles of 39° and 76°, respectively (versus 103° for unmodified silicone), and both decreased *E. coli* adhesion by ~30-fold in comparison to controls. The $(EtO)_3$Si-PEG-tBS surface was additionally bactericidal and reduced the viable bacterial load in solution by a factor of 2.9 relative to unmodified silicone. Hence, with appropriate tuning of their chemical structures, silicone polyether surfactants can create cytophobic, non-biocidal surfaces.

4.2 Introduction

Over the years the rise in resistant microbes has necessitated the development of novel antibacterials or compounds that can limit the adhesion and propagation of bacteria.[1-3] This is particularly important in the context of biomedical implants that are silicone-based. While silicones in general possess several advantageous properties for biomaterials applications,[4-8] they can promote undesirable microbial adhesion[9-11] that, in turn, allows the growth of resistant pathogens in biofilms.

In general, the adhesion of cells to material surfaces is a complex phenomenon,[12] but one very commonly cited influence is that of the surface wettability. Specifically, this refers to the hydrophilic (water-loving) or hydrophobic (water-repelling) nature of the material: the latter is often characterized by water contact angles (CA) of more than 90°.[13, 14] Of these two characteristics, hydrophobicity is often implicated in increased bacterial

adhesion, even though the adhesion response to substrate wettability can be strain-dependent.[15] Conversely, hydrophilic surfaces are thought to create stable interfacial water layers that prevent direct contact between bacteria and the material, thereby reducing adhesion.[16]

Two notable examples include the increased resistance of silicones, which were modified with PEO-silane amphiphiles, to adhesion by bacteria and diatoms,[17] and the increased adhesion seen on hydrophobic silicone hydrogel contact lenses vs. their hydrophilic analogs.[18] In the first case,[17] $(EtO)_3Si(CH_2)_3$-oligodimethylsiloxane$_{13}$-block-poly(ethylene oxide)$_8$–OCH_3 was synthesized and crosslinked by α,ω-dihydroxypolydimethylsiloxane (M_n = 3,000 g mol^{-1}) in a 2:3 M stoichiometric ratio to create a modified silicone (CA ~72°). Confocal laser scanning microscopy was used to analyze the percent coverage by *Pseudoalteromonas sp.* on modified *versus* unmodified silicones; adhesion to the former was ~8x lower than the latter. Since increased hydrophilicity correlates to a reduction of bacterial adhesion, superwetting compounds (agents that cause water/liquids to spread on surfaces to near-zero contact angles, Figure 4-1)[19] may be even more efficient in this regard.

However, explaining adhesion to surfaces by their wetting properties alone is insufficient; the interfacial chemistry is a significant confounding variable in adhesion analysis.[20] This may explain the lack of a consensus on which surfaces (hydrophilic/hydrophobic) are better for microbial control. Cellulosic materials, for example, which are hydrophilic relative to silicones or polystyrene, allow for effective adhesion by *Clostridium thermocellum*; the bacteria may have adhesins with a cellulose-binding factor because its

attachment to cellulose is unaffected by changes in environmental factors like pH and temperature.[21] Such specificity in binding is only possible when moieties on the bacterial membrane interact with specific surface moieties on the substrate. Hence, it is important to select surface modifiers rationally and through a systematic process that considers both the structure-activity relationship of the compound, and the way it affects the physical properties of the interface.

In light of this, we previously studied the bioactivity of various nonionic, silicone polyether surfactants (including a commercially available superwetter) in solution.[22] The goal was to elicit some preliminary guidelines on structural design for antibacterial applications on surfaces. Silicone-based surfactants were chosen for their high surface activity [23] and unexplored potential as antibacterial agents. Accordingly, we found that among other things: (1) surfactants with smaller silicone head groups had almost 4 times the antibacterial activity of the larger analogues; (2) smaller PEG chains correlated with greater biocidal activity; and (3) that the addition of phenyl rings in the hydrophobe decreased the surfactants' overall cytotoxicity. These findings provided tentative design criteria for surfactants based on the type of antibacterial activity required (biocidal/adhesion resistant); a biocidal interfacial surfactant may need small, branched hydrophobes that can effectively interact with proximal bacterial membranes, while the hydrophobes of cytophobic surfactants may need highly branched, cyclic hydrocarbons (like phenyl rings) that, not only seem to interact poorly with cell membranes, but have also been linked with substantially reduced attachment of pathogenic bacteria (like *Pseudomonas aeruginosa*) to surfaces.[20]

In this study, we expand on our work in solution to surfaces. Accordingly, we have synthesized materials from novel silicone-based compounds that were either physically blended or chemically grafted into commercially available or homemade RTV (Room Temperature Vulcanization) silicone rubbers. The subsequent adhesion response of *Escherichia coli,* a model bacteria species, to these materials was studied. Knowing that antibacterial compounds can lose their potency when tethered onto surfaces,[24] but that silicone surfactants generally have unique surface-active properties, we hypothesized that it could be possible to formulate materials that were cytophobic but not necessarily cytotoxic. Bactericidal surfaces can facilitate the development of resistance in microbes if they are not 100% effective. By contrast, cytophobic materials would be advantageous in the context of implantable biomaterials because they would avoid biofilm formation that allows for microbial resistance.

4.3 Experimental

4.3.1 Materials

Sodium dodecyl sulfate (SDS) was purchased from Bioshop Inc. Sodium phosphate dibasic heptahydrate ($Na_2HPO_4 \cdot 7H_2O$), sodium phosphate monobasic ($NaH_2PO_4 \cdot H_2O$) and sodium chloride (NaCl) were purchased from Fisher Scientific, EMD Chemicals Inc. and Caledon Laboratories Ltd. respectively. Hydride-terminated PDMS (7-10 cSt., 1000-1100 g/mol based on the manufacturer's catalog; 1090 g/mol based on ^{1}H NMR analysis), silanol terminated PDMS (2000 cSt., 36,000 g/mol) and bis(trimethylsiloxy)methylsilane

were purchased from Gelest; *t*-butylchlorodimethylsilane, chloro(dimethyl)phenylsilane, chloro(methyl)diphenylsilane, triethoxysilane, tetraethyl orthosilicate ($Si(OEt)_4$), lauric acid, imidazole, *p*-toluenesulfonic acid, Karstedt's platinum catalyst ($Pt_2(H_2C{=}CHSiMe_2OSiMe_2CH{=}CH_2)_3$), isopropyl-beta-D-thiogalactopyranoside (IPTG) and triethylamine were acquired from Sigma Aldrich. Polyethylene glycol monoallyl ether was kindly provided by Clariant as a gift. Siltech Corp provided **ACR-008 UP** (called **ACR** throughout the text) that was used as received. Sylgard 184 silicone elastomer kit was purchased from Dow Corning. The solvents used in this study were dried by passage through an activated alumina column under a nitrogen stream before use. α,ω-Bis-allyl-PEG was synthesized as described elsewhere.[25]

Escherichia coli (*E. coli*) BL21(DE3)pLyS was obtained from the Promega Corporation. Bacto™ yeast extract, Difco™ granulated agar, and Bacto™ tryptone were purchased from Becton, Dickinson and Company (BD). A live-dead *Bac*light™ Bacterial Viability kit (L-7012) was acquired from Invitrogen Life Technologies.

4.3.2 Methods

4.3.2.1 Surfactant synthesis

A total of 18 compounds were received or prepared, each with a PEG backbone and different terminal functionalities (Figure 4-1). All the compounds were rationally selected based on previous work (Chapter 3; Section 4.9.1 (Appendix)). Some of the 18 compounds were commercially available superwetters **4** and **16 (ACR)** while others were novel silicone surfactants (e.g., **1-3, 5-7**). The interfacial behavior of these were compared

with coupling agent molecules that could chemically graft into silicone elastomers (**8-11**) and triblock surfactants (**14**, **15**, **18**) on their own, and when contained in/on a silicone elastomer. The synthesis of the compounds shown in Figure 4-1 is described below.[***] Throughout the chapter, the compounds are referred to by their numbers; the compound names are provided in the synthesis. All ^{1}H and ^{13}C NMR spectra were recorded at room temperature on a Bruker AV-200 (at 200.13 MHz for protons and 50.3 MHz for carbon, respectively) or a Bruker AV-600 (at 600.13 MHz for protons, and 150.9 MHz for carbon, respectively).

[***] Note, compounds **12** and **13** are also commercially available; hence the synthetic protocol is not provided. Chen will provide details on the synthesis for compounds **2** (ally-PEG-TES) and **17** (TES-PEG-PDMS-PEG-TES) before manuscript submission.

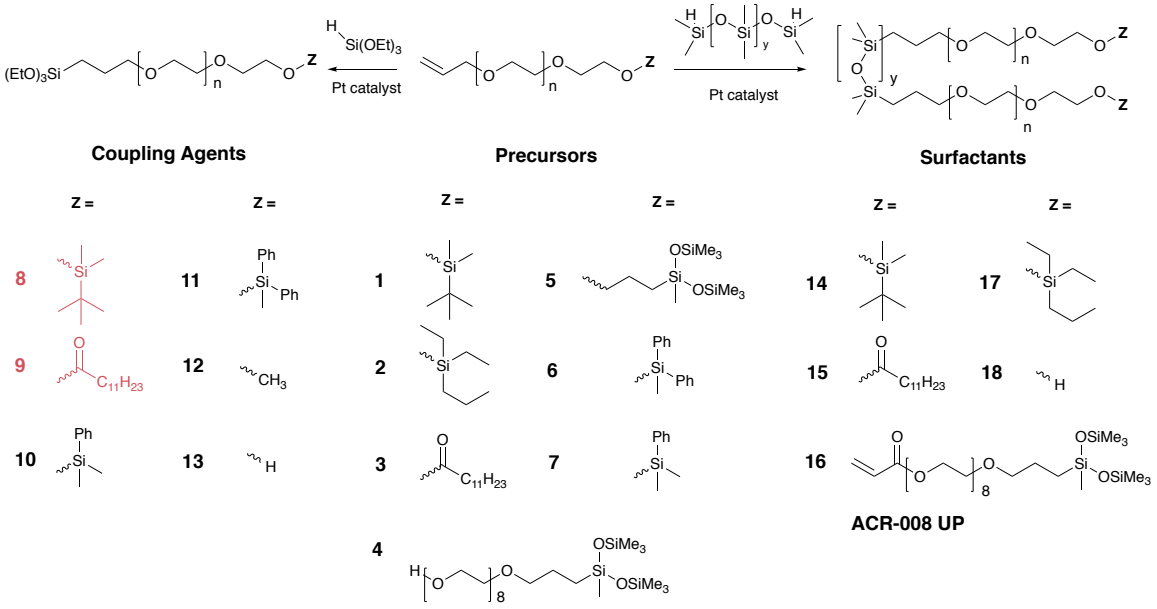

Figure 4-1. Structures of the various compounds tested. The middle column refers to the precursor or starting molecules, which are generally represented by the acrylate- and Z-terminated structure above this column. A triethoxysilane-terminated ($(EtO)_3Si$) coupling agent could then be added to precursors to produce compounds in the column to the left, **or**, the precursors could be used to create surfactant structures in the column to the right. The red structures (**8** and **9,** coupling agents with a *tert*butylsilane (*t*BS) and laurate functionality, respectively) produced the most interesting biological results and become the focus of this work.

4.3.2.1.1 Synthesis of compound **1**: allyl-PEG-*t*BS

To a mixture of polyethylene glycol monoallyl ether (MW 4.0 g, 10.3 mmol) and imidazole (0.70 g, 10.3 mmol) in dry THF (mL) was slowly added *t*-butylchlorodimethylsilane (1.60 g, 10.4 mmol) in dry DCM (100 mL). The reaction mixture was stirred overnight at room temperature. The solvent was removed under reduced pressure, the residue was resuspended in diethyl ether and precipitate was filtered

off. Removal of ether gave the crude product as a yellow oil. The product was purified by dissolution in CH_3CN (150 mL), washing with hexane (3 x 30 mL) and drying *in vacuo*, 4.6 g of colorless oil (89% yield) **1** was obtained.

^{1}H NMR (δ, 200.13 MHz, $CDCl_3$): 0.04 (s, 6 H), 0.87 (s, 9H), 3.71 (m, 32H), 4.00 (d, 2H, *J*=5.6 Hz), 5.20 (dd, *J*=5.6, 1.4Hz, 2H), 5.89 (m, 1H) ppm. ^{13}C NMR (δ, 50.3 MHz, $CDCl_3$): -5.25, 18.4, 25.9 (3C), 62.7, 69.4-70.7 (C of repeat EO), 72.2, 72.6, 117.1, 134.7 ppm.

4.3.2.1.2 Synthesis of compound **3**: allyl-PEG-laurate

A mixture of polyethylene glycol monoallyl ether (4.0 g, 10.3 mmol), lauric acid (2.06 g, 10.3 mmol) and *p*-toluenesulfonic acid (0.010 g, 0.06 mmol) in toluene was refluxed at 110-115 °C using a Dean-Stark trap for continuous removal of water for 5 h. After reaction, the mixture was washed with saturated sodium bicarbonate, twice with water and once with saline, respectively. The organic phase was collected and dried over sodium sulfate, filtered and the solvent removed in vacuo to give *allyl-PEG-laurate* as a colorless oil **3**. Yield: 5.02 g (83%).

^{1}H NMR (δ, 200.13 MHz, $CDCl_3$): 0.85 (t, 3H, *J*=6.0 Hz), 1.23 (m, 6H), 1.59 (m, 2H), 2.30 (m, 2H), 3.66 (m, 30H), 4.01 (d, 2H, *J*=5.6 Hz), 4.18 (m, 2H), 5.18 (dd, *J*=5.6, 1.4Hz, 2H), 5.89 (m, 1H) ppm. ^{13}C NMR (δ, 50.3 MHz, $CDCl_3$): 14.0, 22.5, 24.7, 29.0, 29.1, 29.2, 29.3, 29.4, 31.7, 34.0, 63.2, 69.4-70.7 (C of repeat EO), 72.0, 72.3, 116.8, 134.6, 173.5 ppm.

4.3.2.1.3 Synthesis of compound **5:** allyl-PEG-propylSiMe(OTMS)$_2$

To a solution of *α,ω*-bis-allyl-PEG (4.74 g, 10 mmol) and bis(trimethylsiloxy)methylsilane (2.22 g, 10 mmol) in toluene (50 mL) was added Karstedt's catalyst (10 mL, ~1.0×10^{-3} mmol Pt); the reaction was stirred at room temperature for 5 h. After reaction, the residue of Karstedt's catalyst was removed by activated carbon and volatiles were removed *in vacuo*. The product was purified by dissolved crude product in water (150 mL), washed with hexane (3 x 30 mL), and extracted with CH_2Cl_2 (5 x 30 mL); the CH_2Cl_2 extract was dried over anhydrate Na_2SO_4 filtered, and dried *in vacuo*, giving bis-PEG-allyl as a colorless oil, 4.76 g (68% yield).

^{1}H NMR (δ, 200.13 MHz, $CDCl_3$): -0.02 (s, 3 H), 0.06 (m, 18H), 0.42 (m, 2H), 1.55 (m, 2H), 3.38 (m, 2H), 3.62 (m, 42H), 4.01 (d, 2H, *J*=5.6 Hz), 5.20 (dd, *J*=5.6, 1.4Hz, 2H), 5.86 (m, 1H) ppm. ^{13}C NMR (δ, 50.3 MHz, $CDCl_3$): -0.56, 1.67, 13.3, 23.0, 69.2, 69.6-70.3 (C of repeat EO), 71.9, 73.8, 116.7, 134.6 ppm.

4.3.2.1.4 Synthesis of compound **6:** allyl-PEG-OSi(Me)Ph$_2$

Poly(ethylene glycol) monoallyl ether, allyl-PEG-OH (MW=388, based on ^{1}H NMR) (16.70 g 0.043 mole) and imidazole (2.93 g, 0.043 mole) were dissolved in 100 mL DCM. To the mixture chloro(methyl)diphenylsilane (10.01 g, 0.043 mole) was added dropwise; during the addition a white precipitate formed. The reaction mixture was allowed to stir at room temperature for 4 h. The white precipitate was filtered off, and washed with DCM (10 mL) twice. The combined DCM solutions were passed through a short silica column (4.0 g silica) to remove imidazole residue. The solvent was

evaporated, the residue was redissolved in CH_3CN (80 mL), and extracted with hexane twice(15 mL each time) to remove unreacted chlorosilane. After removal of solvents, a colorless oil was obtained (21.79 g, 87% yield).

^{1}H NMR (δ, 600.13 MHz, $CDCl_3$): 0.57 (s, 3 H), 3.61~3.68 (m, 30H), 3.87 (m, 2H), 4.04 (d, 2H, *J*=5.6 Hz), 5.24 (m, 2H), 5.93 (m, 1H), 7.38 (m, 6H) and 7.61 (d, 4H, *J*=6.4 Hz) ppm. ^{13}C NMR (δ, 150.9 MHz, $CDCl_3$): -2.91, 63.0, 69.5, 70.4 (C of repeat EO), 72.2, 72.4, 117.1, 127.8, 130.0, 134.2, 134.4, 134.8 and 136.1 ppm.

4.3.2.1.5 Synthesis of compound **7**: allyl-PEG-OSi(Me_2)Ph

Poly(ethylene glycol) monoallyl ether, allyl-PEG-OH (MW=388, based on ^{1}H NMR) (22.74 g 0.059 mole) and imidazole (3.99 g, 0.059 mole) were dissolved in 100 mL DCM. To the mixture was added chloro(methyl)diphenylsilane (10.00 g, 0.059 mole) dropwise; during the addition a white precipitate formed. The reaction mixture was allowed to stir at room temperature for 4 h. The white precipitate was filtered off, and washed with DCM (10 mL) twice. The combined DCM solutions were passed through a short silica column (4.0 g silica) to remove imidazole residues. The solvent was evaporated, the residue was redissolved in CH_3CN (80 mL), and extracted with hexane twice (15 mL each time) to remove unreacted chlorosilane. After removal of solvents, a colorless oil was obtained (27.23 g, 89 % yield).

^{1}H NMR (δ, 600.13 MHz, $CDCl_3$): 0.29 (s, 6 H), 3.44~3.66 (m, 32H), 3.92 (d, 2H, *J*=5.6 Hz), 5.12 (m, 2H), 5.81 (m, 1H), 7.27 (m, 3H), 7.48 (d, 2H, *J*=6.40 Hz) ppm. ^{13}C NMR

(δ, 150.9 MHz, $CDCl_3$): -0.02, 64.1, 71.1, 72.1~72.3 (C of repeat EO), 74.0, 74.1, 118.7, 129.4, 131.3, 135.2, 136.5, 139.5 ppm.

4.3.2.1.6 Synthesis of compound **8**: $(EtO)_3$Si-PEG-tBS

To a mixture of *t*BS-PEG-allyl (8.00 g, 15.9 mmol) and triethoxysilane (2.75 g, 15.9 mmol) was added Karstedt's catalyst (10 mL, ~1.0×10^{-3} mmol Pt), the mixture was stirred at room temperature for 5 h. After reaction, the residue of Karstedt's catalyst was removed by activated carbon and volatiles were removed *in vacuo* giving *$(EtO)_3$-PEG-tBS* as a colorless oil, 8.92 g (83 % yield).

^{1}H NMR (δ, 600.13 MHz, $CDCl_3$): 0.00 (s, 6H), 0.57 (m, 2H), 0.83 (s, 9H), 1.16 (t, 9H, *J*=6.98 Hz), 1.63 (m, 2H), 3.38 (m, 2H), 3.48~3.66 (m, 32H), 3.70 (m, 2H) and 3.76 (dd, 6H, *J*=13.96, 6.98 Hz) ppm. ^{13}C NMR (δ, 150.9 MHz, $CDCl_3$): -5.29, 6.40, 18.3, 22.9, 25.9, 58.3, 62.7, 70.0, 70.6, 70.7, 72.6 and 73.6 ppm.

4.3.2.1.7 Synthesis of compound **9:** $(EtO)_3$Si-PEG-laurate

To a mixture of allyl-PEG-laurate (8.00 g, 14.0 mmol) and triethoxysilane, 2.42 g, 14.0 mmol) was added Karstedt's catalyst (10 μL, ~1.0×10^{-3} mmol Pt); the mixture was stirred at room temperature for 5 h. After reaction the catalyst residue was removed using activated carbon and volatiles were removed *in vacuo* giving *$(EtO)_3$-PEG-laurate* as a colorless oil, 8.96 g (86 % yield).

^{1}H NMR (δ, 600.13 MHz, $CDCl_3$): 0.00 (s, 6H), 0.57 (m, 2H), 0.84 (t, 3H, *J*=7.14 Hz), 1.18 (t, 9H, *J*=6.90 Hz), 1.21 (m, 18H), 1.57 (m, 2H), 2.28 (m, 2H), 3.39 (m, 2H), 3.53~3.66 (m, 32H), 3.70 (m, 2H) and 3.78 (dd, 6H, *J*=13.96, 6.90 Hz) and 4.18(m, 2H) ppm. ^{13}C NMR (δ, 150.9 MHz, $CDCl_3$): 6.41, 14.1, 18.3, 22.6, 22.9, 24.9, 29.1, 29.2, 29.3, 29.4, 29.6, 31.9, 34.2, 58.2, 63.3, 69.2, 70.0-70.6 (C of repeat EO), 73.6 and 173.8 ppm.

4.3.2.1.8 Synthesis of compound **10**: $(EtO)_3$Si-PEG-propylSiMe_2Ph

To a mixture of allyl-PEG-OSi(Me_2)Ph (8.04 g, 15.4 mmol) and triethoxysilane, 2.66 g, 15.5 mmol) was added Karstedt's catalyst (10 μL, ~1.0×10^{-3} mmol Pt), the mixture was stirred at room temperature for 5 h. After reaction the catalyst residue was removed by filtration through activated carbon and volatiles were removed *in vacuo* giving *$(EtO)_3$-PEG-OSi(Me_2)Ph* as a colorless oil (9.70 g, 91 % yield).

^{1}H NMR (δ, 600.13 MHz, $CDCl_3$): 0.29 (s, 6 H), 0.54 (m, 2H), 1.14 (t, 9H, *J*=6.96 Hz)), 3.34 (m, 2H), 3.45~3.66 (m, 30H), 3.72 (dd, 6H, *J*=13.96, 6.96 Hz), 3.77(m, 2H), 7.27 (m, 3H) and 7.48 (d, 2H, *J*=6.42 Hz) ppm.

4.3.2.1.9 Synthesis of compound **11**: $(EtO)_3$Si-PEG-propylSiMePh_2

To a mixture of allyl-PEG-OSi(Me)Ph_2 (5.76 g, 9.9 mmol) and triethoxysilane, 1.71 g, 9.9 mmol) was added Karstedt's catalyst (10 μL, ~1.0×10^{-3} mmol Pt), the mixture was stirred at room temperature for 5 h. After reaction the catalyst residue was removed with activated carbon and volatiles were removed *in vacuo* giving *$(EtO)_3$-PEG-OSi(Me)Ph_2* as

colorless oil (6.90 g, 92.5% yield). ^{1}H NMR (δ, 600.13 MHz, $CDCl_3$): 0.56 (m, 2H), 0.58 (s, 3 H), 1.15 (m, 9H), 1.62 (m, 2H), 3.35 (m, 2H), 3.50~3.57 (m, 30H), 3.73 (m, 6H), 3.80 (m, 2H), 7.29 (m, 6H) and 7.51 (d, 4H, *J*=6.42 Hz) ppm.

4.3.2.1.10 Synthesis of compound **14**: *t*BS-PEG-PDMS-PEG-*t*BS

To a mixture of **1** (3.5 g, 7.0 mmol) and hydride-terminated PDMS (7-10 cSt., MW 1090, 3.8 g, 3.5 mol) was added of Karstedt's catalyst (20 mL, ~2.0×10^{-3} mmol Pt); the mixture was stirred at room temperature for 5 h. After reaction, the residue of Karstedt's catalyst was removed filtration through activated carbon and volatiles were removed in vacuo giving *tBS-PEG-PDMS-PEG-tBS* **7** as a colorless oil.

^{1}H NMR (δ, 200.13 MHz, $CDCl_3$): 0.07 (m, 102H), 0.55 (m, 4H), 0.89 (s, 18H), 1.56 (m, 4H), 3.41 (t, 4H, *J*=7.00 Hz), 3.55 (m, 58H), 3.761 (dd, *J*=5.6, 1.4 Hz) ppm. ^{13}C NMR (δ, 50.3 MHz, $CDCl_3$): -5.45, -0.08, 0.84-0.97 (C of repeat Me_2SiO monomers), 13.9, 18.1, 23.2, 25.7(3C), 62.5, 69.8-70.6 (C of repeat EO monomers), 72.5, 73.9 ppm.

4.3.2.1.11 Synthesis of compound **15**: laurate-PEG-PDMS-PEG-laurate

To a mixture of **3** (4.0 g, 7.0 mmol) and hydride-terminated PDMS (7-10 cSt., MW 1090, 3.8 g, 3.5 mol) was added Karstedt's catalyst (20 μL, ~2.0×10^{-3} mmol Pt), the mixture was stirred at room temperature for 5 h. After reaction, the residue of Karstedt's catalyst was removed filtration through activated carbon and volatiles were removed in vacuo giving laurate-PEG-PDMS-PEG-laurate **3** as a colorless oil.

^{1}H NMR (δ, 200.13 MHz, $CDCl_3$): 0.080 (m, 90H), 0.52 (m, 2H), 0.87 (s, 8H), 1.25 (m, 32H), 1.61 (m, 8H), 2.30 (m, 4H), 3.41 (m, 4H), 3.55 (m, 60H), 4.20 (m, 4H) ppm. ^{13}C NMR (δ, 50.3 MHz, $CDCl_3$): 0.01, 0.84-0.97 (C of repeat Me_2SiO monomers), 13.97, 14.02, 22.5, 24.8, 29.0, 29.18, 29.2, 29.3, 29.5, 31.8, 34.1, 63.2, 69.1, 69.8-70.6 (C of repeat EO), 72.4, 74.1, 173.7 ppm.

4.3.2.1.12 Synthesis of compound **18**: HO-PEG-PDMS-PEG-OH

To a mixture of polyethylene glycol monoallyl ether (3.88g, 0.01mol) and hydride-terminated PDMS (7-10 cSt., MW 1090, 5.45g, 0.005mol) was added Karstedt's catalyst (20 mL, ~2.0×10^{-3} mmol Pt); the mixture was stirred at room temperature for 5 h. After reaction, the residue of Karstedt's catalyst was removed by filtration through activated carbon and the volatiles were removed in vacuo giving *HO-PEG-PDMS-PEG-OH* **A** as a colorless oil.

^{1}H NMR (δ, 200.13 MHz, $CDCl_3$): 0.06 (m, 52 H), 0.52 (m, 4H), 1.59 (m, 4H), 3.40 (m, 4H), 3.64 (m, 60H) ppm. ^{13}C NMR (δ, 50.3 MHz, $CDCl_3$): -5.25, 18.36, 25.9 (3C), 62.7, 69.4-70.7 (C of repeat EO), 72.2, 72.6, 117.1, 134.7 ppm.

4.3.2.2 Critical Micelle Concentrations (CMCs)

Pendant drop tensiometry was used to approximate the CMCs for compounds **1**, **2**, **3**, **14**, **15**, **16** (ACR, and the precursors and surfactants containing *t*BS, laurate and TES functionalities). Both the laurate and *t*BS surfactants were shown to confer long-term superwetting properties to simple PDMS elastomers in previous work done by Chen.

Knowing the CMCs was necessary so that the biocidal activity of surfactants in solution, could eventually be measured at appropriate concentrations above the CMC.[26] Dispersions containing different concentrations of each these surfactants (1×10^{-6}, 1×10^{-1}, 1, and 10 w/v % in distilled water) were prepared. Using a standard goniometer/tensiometer setup, with a flat-top, pre-rinsed needle suspended in front of an illuminated screen and camera, the most dilute concentration of one surfactant was gently pushed through the needle to create a droplet that was on the verge of falling. A photo was taken at this point, after which fresh drops were squeezed through the syringe to achieve triplicate measurements. The entire process was repeated from most the dilute to the most concentrated dispersion for each surfactant. Care was taken to rinse the needle and syringe with isopropanol between each type of surfactant. The photographs were subsequently analyzed using the Fiji Pendant Drop Plugin (see section 4.9.2 (Appendix) for sample photos and analysis protocol). The plugin uses the Young-Laplace equation to calculate surface tension - the averages of these are plotted in Figure 4-3.

4.3.2.3 Surfactant cytotoxicity in solution

Luria-Bertani (LB) agar plates were created using 10 g of tryptone, 5 g of yeast extract, 10 g of NaCl, 15 g of agar and 1 L of deionized water (dH_2O), in accordance with accepted protocol.[27] A one-liter stock solution of 0.9% PBS (2.21 g of $NaH_2PO_4 \cdot H_2O$, 11.26 g of $Na_2HPO_4 \cdot 7H_2O$, 9 g of NaCl, 1 L dH_2O (pH 7.4)) was made, sealed, autoclaved and stored at room temperature. LB media (same recipe as for agar plates minus the agar for one liter of LB) was made in required quantities per experiment, autoclaved prior to use and stored at room temperature in between experimental steps.

The sterility of all materials, including pipette tips, was maintained throughout, with all work conducted aseptically in the biosafety cabinet (BSC).

Prior to each of the bacterial experiments detailed below, approximately 50 µL of *E. coli* culture broth were streaked on an agar plate that was incubated at 37 °C overnight in a VWR® Digital laboratory incubator (Model: 1546). Multiple colonies (3-4) were obtained from the resultant lawn using an autoclaved pipette tip and a new vial of broth (5 mL) was inoculated with the same. The vial was incubated for ~12 h at 250 rpm and 37 °C in a Thermo Fisher Scientific Inc. MaxQ8000 Orbital shaker, after which 250 µL of the overnight culture was used to inoculate 50 mL of fresh LB media in a culture flask. The flask was incubated at the same conditions as its predecessor, and the OD_{600} of the dispersion was measured every hour for the first 2 h using the TECAN Infinite® M200 PRO multimode reader, and then every 30 min until the OD_{600} measured 0.5. At this point, the dispersion was treated differently depending on the experiment to be run.

In order to assess the biocidal activity of surfactants in solution, 16 different representative compounds from Figure 4-1 were mixed with PBS (100 mg/mL) to create surfactant solutions at a concentration above their CMC; as previously reported, nonionic silicone surfactants show bioactivity at higher concentrations.[22] Briefly, an overnight *E. coli* culture of 50 mL at OD_{600} = 0.5 was centrifuged to re-disperse the bacteria in PBS. Autoclaved LB media, the bacterial mixture, and the surfactant dispersions were transferred to a fresh 96-well, BD Falcon microplate (each well contained 87.5 µL, 5 µL and 92.5 µL of each surfactant solution respectively). The plate was incubated in a TECAN M200 plate reader for 12 h (37 °C, orbital shaking at amplitude 3), following

which the contents of each well were transferred into correspondingly labeled 2.0 mL flat-top microtubes and centrifuged at 5000 g for 5 min. The supernatant was discarded and the pellet was re-suspended with gentle vortexing (5-6 s, speed 2) in 185 μL of autoclaved PBS. After an additional wash step (centrifugation and re-dispersion), the mixture from each tube was transferred into the corresponding well of a Greiner 96-well black microplate. Exactly 185 μL of live-dead stain (SYTO 9 dye (14.15 μL, 3.34 mM), propidium iodide (14.15 μL, 20 mM), 4.7 mL of filter-sterilized milliQ water) was mixed in each well. After 15 min of incubation, the plate was transferred to the TECAN Infinite® M200 PRO multimode reader where the fluorescence intensity was read from the bottom after gain optimization using an excitation wavelength (λ_{exc}) of 485 nm and emission wavelengths (λ_{emi}) of 530 nm (live) then 630 nm (dead). The ratio of live:dead fluorescence counts was plotted (Figure 4-4).

4.3.2.4 Preparation of surfactant-modified elastomers

Eight compounds (**8**-**15**) were chosen for incorporation into polymers that were made from a defined RTV silicone synthesized in-house. Each compound was added to the pre-elastomer mix in different concentrations (0.5, 1, 2, 5, 10, and 20 wt%), before the mixture was cured by Pt-induced hydrosilylation or Sn-catalyzed hydrolysis and condensation. Note that compounds **14** and **15** were the chemically inactive – *t*BS- and – laurate-terminated surfactants, respectively; they lacked a terminal triethoxysilane to serve as a coupling agent. Hence, these compounds were only physically blended into the

final elastomers and not grafted like the other 6 compounds. Previous work by Chen indicated that the bulky structure of surfactants **14** and **15** allows relatively stable interfacial anchoring of the surfactant in the elastomer,[†††] hence, their physically blended materials were deemed suitable for biological characterization. Compounds **8**, **9, 14** and **15** (10 wt% each) were further crosslinked or blended into a commercial RTV silicone mixture, for which the ingredients are only partly known. Such a polymeric system was considered an interesting comparison to those based on the homemade RTV. After all the materials were synthesized, a 0.635 mm punching tool was used to obtain circular discs (n = 3, ~0.5 mm thick) from each material that were placed in separate wells of a 96-well microplate. Care was taken to ensure discs were inserted in the correct orientation; the air-polymer interface prior to punching was placed facing upwards when the discs were put in the plate. Silicones can undergo dynamic rearrangement and different concentrations of surfactants could present at the air or polymer interface. Placing all the interfaces face up (during biological characterization of the materials) permits a consistent response to be obtained.

4.3.2.5 Light transmittance and surface wettability of modified elastomers

Coupons of each polymer and controls (n = 4 for each type) were placed in a 96-well Greiner transparent flat-bottom plate, and absorbance readings over the range of visible wavelengths (400-750 nm) at 10 nm intervals were obtained from a TECAN M1000 plate

[†††] Unpublished work.

reader. The absorbance values were converted to percent light transmittance using the following equation:

$$(1/10^{absorbance}) \times 100\% \quad (1)$$

Separately, the surface wettability of freshly punched coupons for each polymer (n = 3) was acquired by measuring their sessile drop CAs. A Future Digital Scientific high-speed contact angle measurer (Model: OCA20) was used to both dispense 5 µL of milliQ water onto each coupon, and to calculate the resulting angle made by the droplet at the interface. For most surfaces, the CA was acquired after a 3 min wait time, which ensured that any surface rearrangement[28-31] of molecules had occurred prior to measurement, and the drop was stable. The average light transmittance and contact angle data for representative materials are shown in Figure 4-5 and Figure 4-6, respectively. The remaining data can be found in section 4.9.3 (Appendix).

4.3.2.6 Biocidal activity of modified elastomers

Once the OD_{600} of an overnight 50 mL culture had reached 0.7, the bacteria was pelleted via centrifugation (5000 g, 5 min) and resuspended in an equivalent volume of autoclaved PBS. The new mixture was transferred into 2 microplates containing coupons for each material (100 µL/ well), before the plates were covered and placed in a VWR® symphony™ incubating plate shaker. After 2 h, the solutions from each well were aspirated into the corresponding well of a fresh black-well microplate, and mixed with 100 µL each of the live-dead stain (33 µL, 3.34 mM of SYTO 9 and 33 µL, 20 mM propidium iodide in 21 mL of filter-sterilized milliQ water). As before, after 15 min of

incubation, the fluorescence intensity of each plate was measured using the TECAN Infinite® M200 PRO multimode reader (λ_{exc} = 485 nm, λ_{emi} = 530 nm (live), 630 nm (dead)). The results were plotted in Figure 4-7 and Figure 4-8.

4.3.2.7 Cytophobicity of modified elastomers

IPTG (50 µL, 1 mM) was added to a 50 mL overnight culture of *E. coli* at OD_{600} = 0.5. The culture was re-incubated at 37 °C and 250 rpm for an additional 2 h. The bacteria were then harvested by centrifugation at 5000 g for 5 min, the supernatant was discarded, and the pellet was resuspended in 50 mL of autoclaved PBS via agitation. The mixture was then pipetted onto the modified surfaces (100 µL/well) and allowed to incubate at 24 °C and 250 rpm for ~ 12 h in the incubating plate shaker; note the plate had been wrapped in foil to prevent photobleaching of the GFP. After the allotted time, the PBS from each well was aseptically aspirated and discarded. PBS was used to rinse each surface three times to remove any loosely adhered bacteria; 100 µL was dispensed and aspirated twice/well to constitute one wash step (solutions from each wash were transferred into the corresponding well of a fresh Greiner black-well, non-binding microplate – hence three microplates were generated per plate full of polymers). Care was taken to use a fresh pipette tip for each rinse, and to aspirate the PBS in its entirety between each step. The GFP fluorescence intensity from the wash plates was then scanned using the TECAN infinite M200 plate reader (λ_{exc} = 395 nm, λ_{emi} = 509 nm, optimized gain), to ensure loosely adhered *E. coli* was indeed rinsed off (section 4.9.4 (Appendix)). Similarly, the surfaces in the original plates were scanned for GFP fluorescence intensity, the data for which is shown in Figure 4-9.

4.4 Results

4.4.1 Surfactant synthesis and characterization

4.4.1.1 Synthesis

Three types of PEG and PDMS block surfactants and crosslinkers were prepared: allyl PEG surfactants; $(EtO)_3Si$-terminated surfactants and triblock surfactants.

Heterofunctional PEG terminated with an OH at one end and Me or allyl group at the other end are commercial available. Silyl protected PEG terminated with an allyl group at one terminus (**1**, **5** and **6**) were prepared using classical routes; α-allyl-ω-hydroxy-PEG was reacted with the corresponding chlorosilane in the presence of imidazole in dichloromethane (DCM) at room temperature to give the silyl ethers in moderate to high yields. Allyl-PEG-laurate **3** was prepared using standard acid-catalyzed esterification in which the mixture was refluxed in toluene for 5 hours; the formed water was trapped in a Dean Stark apparatus.

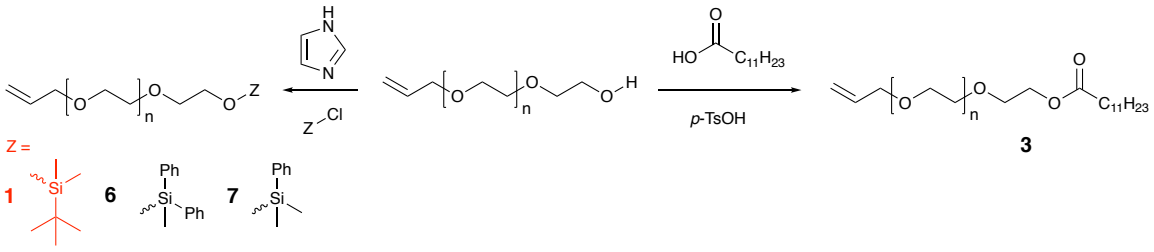

Figure 4-2. Synthetic route to wetting agents

Heterofunctional PEG terminated with an allyl group at one end and propyltriethylsilane

or propyltrisiloxane (propylSiMe$(OTMS)_2$) at the other end were prepared using hydrosilylation catalyzed by Karstedt's platinum catalyst to convert α-allyl-ω-hydroxy-PEG into α-allyl-ω-propyltriethylsilane-PEG **2** and α-ω-diallyl-PEG into α-allyl-ω-propyltrisiloxane **5**, respectively (Figure 4-1).

Hydrosilylation catalyzed by Karstedt's platinum catalyst was again used both to convert heterofunctional PEG **1**, **2**, **5**, **6** and **7** into functional PEG crosslinkers and PDMS block surfactants **14**, **15** and **17**. In the cases of functional PEG crosslinkers, triethoxysilane was reacted with a stoichiometric quantity of allyl-PEG silylether **1**, **6** and **7** or allyl-PEG-laurate, respectively. The triethoxysilyl group attached to PEG silylethers or PEG laurate can be used as an additional crosslinker when combined with a more traditional crosslinker, e.g., $Si(OEt)_4$, in RTV silicone elastomers. In such case, PEG silylether or PEG-laurate can be covalently linked to silicone elastomer's network.

The functional PEG PDMS block surfactants **14**, **15** were prepared by hydrosilylation reaction of **1** or **3** with hydride-terminated PDMS using Karstedt's platinum catalyst. The surfactants were all soluble in most organic solvents, but exhibited poor solubility in water.

The surfactants were introduced to a silicone elastomer in two different ways: the surfactants that were chemically active (**8-11**) were added to the pre-cured elastomer ingredients that were then induced to cure to give an elastomer; or the surfactants, which were not chemically active (**14**, **15**) were added into the pre-cured elastomer mixtures that were cured by Pt-induced hydrosilylation or Sn-catalyzed hydrolysis and condensation.

4.4.1.2 Critical Micelle Concentrations (CMCs)

Surfactant (**1**, **2**, **3**, **14**, **15**, **16)** dispersions of different concentrations were made via serial dilution for analysis by pendant drop tensiometry. The dispersions were stable at room temperature for at least 15 minutes, after which signs of phase separation were apparent in many cases. As can be seen from Figure 4-3, these materials do not exhibit the classic CMC curves for small organic surfactants because they contain relatively large silicone hydrophobes. Plots of surface tension against the weight percent of surfactants in distilled water showed changes in surface tensions from ~63 mN/m to an average of 28 mN/m, indicating that the approximate CMC for all surfactants lay in the (high) 1 -10 w/v% range. The most notable difference in surface tension was between compounds **14** and **15**, with the latter clearly lower than the former (29 and 21 mN/m, respectively). Interestingly, the apparent CMC of the small commercial surfactant ACR (0.03 w/v%), as per Figure 4-3, was an order of magnitude higher than that previously reported and provided by the manufacturer (0.001 w/v%).

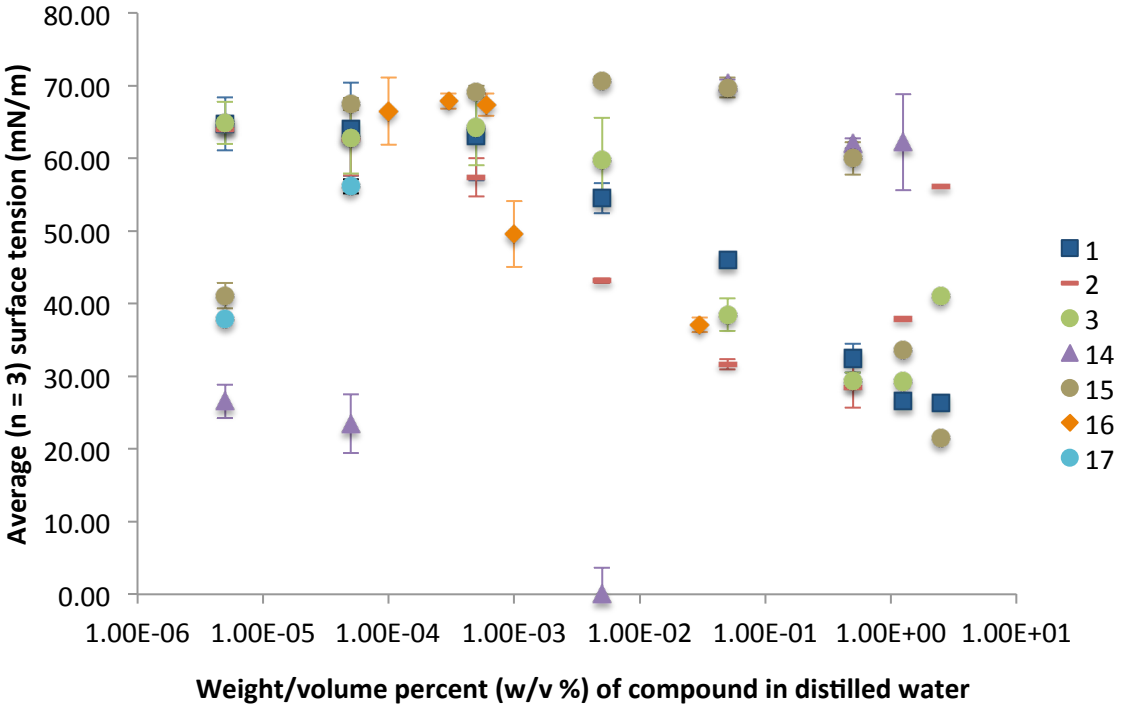

Figure 4-3. The approximate critical micelle concentrations (CMCs) of tested compounds as indicated by the dip in the curves seen in the graph. Compounds **1-3** correspond to the allyl-terminated precursor molecules with -*t*BS, -TES and laurate endgroups, respectively. Compounds **14**, **17** and **15** are surfactants based of the same functional groups, in that order. Compound **16** is the commercially available superwetter ACR. Error bars result from the standard deviation around the average.

4.4.1.3 Cytotoxicity of surfactants in solution

Based on Figure 4-3, 0.1 w/v% of each compound (Figure 4-1) was used to make dispersions in PBS. This concentration was greater than the CMCs of all the compounds; a necessary requirement to observe any bioactivity of silicone surfactants.[22] An overnight culture of *E. coli* was harvested for bacteria, which were re-suspended in PBS, and then incubated with the different surfactants for ~ 12 hours (control wells lacked a compound

but were otherwise identical to the treatment wells). A live-dead stain was then conducted (Figure 4-4). The most and least antibacterial compounds were **16** (ACR) and **7** (the allyl-terminated PEG with one phenyl ring), respectively, with LDRs of 0.12 and 0.89. The other phenyl-containing precursor **6** was also only mildly antibacterial, with comparable LDRs to compounds **8**, **10**, **11**, **14** and **17**. However, the compounds with smaller silane head groups (**2**, **4**, and the commercial wetting agents **5** and **16**) were about 4 times more active. Lastly, while surfactants **3**, **9** and **15** had similar, fatty acid-based structures compound **3** had antibacterial activity (LDR = 0.16) comparable to that of **9**, but was twice as potent as compound **15** (LDR = 0.35); 3 > 9> 15.

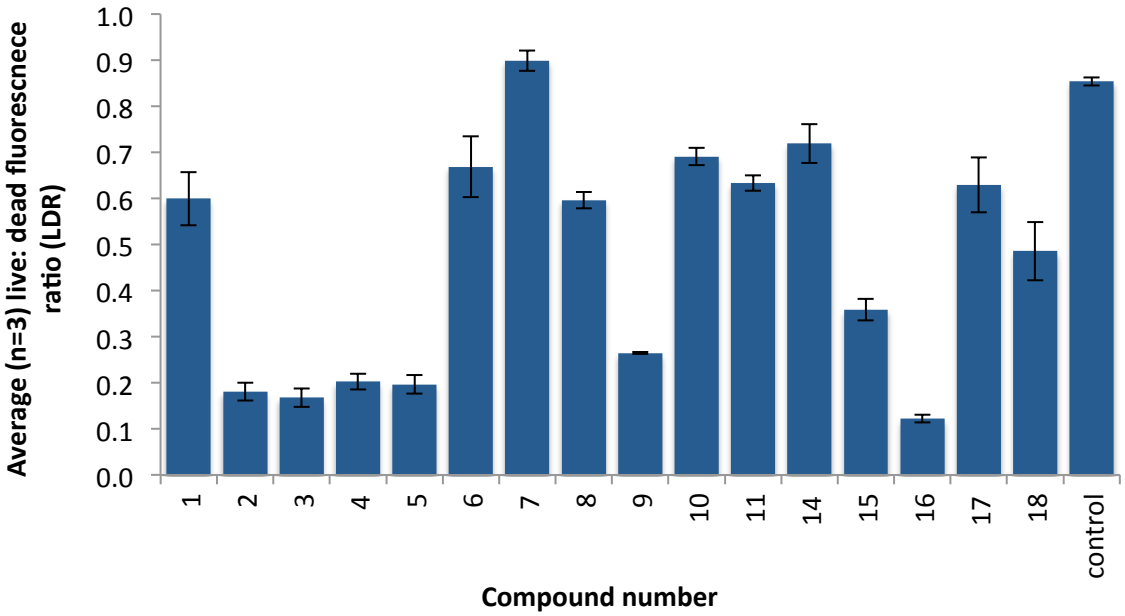

Figure 4-4. Average live:dead fluorescence ratios produced after *E. coli* was exposed to 0.1 w/v% of each compound for 12 hours. The error bars represent standard deviations around the mean. Fluorescence counts are uncorrected.

4.4.2 Surfactant-modified elastomers

Based on qualitative observations, the elastomeric materials appeared very smooth, with those containing 20 wt% of compound **7** demonstrating the most elasticity. All seemed to have comparable hardness when indented or handled with tweezers, with the exception of materials containing the surfactant with two phenyl rings in their hydrophobe (compound **11**). The elastomers of compound **11** were soft, easily deformed and tacky; materials containing ≥ 5 wt% of compound **11** were highly viscoelastic.

4.4.2.1 Light transmittance and surface wettability

Absorbance values were collected for elastomers in which the surfactants had been crosslinked into homemade RTV. The measurements were made using a TECAN M1000 plate reader, and then converted to percent transmittance, as an indication of optical transparency. The results for compound **8** (Figure 4-5) are representative of all the compounds (section 4.9.3 (Appendix)); all crosslinked materials containing high weight percentages of a surfactant (20, 10 wt%) had the lowest transmittances and were more opaque, while those with low concentrations of any surfactant (1, 0.5 wt%) had the highest transmittance (80-90 %). Materials with 5 wt% surfactant typically had median light transmittance values. This concentration-dependent effect on opacity suggests that at higher concentrations, the surfactants are forming separate domains of sufficient size to scatter light. A homemade RTV (the control elastomer with no surfactant) had the greatest optical transparency (92 %).

Note that elastomers in which the surfactants (**14**, **15**) were dispersed (physically blended)

produced grease-like droplets at the interface when handled with tweezers, especially at high surfactant concentrations. This indicates the presence of a second, mobile phase. The effect was visibly reduced at lower surfactant concentrations provided the material was carefully handled. As a consequence of a mobile phase within the elastomer, these materials were not deemed amenable for absorbance testing.

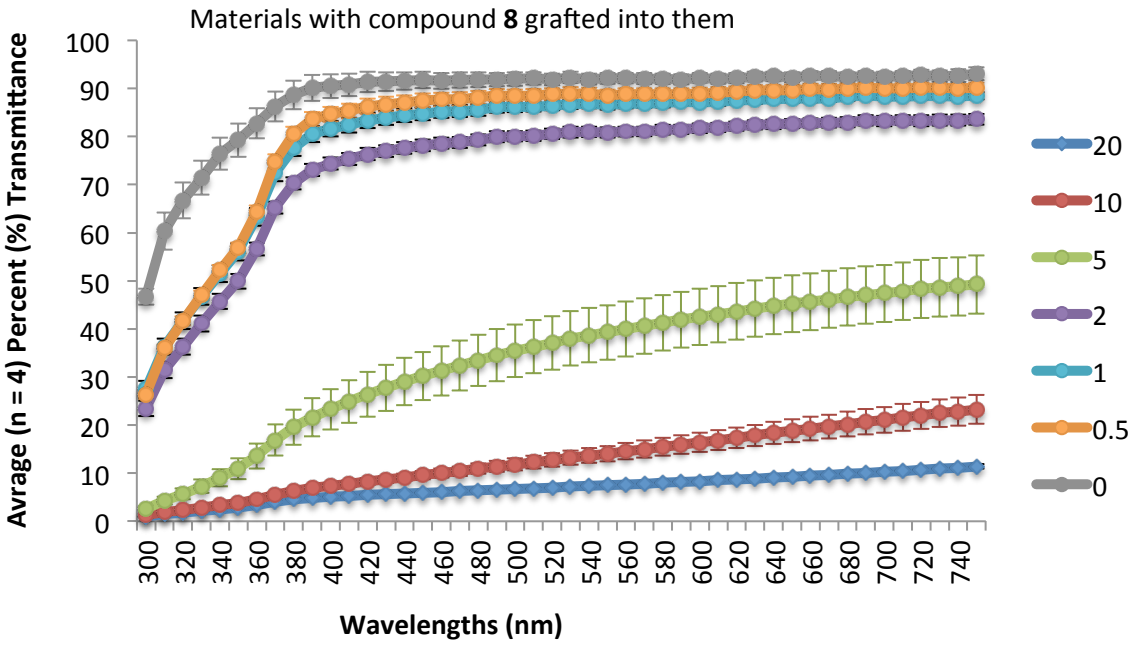

Figure 4-5. Average light transmittance data, across the range of visible light wavelengths, for homemade RTV modified with varying weight percentages (0-20 wt%) of the coupling agent **8.** The trends seen are representative of the light transmittance for all materials. The error bars are standard deviations around the average.

As with light transmittance, the surface wettability of most materials was also comparable. A standard goniometer was used to calculate the sessile drop contact angles of all surfaces in triplicates, and the averaged data indicated contact angles of ~80-100°

for the elastomers in which surfactants were crosslinked (Figure 4-6). The highest contact angle was seen for the control elastomer, homemade RTV (103°), followed by the surface containing cross-linked compound **8** (~80°). Materials into which **9** had been grafted showed significantly smaller contact angles (~40°), while the blend of compound **14** had the lowest (~20°). Interestingly, the contact angles in all cases were consistent across each the materials of different surfactants; the concentration of the surfactant in the system seemed to have to no effect on the interfacial contact angle.

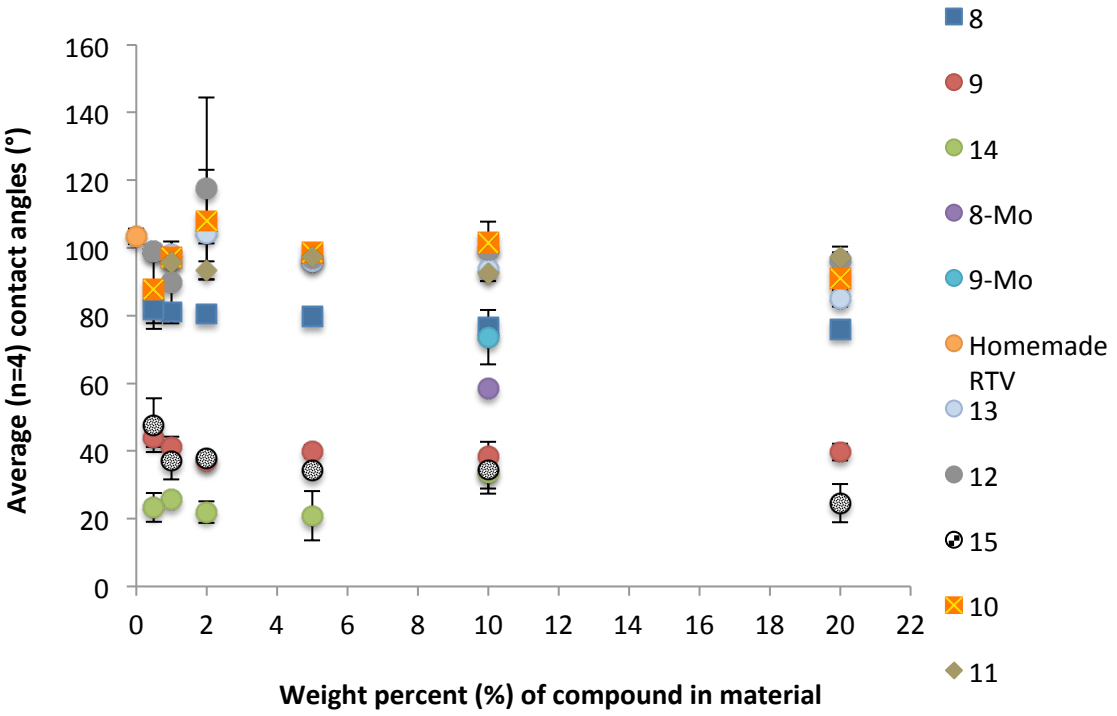

Figure 4-6. Water contact angles at the air-polymer interfaces. 'Mo' stands for Momentive™ silicone mixture (as opposed to all other materials made with homemade RTV and a surfactant). Error bars are standard deviations around the mean.

4.4.2.2 Contact-killing of E. coli by surfactant-modified silicone surfaces

Bacteria from an overnight culture were harvested and re-suspended in PBS, and the resulting mixture was transferred into microplates containing discs of each elastomer type in triplicate. After 2 hours of incubation at room temperature in a plate shaker, the fluid from each well was transferred into a fresh microplate and a live-dead stain was conducted. As with the contact angles, the weight percent of surfactant in the system had no effect on the bioactivity of the material for compounds **10, 11, 12** and **13** (Figure 4-7). For all these materials the LDR for the *E. coli* that had been exposed to the surface was ~0.8 and near identical to homemade RTV (LDR 0.79).

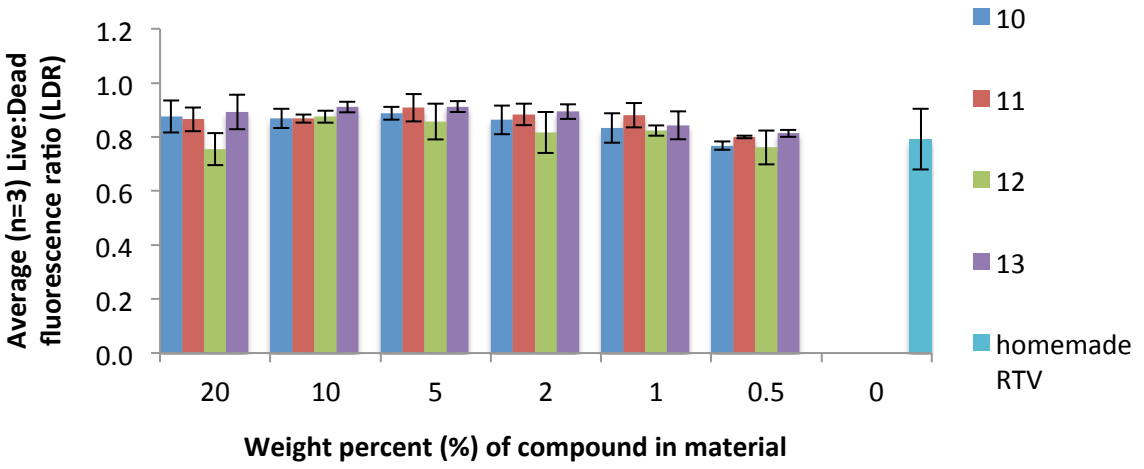

Figure 4-7. Average live:dead fluorescence ratios for *E. coli* after 2 hours of exposure to modified RTV materials with varying weight percentages of different compounds. Fluorescence counts are uncorrected while the error bars represent the standard deviation around the mean.

Differences, however, were observed between materials containing compounds **8** and **9**, respectively. Materials of the former showed up to 3 x the reduction in live bacteria than the control well, while latter allowed for the highest number of live bacteria in all the materials tested, and even more so than the control (LDR = ~1.3, control LDR = 0.78). Interestingly, this trend is a reversal of that seen for the antibacterial analysis of each compound in solution: the ester-based compound **9** was far more antibacterial than **8** in solution (had lower LDRs), but it seemed to lose its biocidal behavior when incorporated into silicone elastomers, while **9** gained it.

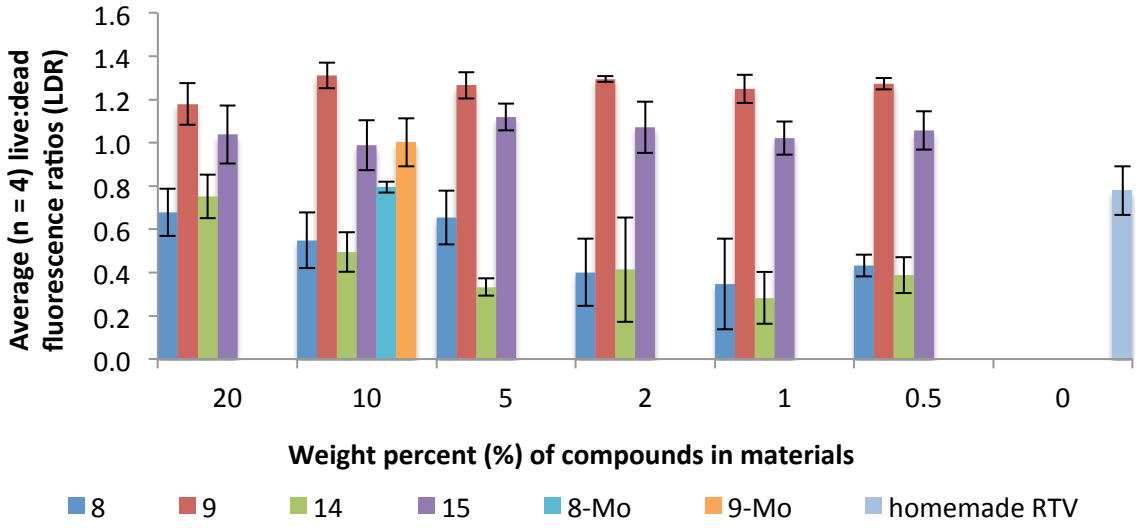

Figure 4-8. Average live:dead fluorescence ratios for *E. coli* after 2 h of exposure to modified RTV materials with varying weight percentages of different compounds. Fluorescence counts are uncorrected while the error bars represent the standard deviation around the mean.

4.4.2.3 Material cytophobicity

An overnight culture of *E. coli* was diluted and brought to its mid-exponential growth phase before the addition of IPTG. The culture was re-incubated and eventually harvested for its bacteria, all of which were re-suspended in PBS. The mixture was transferred into microplates containing the discs of each material type, and the whole set-up was placed in a microplate shaker overnight. PBS was then used to rinse each surface three times before being scanned for GFP fluorescence.

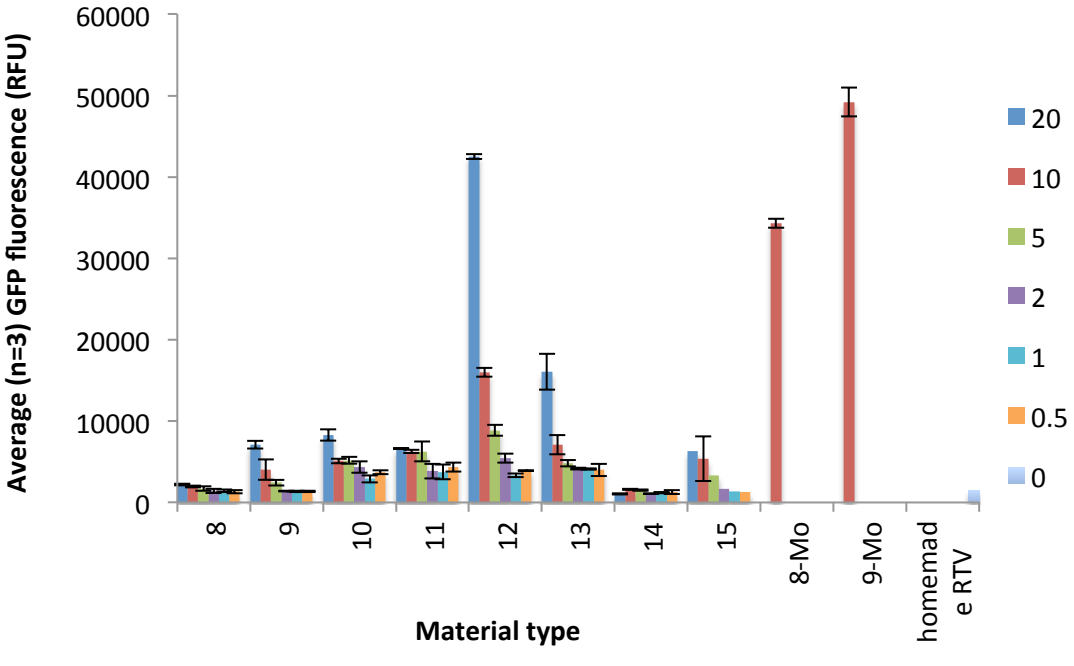

A

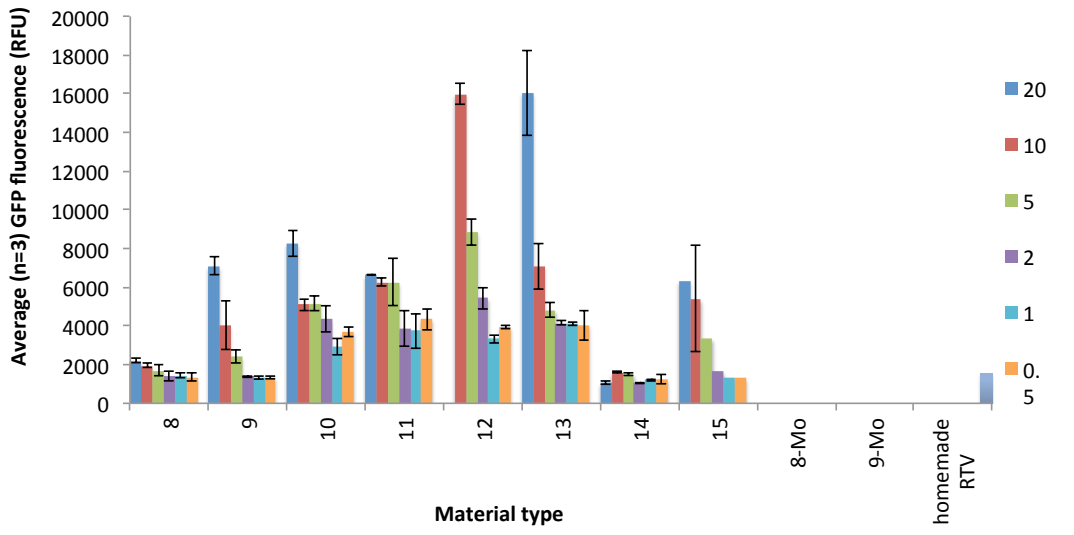

B

Figure 4-9. *E. coli* adhesion response to synthesized materials. (A) The adhesion response to the full set of materials; (B) Large fluorescence signals have been removed from 'A' to better see the adhesion trends. Error bars represent the standard deviation around the mean of triplicate measurements. Note that the fluorescence counts are uncorrected.

Interestingly, the fluorescence counts from almost all surfaces made from homemade RTV (that lacked fillers or other excipients) were significantly lower than that of the Momentive^{TM}-based controls (up to 38 x lower in the cases of compound **9** and the alkylsilane (**8)**-containing elastomers). A notable exception was the material made using 20 wt% of **12**, the relative fluorescence units (RFUs) for which were ~42,500 and comparable to that of the controls. In the absence of extreme values like this, a concentration-dependent affect on RFUs was observed (see Figure 4-9.B), such that the higher the weight percent of surfactant in the rubber, the higher the fluorescence counts. The effect of concentration seemed negligible in the case of surfaces for compound **8**.

4.5 Discussion

Antibacterial materials, and particularly anti-adhesive surfaces, are of great import in many aspects of healthcare, including biomedical devices. Anti-adhesive surfaces, for example, may dually limit post-operative infections and the development of microbial resistance by preventing bacterial colonization of implanted materials. In this regard, generating hydrophilic or wettable surfaces using surfactants has gained popularity, however, hydrophilicity alone cannot explain the adhesive response of bacteria to surfaces; the chemical nature of the interface matters. To examine this further, a range of nonionic, silicone surfactants (that have not been well studied previously) were synthesized for evaluation of their bioactivity in solution and in materials.

4.5.1 The similarity of critical micelle concentrations (CMCs)

The critical micelle concentration is the concentration at which the air-water interface is

saturated with surfactant molecules, such that the surfactants begin forming micelles or other aggregated structures in solution to shield their hydrophobic portions from the aqueous environment. Since the surfactant displaces water molecules at the hydrophobe interface, the surface tension of the liquid drops; the cohesive forces between water molecules are stronger than those between surfactant and water molecules. Hence, on a plot of surface tension versus surfactant concentration in solution, the lowest point at which the surface tension plateaus indicates the surfactant CMC. The CMC can be determined via several methods, however, shape analysis of pendant drops is both reproducible and convenient and was consequently used herein.

Compounds **1**, **3**, **14** and **15** had comparable CMC values, although compound **15** had a somewhat lower surface tension that that of **14** (Figure 4-3). This was surprising given that the CMC value is affected by the molecular structure of the compound, and these surfactants (particularly **14** and **15**, which have short and long chain terminal groups, respectively) vary significantly in this regard. The similarities in CMC may be due to timing of the photographs, which were taken instantly after the maximal, stable drop volume had been reached. While this deals with the issue of evaporative loss of fluid from the droplet, it may be problematic given the large, polymeric nature of the surfactants, and the time required for diffusion from the bulk phase to the interface. Hence, compounds **1**, **3**, **14**, **15** and **17** may exhibit a time-dependent variation in surface tension, the eventual stabilization of which might occur at slightly different concentrations, thereby indicating a difference in CMCs. A need for technique optimization may also explain why compound **16** (ACR) showed a higher CMC value than previously

reported.[22] Since the antibacterial activity of nonionic surfactants was shown to be greatest at above their CMC values,[22] tests for bioactivity should be conducted above this point and, therefore, it is important to know the correct CMCs. However, antibacterial testing in this report was conducted at concentrations much higher than the approximated CMC of each surfactant (Figure 4-3), hence, any measurement errors (as was possible with ACR) were deemed negligible.

4.5.2 Differential cytotoxicity in solution based on size and hydrophobe

The approximate values obtained via pendant drop analysis were used to create surfactant dispersions at concentrations above the CMCs of each compound. These mixtures were incubated with *E. coli* overnight (~12 hours), after which time the bacteria were isolated and subjected to a live-dead stain. Note that, given the length of *E. coli*-surfactant exposure, the effect of any time-dependent variation in saturation of the air-water interfaces by compounds (owing to their size differences) prior to micelle formation is likely negligible.

The results of solution toxicity seen in Figure 4-4 seem aligned with our previously published hypothesis on the antibacterial mechanism of action (MOA) for nonionic, silicone polyether surfactants. Namely, small molecules with simple (not hyperbranched) hydrophobes may better penetrate bilayers to solubilize membranes and cause lysis of *E. coli*. Accordingly, small surfactant molecules **2**, **4**, **5** and **16** showed the greatest antibacterial activity; the most toxic of these small molecules was **16** (ACR) which is unsurprising both because of well-documented cytotoxicity of acrylic monomers,[32, 33] and

the small size of the silicone hydrophobe. Note that both ends of such a heterofunctional PEG contribute to the overall antibacterial activity of a compound when it is *mobile* in solution. This was evident during a preliminary screen of ACR derivatives against *E. coli*, where replacement of the terminal acrylate with a hydroxyl group rendered the surfactant less bacteriotoxic (Figure 4-10, Appendix). It is likely that the two ends (acrylate and hydrophobe) have different MOAs in solution. It is proposed that, during incorporation into polymers, curing involves reaction of the acrylate such that any interfacial bioactivity of the resulting material will be linked to the silicone hydrophobe alone.

Compound **3** had potency similar to that of ACR, despite the larger laurate head group. However, this longer, linear alkyl chain may allow for better insertion between the structural lipids of a membranous bilayer, given that they too have linear fatty acid chains (16-18 carbons long).[34] Conversely, compounds with branched structures (**14**) or two phenyl substituents (**6**) had markedly lower antibacterial activity as would be expected for compounds that cannot easily insert into a cell membrane. The behavior of **7** is intriguing; it was less toxic than compound **10,** even though the only difference between the two compounds is in the endgroup (**7** has an allyl group instead of the ethoxysilylpropyl group of **10**). While a satisfactory explanation still needs to be found, this phenomenon may be explained by an orientation change for insertion into the bilayer. Perhaps, for example, the ethoxysilylpropyl of **10** is hydrophobic enough (in comparison to the allyl group of **7**) that it disrupts, to a small degree, the interactions between phospholipids in a bilayer (i.e., since the phenyl rings cannot insert into membranes, perhaps the other hydrophobic portion of the same molecule does). Only a few of these compounds exhibited biocidal

activity in solution. It is unclear at this stage whether they hold any benefit over traditional organic surfactants. However, it was still of interest to understand how the surface-active structures would affect the adhesion of bacteria to surfaces. Therefore, the compounds were incorporated into silicone elastomers to create novel materials, which were then characterized physically and biologically.

4.5.3 Concentration-dependent transparency and moderate hydrophilicity

Absorbance readings for all elastomers were measured using a standard microplate reader and then converted to percent light transmittance as an indication of transparency. The latter decreased with increasing concentration of each surfactant in the system such that 20 wt% materials appeared opaque and 0.5 wt % materials were highly transparent. This phenomenon may be attributed to the formation of surfactant-governed microdomains[35, 36] in the silicone rubber that prohibit the propagation of light through the system. With increasing surfactant concentration therefore, there may be a greater number of these domains and/or the domains may grow in size with surfactant concentration. Release of surfactants may be expected from these regions if the surfactant is not grafted into the rubber, as was observed during physical manipulation of materials **14** and **15**. Additionally, further studies to determine optimal domain sizes for specific refractive indices may be relevant if any of these materials are considered for ophthalmic applications.

Surface wettability of the materials was characterized by measuring the contact angle (CA) of a sessile drop on the air-material interface. This would allow comparison of

hydrophilicity to any bacterial adhesion resistance. Most materials exhibited only moderate wettability (73-108°), with the exception of materials containing physically blended surfactants, and those comprised of $(EtO)_3Si$-PEG-laurate. As per the data in Figure 4-6, materials with compound **14** (the -*t*BS surfactant) exhibited CAs as low as 20°. However, this may result from the grease-like microdroplets that appeared at the interface, which caused immediate wicking of added water. Similarly, the CAs of materials with compound **13** seem anomalous, because its polar hydroxyl endgroup should confer CAs lower than those seen (85-108°). This compound has a terminal coupling agent and hydroxyl group, and the latter should theoretically present a polar, hydrophilic interface with low CAs. However, its CAs were comparable to materials with phenyl containing compounds **10** and **11**.

All other materials followed the predicted general trends. In comparison to the alkylsilane materials, for example, the laurate functionality in **9** (coupling agent) and **15** (triblock surfactant) promoted instant spreading of water to CAs as low as 37° and 24° respectively, likely due to the dynamic rearrangement of interfacial surfactant molecules. Since PEG chains are known to have rotational mobility,[37] it is thermodynamically favourable for PEG-based surfactants to reorient at the interface such their exposure to the aqueous environment is maximized while that of the hydrophobe is minimized. In the case of a linear laurate, the alkyl chains may better embed themselves into the underlying silicone matrix in comparison to the branched alkylsilanes that should be sterically hindered, even though the latter match the surface energy better and can adsorb to the interface. Hence, the presence of the alkylsilanes at the surface may account for the

highest CAs of such materials (**10, 11**), higher than even the pure silicone control (homemade RTV). It would also explain why the –*t*BS material (**8**) had higher CAs than the corresponding laurate material (**9**). Both compounds **8** and **9** (10 wt%) in homemade RTV had comparable CAs to the analogous materials made from Momentive™ silicone (**8-Mo**, **9-Mo**), hence any fillers or excipients in the commercial silicone mixture seemed to have little effect on CAs. Interestingly, in all cases, the concentration of compound in the material system had little effect on the CAs across any series of materials. Higher concentrations (20 and 10 wt%) of compounds in materials did produce lower CAs than low concentrations (0.5 and 1 wt%) for select samples; for example, the CA of materials with the laurate surfactant **15** had a CA of 25° at 20 wt% and a CA of 37° at 1 wt% (hence more surfactant allows more wetting). In light of this data, the cytophobicity and contact killing of all materials is discussed below.

4.5.4 Limited contact-killing and high cytophobicity; a winning combination

In theory, the attachment of polymeric biocides onto appropriate surfaces can create materials that kill microbes on contact. However, depending on the polymer, tethering it at the interface can render it benign for microbes.[24] This phenomenon was observed for the laurate-based compounds **9** (with coupling agent) and **15** (surfactant), which had potent bioactivity in solution but not when it was part of the RTV rubber. As with the contact angles, it is highly probable that when grafted at the interface and exposed to the aqueous environment, compounds **9** and **15** reorient to embed their hydrophobic ester

groups into the underlying silicone. Consequently, bacterial cells in solution are faced predominantly with hydrated PEG chains (that can sterically prevent surface attachment as seen in Figure 4-9), and not the alkyl chains that can readily disrupt the bilayer to cause lysis (Figure 4-4). Note that while there was no concentration-related effect on the contact killing for compound **9**; high concentrations above 2 wt % of surfactant in the system showed higher fluorescence counts during analysis for cytophobicity (therefore implying more adhesion) then those with 2 wt% or less. This may result from saturation of the interface with surfactant such that its reorientation to shield the ester is no longer homogenous across the surface. Hence, it may be possible that there are microdomains where the laurate is not fully embedded in the surface, but sufficiently exposed to create hydrophobic pockets for microbial attachment, without altering the hydrophilicity of the surface on a whole. This piece of adhesion data becomes even more interesting when compared with that for compound **8** and the CAs in Figure 4-6; using only wettability as a predictor of bacterial adhesion is clearly limiting since materials of compounds **8** and **9** *cause different amounts of wetting but both limit adhesion* in comparison to controls Figure 4-9.

In the case of compound **8**, the switch between relatively limited toxicity in solution to biocidal behavior at a material interface is not unique for compounds being studied for antibacterial activity. In one study, for example, *N*-hexylated polyvinylpyrrolidone (PVP) (a polymer with linear hexadecyl bromides attached to the pyridine rings) killed Gram-negative *Pseudomonas aeruginosa* when grafted onto a surface, but was largely ineffective against the same in solution.[24] One possible explanation is that grafted

polymers are presented in such a high concentration to an adhering cell, that they might even kill microbes that are not very susceptible to those polymers in solution. Perhaps this is the way in which compound **8** acts. Interestingly, when compounds **8** and **9** were cured into Momentive™ silicones, the materials that were generated showed significantly higher adhesion than their analogues made of homemade RTV. This seems to suggest that the combination of additives present in commercial mixtures of silicones may be responsible for the high adhesion often seen on PDMS (polydimethylsiloxanes), rather than the silicones themselves; the fillers are likely conferring the higher surface rigidity that was qualitatively observed for Momentive™ silicones relative to the homemade RTV, and surface rigidity has been positively correlated with bacterial adhesion.[38] The fact that unmodified homemade RTV (Figure 4-9) had very little adhesion despite an appropriate contact angle (103°) for silicones, further supports this hypothesis.

Another interesting observation was the increased adhesion seen to homemade RTV after modification with surfactants. This fact is difficult to explain and is still being probed by repeat adhesion assays for the unmodified control. However, it does not detract from the differences produced among compounds owing to their chemistry; clearly some allow more adhesion than others, while some also create contact-killing materials. These results also seemed to follow the general trends and design criteria outlined in previous work, whereby wetting agents of a defined PEG length can be functionalized with small hydrophobes to confer biocidal activity along with minimal adhesion (compound **8**) while wetting agents with much larger hydrophobes can be created that are cytophobic and non-bactericidal (for example compound **9**, **10**, **11**). As a preliminary study, therefore, the data

still yields promising candidates for anti-adhesive, non-bactericidal materials (compound **9** at 1-2 wt % in homemade RTV) that need to be studied in more depth.

4.6 Conclusion

The colonization of opportunistic pathogens on implantable biomaterials is an ongoing concern, and various mitigative strategies have been tried. Chief among these is the modification of surface wettability, particularly for silicones that form a large portion of the biomaterial industry, but have hydrophobicity that may facilitate undesirable adhesion. While such surfaces can be rendered hydrophilic with the use of surfactants, not all hydrophilic surfaces are cytophobic, and care must be taken to ensure the interface is not biocidal so as to prevent the spread of microbial resistance. As a consequence of this and the confounding effects of interfacial chemistry, materials that are both cytophobic and wetting, but not bactericidal, can be difficult to achieve. Our study successfully reports on the use of nonionic, silicone polyether surfactants, an understudied class of antibacterials, to modify silicone rubbers for this purpose. Out of the eight new material formulations that were tested, seven showed high cytophobicity at low weight percentages of surfactant in the system, without any biocidal activity. The contact killing by materials of compound **8** allows us to refine our design parameters for surfactant-based surface modifiers of silicones; longer, linear hydrophobes (while clearly toxic to bacteria in solution) may better penetrate the underlying silicone, thus providing wettable and cytophobic interfaces.

4.7 Acknowledgements

We thank the Natural Sciences and Engineering Research Council of Canada for financial support and Siltech Corp. for the gift of ACR. Prof. Christine DeWolf kindly provided access to her facilities at Concordia University to measure CACs and we thank her and Rolf Schmidt (DeWolf lab) for their help with the installation and suggested workflow of the CAC measurements.

4.8 References

1. H. W. Smith, *New Zealand veterinary journal*, 1967, **15**, 153-166.
2. C. A. Arias and B. E. Murray, *New England Journal of Medicine*, 2009, **360**, 439-443.
3. T. F. O'Brien, *Clinical Infectious Diseases*, 1997, **24**, S2-S8.
4. L. V. Interrante, Q. Shen and J. Li, *Macromolecules*, 2001, **34**, 1545-1547.
5. J. H. Park, K. D. Park and Y. H. Bae, *Biomaterials*, 1999, **20**, 943-953.
6. A. Mata, A. J. Fleischman and S. Roy, *Biomedical Microdevices*, 2005, **7**, 281-293.
7. S. I. Ertel, B. D. Ratner, A. Kaul, M. B. Schway and T. A. Horbett, *Journal of Biomedical Materials Research*, 1994, **28**, 667-675.
8. T. G. van Kooten, J. F. Whitesides and A. F. von Recum, *Journal of Biomedical Materials Research*, 1998, **43**, 1-14.
9. H. J. Busscher, G. I. Geertsema-Doornbusch and H. C. van der Mei, *Journal of Biomedical Materials Research*, 1997, **34**, 201-209.
10. T. Neu, H. Van der Mei, H. Busscher, F. Dijk and G. Verkerke, *Biomaterials*, 1993, **14**, 459-464.
11. M. J. Giraldez, C. G. Resua, M. Lira, M. E. C. D. Real Oliveira, B. Magariños, A. E. Toranzo and E. Yebra-Pimentel, *Optometry & Vision Science*, 2010, **87**, E426-E431 410.1097/OPX.1090b1013e3181da8656.
12. M. C. Lensen, V. A. Schulte, J. Salber, M. Diez, F. Menges and M. Möller, *Pure and Applied Chemistry*, 2008, **80**, 2479-2487.
13. J. Drelich and E. Chibowski, *Langmuir*, 2010, **26**, 18621-18623.
14. R. Förch, H. Schönherr and A. T. A. Jenkins, *Surface Design: Applications in Bioscience and Nanotechnology*, Wiley, 2009.
15. M. Ribeiro, F. Monteiro and M. Ferraz, *Biomedical Materials*, 2012, **7**, 045010.
16. V. A. Tegoulia and S. L. Cooper, *Colloids. Surf. B:*, 2002, **24**, 217-228.
17. M. L. Hawkins, F. Faÿ, K. Réhel, I. Linossier and M. A. Grunlan, *Biofouling*, 2014, **30**, 247-258.
18. G. M. Bruinsma, H. C. van der Mei and H. J. Busscher, *Biomaterials*, 2001, **22**, 3217-3224.

19. X. Feng and L. Jiang, *Advanced Materials*, 2006, **18**, 3063-3078.

20. A. L. Hook, C.-Y. Chang, J. Yang, J. Luckett, A. Cockayne, S. Atkinson, Y. Mei, R. Bayston, D. J. Irvine, R. Langer, D. G. Anderson, P. Williams, M. C. Davies and M. R. Alexander, *Nat Biotech*, 2012, **30**, 868-875.

21. E. A. Bayer, R. Kenig and R. Lamed, *Journal of Bacteriology*, 1983, **156**, 818-827.

22. M. F. Khan, L. Zepeda-Velazquez and M. A. Brook, *Colloids and Surfaces B: Biointerfaces*, 2015.

23. R. M. Hill, *Silicone surfactants*, CRC Press, 1999.

24. F. Siedenbiedel and J. C. Tiller, *Polymers*, 2012, **4**, 46-71.

25. H. Chen, M. A. Brook and H. Sheardown, *Biomaterials*, 2004, **25**, 2273-2282.

26. M. F. Khan, L. Zepeda-Velazquez and M. A. Brook, *Colloids. Surf. B:*, 2015, **132**, 216-224.

27. M. F. Khan, Masters of Applied Science (MASc), McMaster University, 2013.

28. J. L. Fritz and M. J. Owen, *J. Adhes.*, 1995, **54**, 33-45.

29. H. Hillborg and U. W. Gedde, *Polymer*, 1998, **39**, 1991-1998.

30. H. Hillborg, M. Sandelin and U. W. Gedde, *Polymer*, 2001, **42**, 7349-7362.

31. H. Hillborg, N. Tomczak, A. Olah, H. Schonherr and G. J. Vancso, *Langmuir*, 2004, **20**, 785-794.

32. J. Autian, *Environmental health perspectives*, 1975, **11**, 141.

33. S. Mageswari and K. Subramanian, *Polymer-Plastics Technology and Engineering*, 2012, **51**, 1296-1302.

34. B. Alberts, A. Johnson, J. Lewis, D. Morgan, M. Raff, K. Roberts and P. Walter, *Molecular Biology of the Cell, Sixth Edition*, Taylor & Francis Group, 2014.

35. M. Laradji, H. Guo, M. Grant and M. J. Zuckermann, *Journal of Physics: Condensed Matter*, 1992, **4**, 6715.

36. M. E. Whinton, 2016.

37. J. M. Harris, *Poly(Ethylene Glycol) Chemistry: Biotechnical and Biomedical Applications*, Springer, 1992.

38. C. Guegan, J. Garderes, G. Le Pennec, F. Gaillard, F. Fay, I. Linossier, J.-M. Herry, M.-N. B. Fontaine and K. V. Réhel, *Colloids and Surfaces B: Biointerfaces*, 2014, **114**, 193-200.

4.9 Appendix

4.9.1 Live-Dead fluorescence ratios (LDR) of ACR derivatives[‡‡‡]

The following preliminary data was acquired using the same protocol detailed in Section 4.3.2.3 (*Surfactant cytotoxicity in solution*), and it was analyzed after the completion of work in Chapter 3, but prior to initiating the study in this chapter. The compounds tested were structurally similar to ACR shown in Figure 4-10. The notation used in the graph corresponds to the terminal functional groups on either end the PEG backbone of ACR-based superwetters; ACR, for example, can be symbolized by $(OTMS)_2$-PEG_8-$COCHCH_2$, and is abbreviated to OTMS2-COCH2 in the graph. Similarly, OTMS2-OH indicates the PEG_8 backbone has a hydroxyl group on one end, and two OTMS groups on the other. NT signifies 'no treatment' and PEG, which is another control, has an equivalent number of units to ACR but lacks terminal functional groups.

As evident from Figure 4-10, ACR lost its biocidal activity when a hydroxyl group replaced its acrylate. This was interesting, since the data of Chapter 2 seemed to link bioactivity to the presence of a small hydrophobe alone. Based on Figure 4-10, however,

---

[‡‡‡] Recall, this preliminary work was motivated by ACR's biocidal nature, as demonstrated in Chapter 2.

a small hydrophobe is important but insufficient since both the methoxy compounds (with OTMs groups, albeit less than ACR) produced LDRs that were more than double that of the acrylate-containing analogue (they killed less bacteria). It seems, therefore, that the nature of the terminal groups on both ends of a bi-functional PEG backbone can significantly affect the biocidal behavior of these silicone surfactants. Since the ACR and hydroxyl-terminated derivative displayed the 'extreme' LDR values of all the derivatives used, they were re-utilized as comparators to other surfactants in Chapter 4. Methyl-end groups were also incorporated into the newly synthesized coupling agents and surfactants.

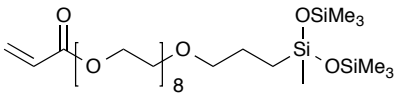

ACR-008 UP

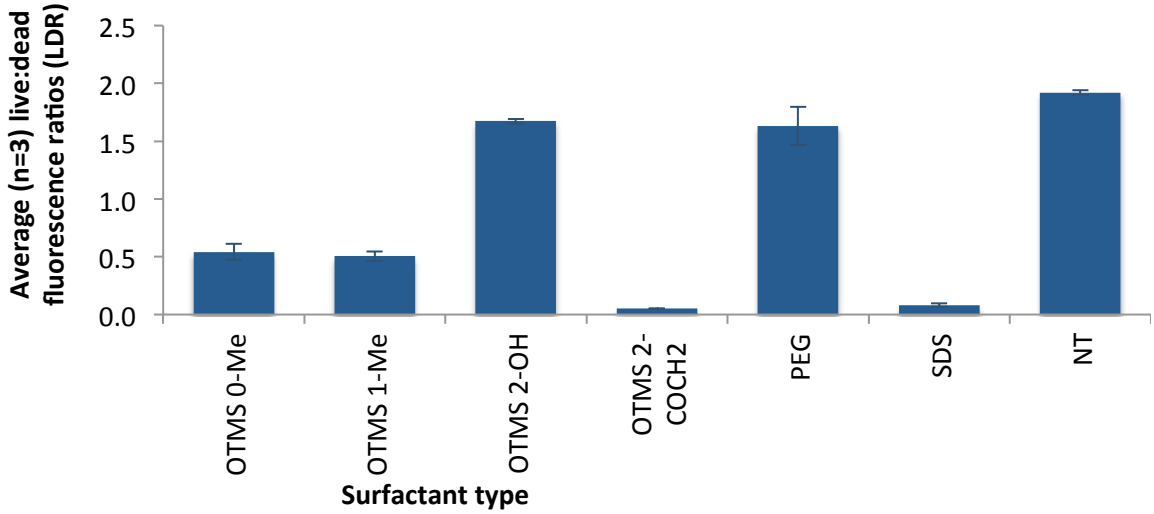

Figure 4-10. Average live:dead fluorescence ratios produced after *E. coli* was exposed to 0.1 w/v% of each compound for 12 hours. Error bars result from the standard deviation around the average.

4.9.2 Protocol used to determine Critical Micelle Concentrations (CMCs)

Downloaded and unzipped Fiji:

- http://fiji.sc/Downloads
- Downloaded the latest version of the pendant drop plugin:
  - http://sites.imagej.net/Daerr/plugins/
- Changed the file extension to 'jar'
- Copied the jar file into Fiji.app/plugins
- Copied and pasted the ActionBar and Scale folders into Fiji.app/plugins
- Opened Fiji.app/macros
- Opened StartupMacros.fiji.ijm with WordPad
- Found the 'AutoRun' macro: macro "AutoRun" {…}
- Added the following command right before the closing bracket:
  - run("Action Bar", "/plugins/Scale/_Set scale.txt");
- Saved StartupMacros.fiji.ijm

Created shortcut for pendant drop analysis

- Started Fiji
- Went to Plugins/Shortcuts/Add Shortcut by Name…
- Selected an appropriate shortcut from the dropdown
- Typed Pendent drop
- Clicked OK

Suggested workflow

- Opened an image of a pendant drop
- Clicked on 'Settings' in the 'Set scale' window.
- Changed the settings as required, checked 'Global' to apply the same calibration to all images upon opening

- Clicked on ‘Pendant drop’ in the ‘Set scale’ window to apply the calibration for the pendant drop set-up
- Used the shortcut created in the previous section to open pendant drop analysis
- Ran the pendant drop fit and recorded the surface tension
- Opened the next image (can use Ctrl-Shift-O) and repeat
- Clicked ‘Add scale bar’ to add a scale bar if necessary

To change a scale bar

- Editing scale bar settings is not supported in Fiji. Follow the instructions below to change the scale bar.
- Click ‘Delete scale bar’ to delete the scale bar
- Click on ‘Settings’ in the ‘Set scale’ window.
- Change the settings as required, check ‘Global’ to apply the same calibration to all images upon opening
- Click ‘Add scale bar’ to add a scale bar

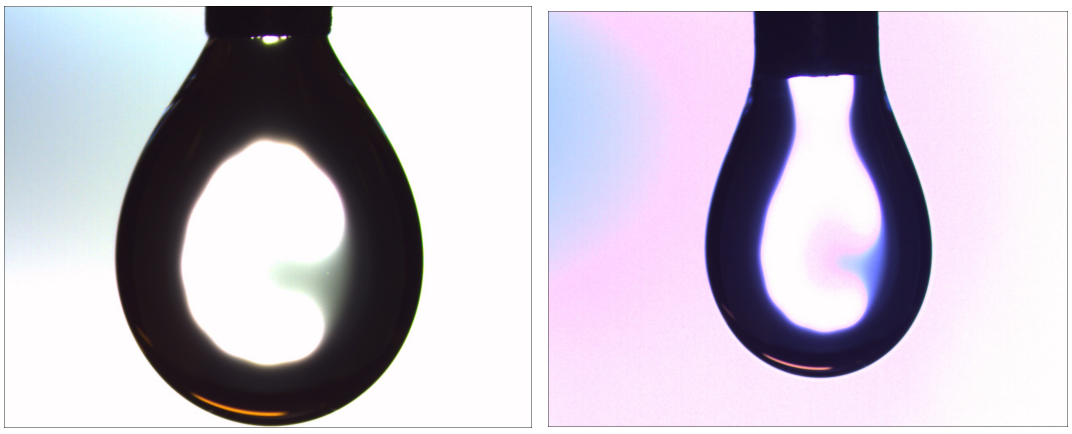

Figure 4-11. Pendant drop images obtained during CMC measurements for water (left) and compound **2** (allyl-PEG-TES) at a concentration of 0.1 w/v % in distilled water (right). Note these pictures are not to scale, however, the difference in droplet curvature resulting from the differences in surface tension of the liquid is apparent.

4.9.3 Light transmittance data for modified elastomers

The following multi-part figure indicates the transparency of homemade RTV elastomers that were modified with select coupling agents (**9-13**)

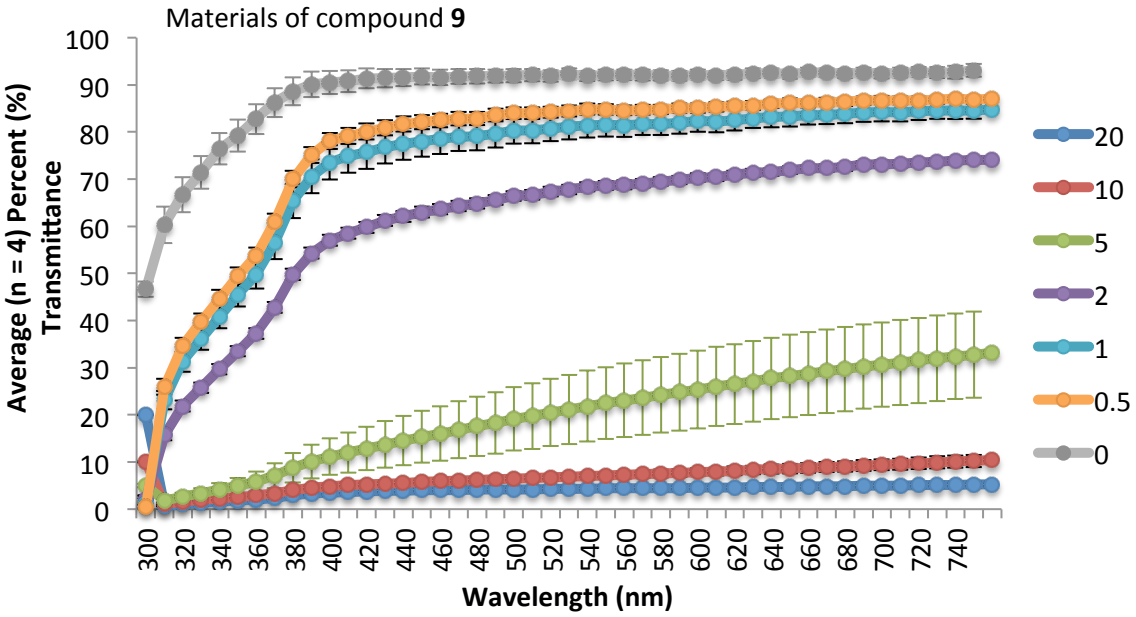

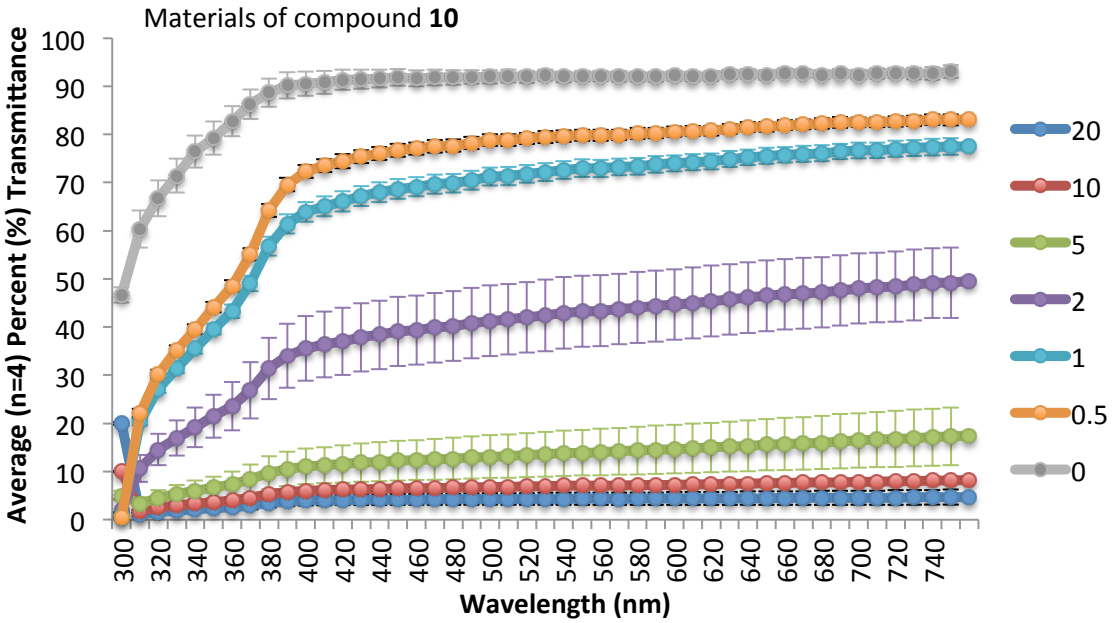

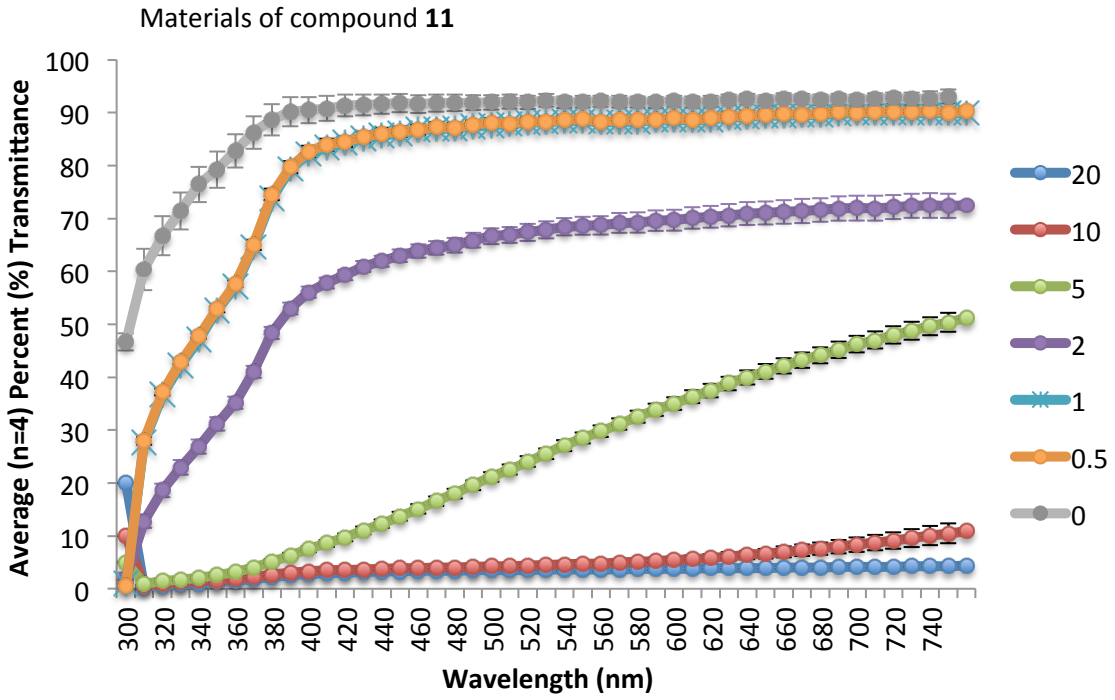
Materials of compound **11**
Average (n=4) Percent (%) Transmittance
Wavelength (nm)
20
10
5
2
1
0.5
0

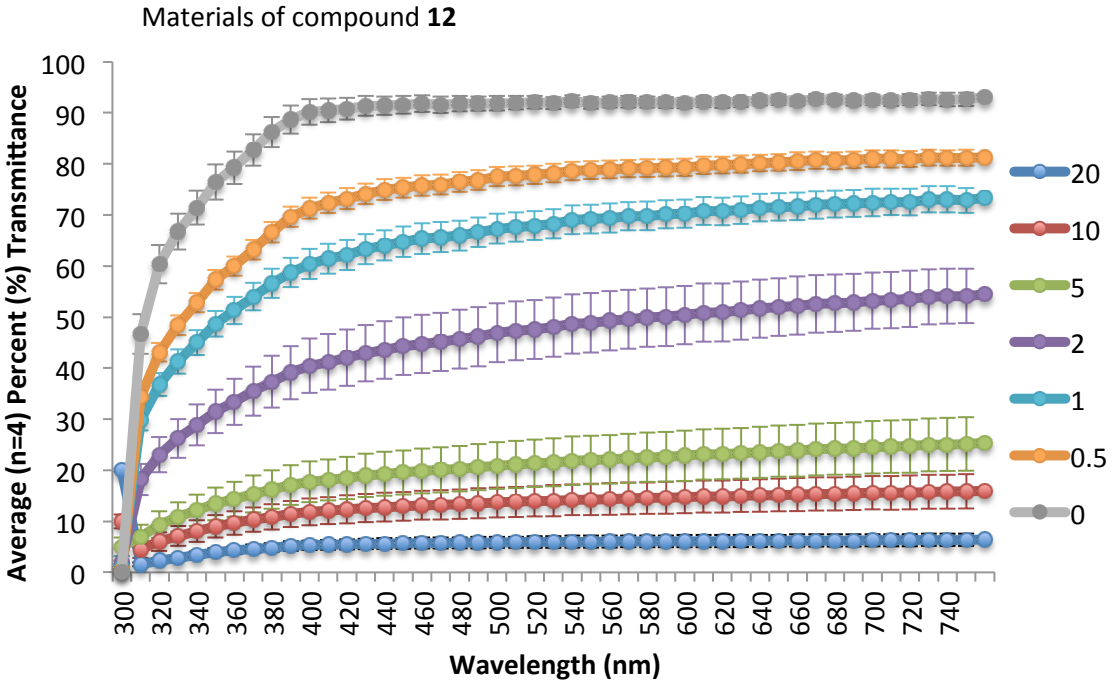
Materials of compound **12**
Average (n=4) Percent (%) Transmittance
Wavelength (nm)
20
10
5
2
1
0.5
0

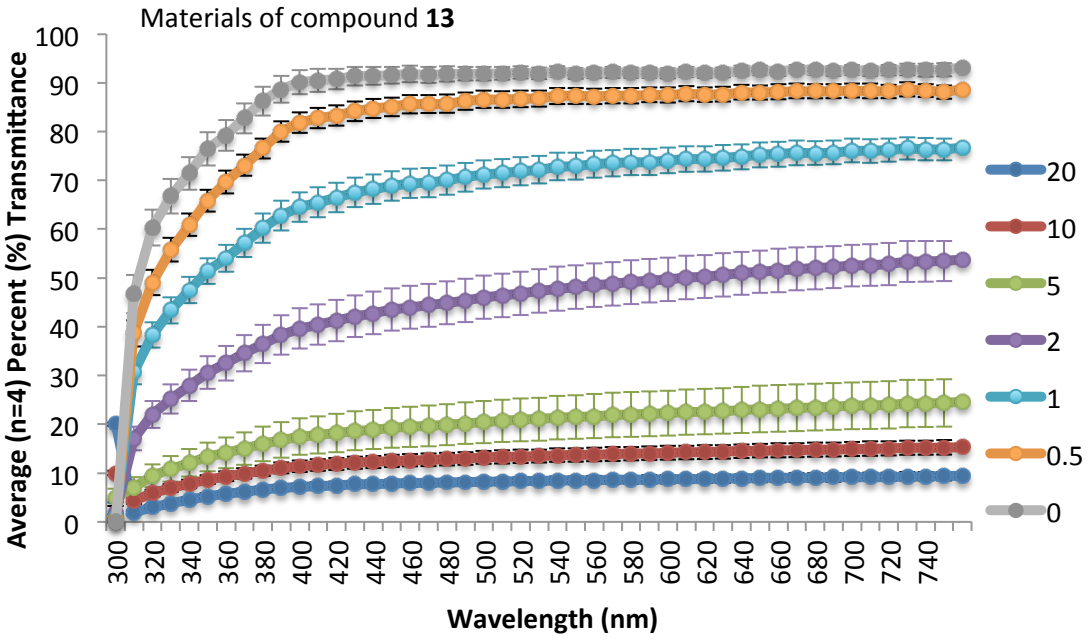

Figure 4-12. Average light transmittance values, across the range of visible light wavelengths, for homemade RTV materials that were modified with varying weight percentages (0- 20wt%) of coupling agents **8-13**. The error bars are standard deviation around the average.

4.9.4 GFP Fluorescence of material washes during cytophobicity analysis

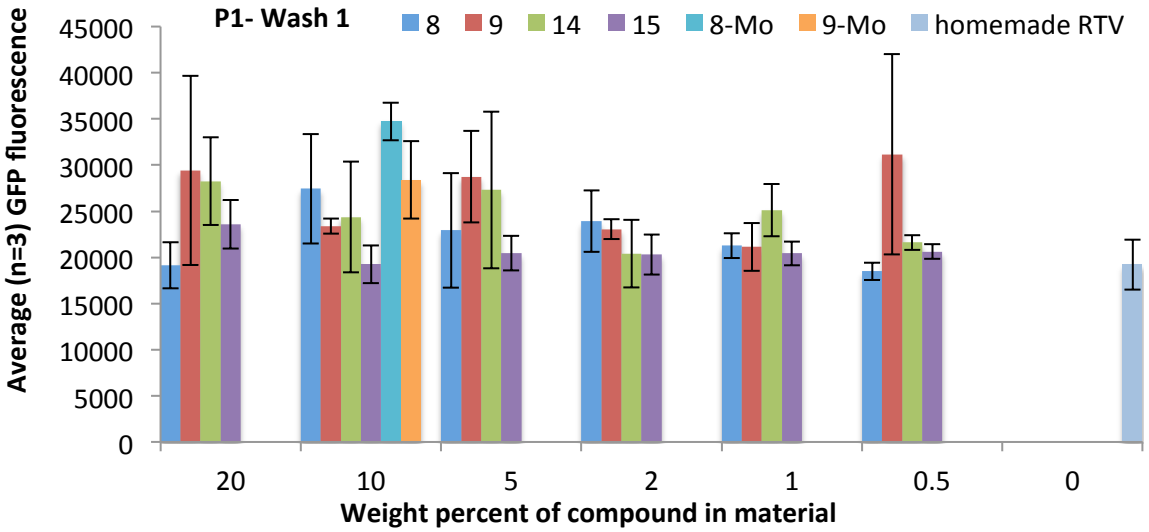

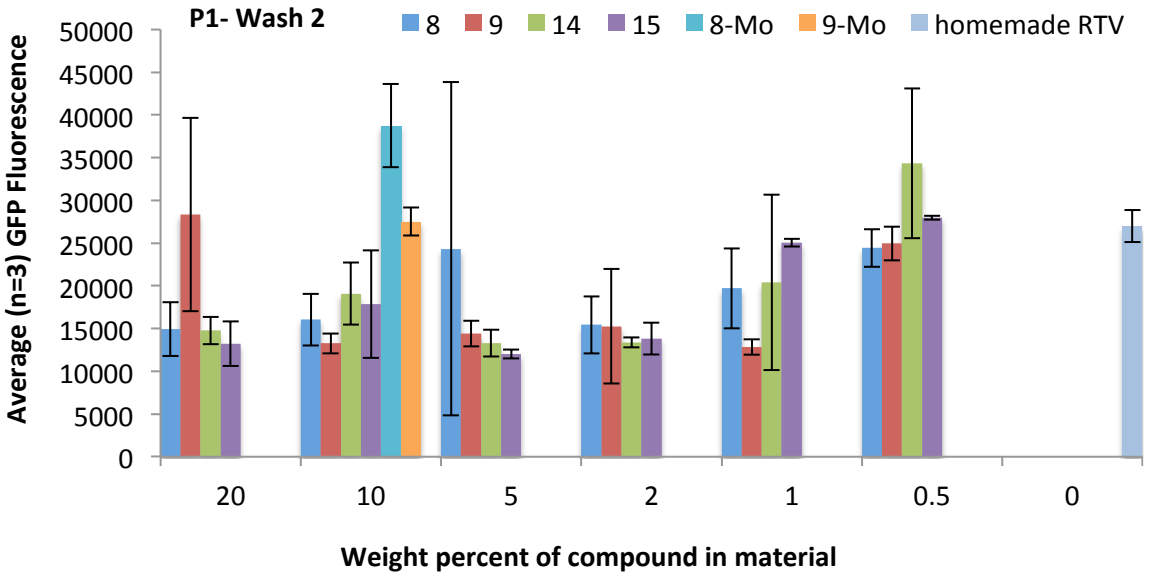

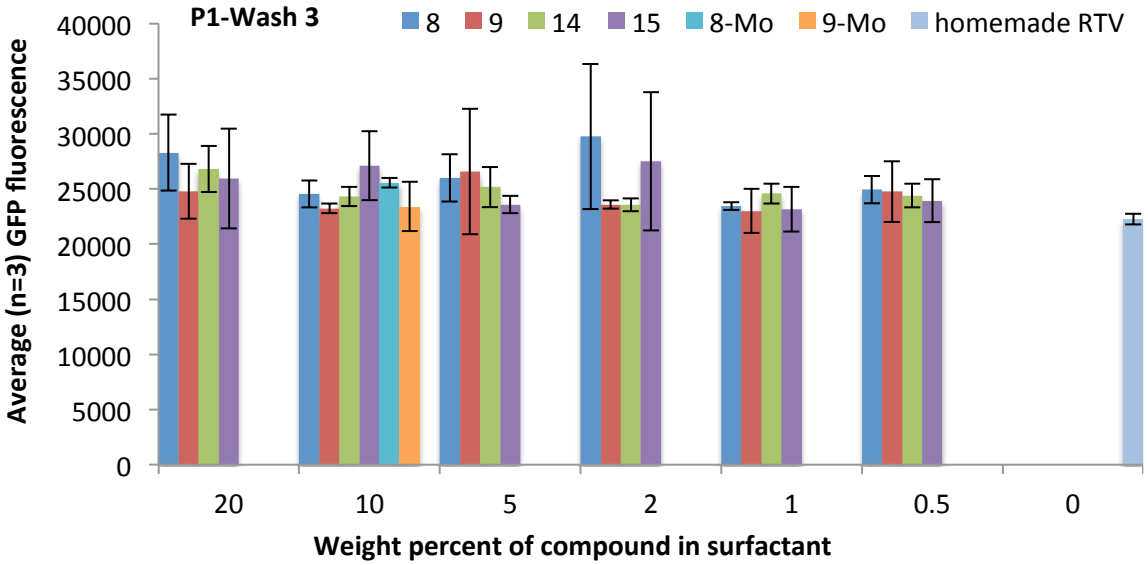
P1-Wash 3
8
9
14
15
8-Mo
9-Mo
homemade RTV
Average (n=3) GFP fluorescence
40000
35000
30000
25000
20000
15000
10000
5000
0
20
10
5
2
1
0.5
0
Weight percent of compound in surfactant

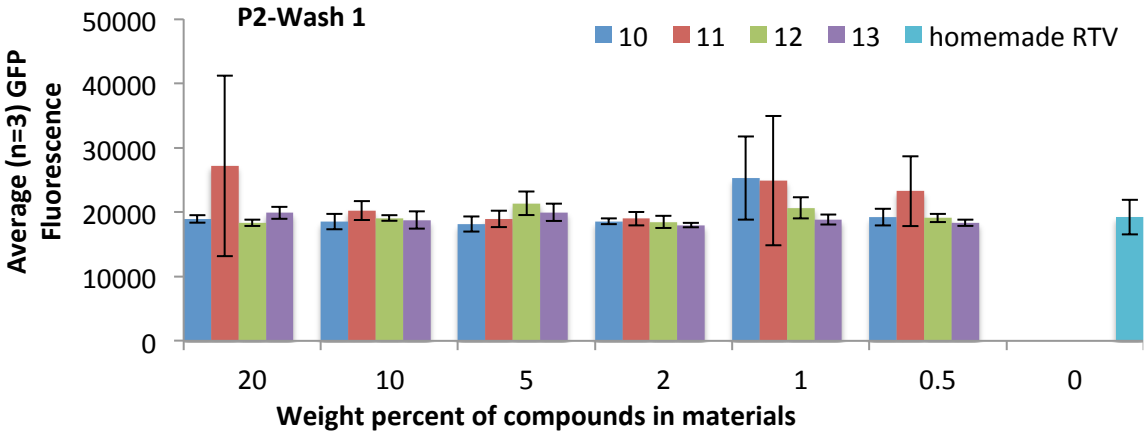
P2-Wash 1
10
11
12
13
homemade RTV
Average (n=3) GFP Fluorescence
50000
40000
30000
20000
10000
0
20
10
5
2
1
0.5
0
Weight percent of compounds in materials

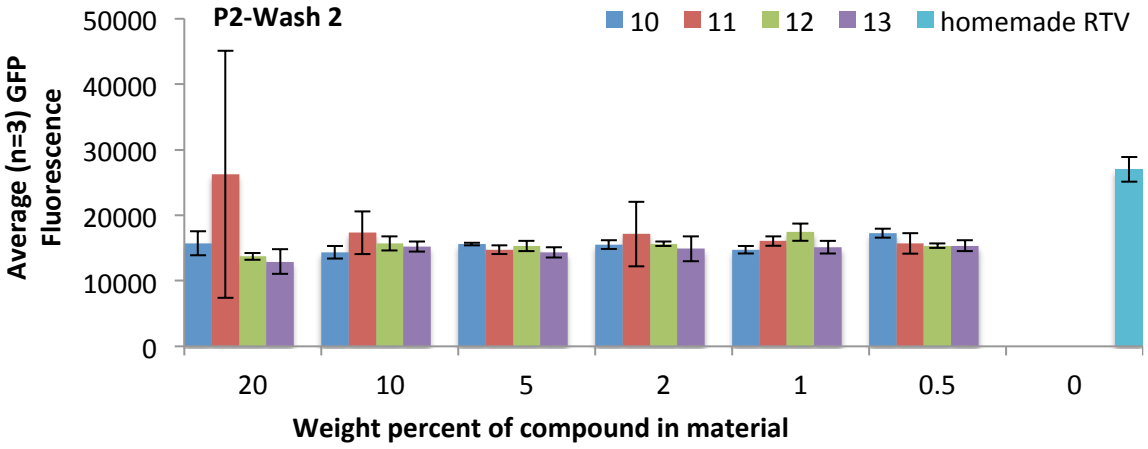
P2-Wash 2
10
11
12
13
homemade RTV
Average (n=3) GFP Fluorescence
50000
40000
30000
20000
10000
0
20
10
5
2
1
0.5
0
Weight percent of compound in material

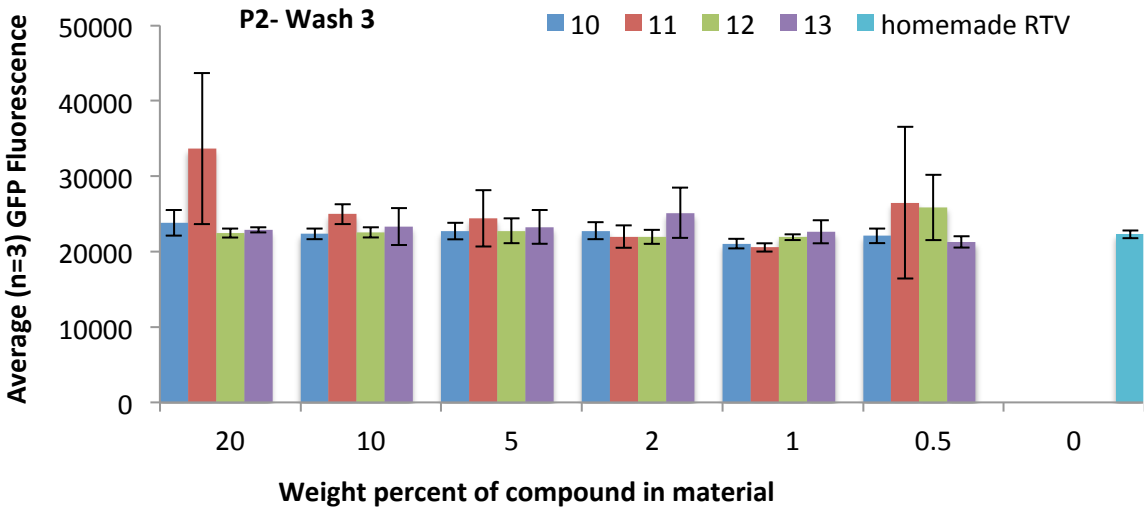

Figure 4-13. The average GFP fluorescence measured from each of the three wash steps for plates (P1/ P2) during cytophobicity analysis of materials. Error bars represent the standard deviation form triplicate measurements. Note that fluorescence values are uncorrected.

CHAPTER 5: General conclusions

As detailed in Chapter 1, microbial contamination of surfaces is of socioeconomic concern in a variety of settings, including, but not limited to, that of healthcare, food packaging, water and sanitation, as well as the petrochemical industry. The problem is not the introduction of microbes to a surface, but rather the subsequent development of biofilms, which results from colonies of microbes secreting a protective polysaccharide matrix. This film allows the embedded cells to: (1) withstand antibiotics, biocides and other harsh and/or nutrient-depleted environmental conditions; (2) secrete problematic toxins; (3) exchange genetic information with neighboring cells (and therefore transfer antibacterial resistance); (4) degrade the underlying substrate and cause material failure or general spoilage; (5) serve as a microbial depot for the colonization of other proximal surfaces; and (6) cause problematic restrictions of openings. Biofilms are particularly concerning for medical devices or implants such as stents, where they can block the blood flow in key arteries with serious consequences. Since almost all synthetic materials are vulnerable to contamination, the control of microbial growth on surfaces is of significant interest in the fields of material science and medicine.

Several strategies are used for preventing biofilm formation. One is to sterilize the interface and surrounding environment using disinfectants such as hypochlorite or hydrogen peroxide. This strategy is impermanent and the reintroduction of bacteria to the material is relatively easy. Surface modification to create antibacterial interfaces is

another advocated solution. This is typically achieved via the introduction of polymer brush layers, coatings that allow the incorporation and release of antibiotics, and the grafting of quaternary ammonium (QA) or silver containing compounds onto the surface. The limitations of use are common to all: impermanence of the antibacterial effect (as is the case when using disinfectants); leaching of cytotoxic compounds from the surface (e.g., QA compounds, and silver ions); and, in the case of antibiotic doped surfaces; the achievement of controlled release kinetics is difficult. In each case, the exposure of bacteria to sublethal concentrations of antibacterials is concerning, because it may facilitate the formation of resistant strains (a growing problem as evident by antibiotic resistant pathogens). Additionally, many biocidal moieties (such as triclosan) attached to antimicrobial polymers can be of environmental concern.

Hence, the focus has shifted from trying to kill bacteria, to simply preventing their adhesion. In this regard, silicone surfactants may be the ideal surface modifiers since they are highly surface active, even more so then their hydrocarbon analogues, are eco-friendly, since their degradation products are sand and glycolic acids, are generally biocompatible, because they are derivatives of silicones that are widely used, and because they have as of yet, unexplored potential. Their superwetting properties in particular may disrupt the initial hydrophobic interactions used by bacteria to begin their attachment to material surfaces.

With this in mind, Chapter 2 studied the adhesion response of gram-negative *E. coli* to the improved interfacial wetting provided by a commercially available silicone surfactant, ACR, which has a heterofunctional PEG backbone of eight units, and terminal acrylate

and trisiloxane functionalities. Mixtures of MMA and/or BMA were radically polymerized with increasing amounts of the surfactant (0-100 wt %). As a result, three distinct polymer series were synthesized: ACR:BMA:MMA (with equal parts BMA and MMA), ACR:MMA and ACR:BMA, respectively. These materials where then characterized physically and biologically to produce two very interesting results.

The first was that the surface wettability of the materials did not positively correlate with surfactant concentration, even though more wetting agents at the interface should have increased the surface hydrophilicity. Since trisiloxane surfactants are highly mobile, it is likely that they respond to environmental stimuli (wet vs. dry) by reorienting at the interface. In aqueous conditions, for example, the trisiloxane of the ACR likely adsorbs to the underlying silicone, while its PEG chain interacts with the water. This concept helps explain the high to low to high sessile drop CAs observed with increasing ACR concentration in materials: at low surfactant concentrations, we suggest that the number of interfacial PEG chains will be insufficient to confer hydrophilicity, and the droplet will see the hydrophobic methacrylate body (hence the high CAs); at intermediate ACR concentrations, enough interfacial PEG chains should be present to increase the surface wettability (low CAs); and at high ACR concentrations, reorientation of the surfactant may be hindered by the density of interfacial surfactant molecules, hence, the surfactant likely forms a brush layer of trisiloxanes to re-create a hydrophobic surface (high CAs).

The second interesting phenomenon was similar in that *E. coli* adhesion also tracked imperfectly with the amount of ACR in the system. Materials with 0 and 50 wt % surfactant, for example, showed greater adhesion than those of 20 wt % ACR (ACR-

MMA and ACR-BMA materials). In fact, the adhesion on surfaces of 20 wt % ACR were the lowest of all series. This was unsurprising, since low concentrations of surfactants significantly decrease the adhesion of bacteria on synthetic surfaces, possibly because they disrupt the initial hydrophobic interactions required for bacterial attachment. Hence, while the surface concentration of surfactant groups at 20 wt % ACR may have been insufficient to show a net change in the surface wettability, this concentration may have been enough for the very mobile ACR to interact with proximal bacterial membranes to disrupt adhesion.

Both observations emphasize that the effect of surface modification on *E. coli* adhesion is not one-dimensional; a lack of adhesion cannot be attributed to the wettability conferred by the superwetting silicone surfactants alone. The chemistry of the surface modifier, and therefore its behavior at the interface, clearly matters. Consequently, a more robust screening of antibacterial activity as it relates to the chemical structure of a silicone surfactant was deemed necessary.

A small library of seven, closely related nonionic silicone polyether surfactants was used for further study in Chapter 3. Based on the MOA described for nonionic detergents in pharmaceutical applications, it was proposed that the hydrophobes of each surfactant would serve as the bioactive moiety. Hence, creating silicone surfactants with well-defined hydrophobes was important. While historically difficult, this was accomplished using the Piers-Rubinsztajn reaction to generate explicit head groups, which were then clicked onto hydrophilic tails using azide-alkyne click chemistry. The tails were methyl-terminated, low polydispersity $(PEG)_{44}$ or $(PEG)_{15}$ polyethers, while the hydrophobes

varied in size, number of silicone groups (4, 7 or 10) and the number of phenyl groups (1 or 3). In an attempt to understand the bioactivity of these compounds they were tested against 5 concentrations of *E. coli* in solution at concentrations below, at, and above their (CMCs). The antibacterial assay consisted of a turbidometric screen, a live-dead stain and viable colony counts.

Data for the three phenyl-containing compounds did not match the trends evident for all other surfactants: there appeared to be no difference in the activities seen at surfactant concentrations above and below the CMCs. This suggests that the phenyl nature of the head groups (rigidity, ability to pi-stack, and ease/ difficulty of intercalation with the bilayer phospholipids) may be confounding variables, the exact effect of which requires further experimentation to elucidate. For all other surfactants, however, antibacterial activity was higher at above the CMC. Additionally, surfactants with smaller silicone head groups had almost 4 times the activity of the larger analogues. Smaller PEG chains also correlated with greater biocidal activity, and in all cases bacterial concentration had little or no effect on biocidal behavior.

Greater activity above CMC concentrations was likely due to membrane saturation by surfactant molecules, such that enough lipid-lipid-bonds were disrupted to cause cell lysis. Surfactants may penetrate the hydrophobic membrane directly from solution or from the surfactant micelles; hence, larger branched silicones had decreased activity on account of impaired integration, while long PEG chains likely formed larger hydrophilic coronas around micelles that hindered surfactant-membrane interactions. While these proposed action mechanisms warrant further investigation, which would also allow an

assessment of activity against other bacteria, the fact that these surfactants were not ill-defined mixtures like most other silicones (the Piers-Rubinsztajn provides great control over the hydrophobe structure) means that the article in Chapter 3 was a first in reporting structure-dependent antibacterial activity for silicone polyether surfactants. Interestingly, the superwetting compound ACR-008UP (provided by Siltech Corp.) showed antibacterial activity greater than even sodium dodecyl sulphate (SDS), which is a known and potent lysing agent. Hence, it and other superwetting compounds were deemed good candidates for the modification of surfaces. Surfactants that did not significantly affect organisms, but conferred wettability owing to their PEG backbones, could give rise to anti-adhesive (cytophobic) materials. Alternatively bacteriotoxic surfactants could allow for contact-killing surfaces.

Chapter 4, therefore, capitalizes on the design criteria from its predecessor, and describes 18 new compounds that were rationally synthesized or purchased. Unlike the compounds of Chapter 3, these new surfactants had smaller PEG backbones and were grouped into 3 categories: (1) surfactants that were allyl-terminated and served as precursors to compounds in other groups; (2) surfactants with terminal ethoxysilylpropyl coupling agents; and (3) triblock surfactants. The head groups of all surfactants differed in their functionalities, which ranged from simple hydroxyl and methyl groups to more complex phenyls, laurates and *t*BS groups.

As before, these compounds were first assessed for antibacterial activity in solution at concentrations above their CMCs. The results supported our previously proposed MOA, whereby surfactant molecules with smaller hydrophobes had the greatest antibacterial

activity, while those with phenyl rings had the least. The MOA was further evidenced by the comparable toxicity of ACR and the laurate- and ethoxysilylpropyl- terminated surfactant; its longer, linear alkyl group, which resembles membranous fatty acid chains, likely allowed for better insertion between, and the disruption of, structural lipids in the bacterial bilayers. In contrast, the corresponding *t*BS- functionalized surfactant showed markedly lower toxicity to *E. coli*.

Interestingly, these results were reversed when the *t*BS- and laurate-based surfactants were incorporated into PDMS elastomers; materials of the former showed higher contact killing than the latter. It is possible that the tethered laurate, once exposed to the aqueous environment, is more effective at penetrating the underlying silicone matrix than the *t*BS group. This would sufficiently shield the laurate and prevent it from interacting with the *E. coli.* The *t*BS- containing analogue, with its high affinity for surface adsorption but branched head group may be sterically hindered and unable to incorporate into the underlying matrix as effectively. Such differences in behavior between the two surfactants may also explain the differences observed in their surface wettabilities; the laurate modified surface had CAs around 40°, while the other average 80°. In theory, the steric hindrance experienced by the *t*BS group should also prevent it from disrupting proximal bilayers in solution (assuming accuracy of our simple MOA), however, the literature explains this phenomenon to be a function of bacteria facing higher concentrations of surfactant when it is tethered than when it is in solution. Regardless of the reason, it is clear that the differences in surfactant chemistry allowed for the creation of biocidal and non-biocidal surfaces.

These results become more even more striking when combined with the *E. coli* adhesion data, which show that the laurate and *t*BS functionalized surfaces caused different amounts of wetting but *both* limited adhesion. The adhesion data correlated with surfactant concentration, such that the greater the amount of surfactant in the system, the greater the adhesion observed. This may result from saturation of the interface with surfactant, so that insufficient reorientation and shielding of the surfactant head groups created hydrophobic microdomains for bacterial attachment. This was not a concern at low surfactant concentrations. As such, and in the context of this study, the elastomer modified with the laurate-functionalized surfactant (at concentrations less than 5 wt %) created the ideal material surface: cytophobic and non-toxic.

To summarize, the body of work presented in this thesis accomplishes its intended goal; to demonstrate that nonionic silicone polyether surfactants are a viable source of novel antibacterial agents. While the work began with a naive attempt at decreasing bacterial adhesion on surfaces using superwetting silicone surfactants, it has since shown that such compounds can have potent structure-dependent activity. Hence, manipulating their chemistry allows for potentially tunable biological responses that further diversify the utility of these compounds. One use is the creation of anti-adhesive materials, which have multi-industry applications, but are particularly relevant in the context of health care where the development of biofilms is highly problematic. To this end, the *in vitro* efficacy of these surfaces against different, clinically relevant strains of bacteria must be determined, and their effect on mammalian cells must also be addressed. Lastly, additional studies to determine the exact MOA may help validate the models proposed

herein. MOAs are generally difficult to elucidate, given the complexity of bacterial-surface interactions, but doing so will further aid structural optimization of the surfactants for specific biological responses. It seems, therefore, that there is still much work to be done before these surfaces can be practically applied. However, since this is the first time the structural parameters of nonionic silicone polyether surfactants have been examined in terms of bioactivity, the work included in this thesis is an important start towards novel silicone surfactant based antibacterial materials to limit biofilm formation.